

University of Southampton Research Repository

Copyright © and Moral Rights for this thesis and, where applicable, any accompanying data are retained by the author and/or other copyright owners. A copy can be downloaded for personal non-commercial research or study, without prior permission or charge. This thesis and the accompanying data cannot be reproduced or quoted extensively from without first obtaining permission in writing from the copyright holder/s. The content of the thesis and accompanying research data (where applicable) must not be changed in any way or sold commercially in any format or medium without the formal permission of the copyright holder/s.

When referring to this thesis and any accompanying data, full bibliographic details must be given, e.g.

Thesis: Author (Year of Submission) "Full thesis title", University of Southampton, name of the University Faculty or School or Department, PhD Thesis, pagination.

Data: Author (Year) Title. URI [dataset]

UNIVERSITY OF SOUTHAMPTON

Faculty of Social Sciences

Mathematical Sciences

NONLINEAR MODELS FOR MIXTURE EXPERIMENTS
INCLUDING PROCESS VARIABLES

by

Shroug Abdullah Alzahrani

<https://orcid.org/0009-0004-3862-7316>

Thesis submitted for the degree of Doctor of Philosophy

April 28, 2024

UNIVERSITY OF SOUTHAMPTON

ABSTRACT

FACULTY OF SOCIAL, HUMAN, AND MATHEMATICAL SCIENCE

Mathematical Sciences

Doctor of Philosophy

Nonlinear Models for Mixture Experiments Including Process Variables

Shroug Abdullah Alzahrani

Mixture experiments are applied in a variety of fields, for example, food processing, chemical engineering, and product quality improvement. All these examples have in common that they rely on experiments that mix multiple components. In mixture experiments, the measured response is a function not of the amount of the mixture components but their proportions. This adds a layer of complexity to the modeling of such experiments. In some mixture experiments, the blending properties of the mixture may be affected by the processing conditions, such as temperature and pressure, besides the mixture components' proportions. Such types of mixture experiments are known as mixture-process variables experiments.

This present work is concerned with finding and assessing a class of models that flexibly fits data from mixture experiments and mixture-process variables experiments, and with providing guidelines for how to design mixture experiments and mixture-process variables experiments when these models are fitted. Most models in the literature are either based on polynomials and are therefore not very flexible, or have a large number of parameters that make the response surface interpretation difficult to understand. The modified fractional polynomial models are a recent class of models from the literature that are flexible and parsimonious but quite restrictive. We contribute to mixture experiments by proposing a new class of nonlinear models, the complement mixture fractional polynomial (CMFP) models, by making an additional transformation of the fractional polynomial, which results in less restrictive models while retaining (and indeed exceeding) the advantages of this class. Moreover, we suggest an extended form for the modified fractional polynomial models to fit data from mixture-process variables experiments.

A further main concern of this thesis is to optimize the response by finding the optimal combinations of proportions of the mixture components. Therefore, we found the maximum response by determining the corresponding proportions of the mixture components that achieved this. We conducted a simulation study in which we evaluated the performance of the CMFP models and compared them with different models from the literature.

An efficient design can greatly improve the analysis of an experiment. We constructed exact and near-optimal mixture designs in constrained experimental regions for CMFP models with respect to the D-optimal criteria. Comparisons between the obtained designs in terms of their efficiency and robustness assessment are illustrated with several examples.

Contents

List of Figures	v
List of Tables	viii
Declaration of Authorship	xiii
Acknowledgments	xiv
1 Introduction	1
1.1 Mixture Experiments	1
1.2 Design of Experiments	3
1.3 Organization of the Work	4
2 Literature Review and Background	5
2.1 Modelling of Mixture Experiments	5
2.2 Modelling of Mixture-Process Variables Experiments	7
2.3 Finding Optimal Proportions of Mixture Components	10
2.4 Optimal Design of Mixture Experiments	11
2.5 Mixture Designs Settings	13
2.5.1 Simplex-Lattice Design	13
2.5.2 Simplex-Centroid Design	14
3 Models for MPV Experiments	16
3.1 Models for Mixture Experiments	17
3.2 Models for Process Variables	20
3.3 Mixture Model Including Process Variables	20
4 Estimation in MPV Experiments	24
4.1 Statistical Criteria for Model Comparison	24
4.2 Example 1: Estimate a Mixture Experiment with a 2-Level Process Variable	25

4.3	Example 2: Estimate a Mixture Experiment with a 3-Level Process Variable	29
4.4	Example 3: Estimate a Mixture Experiment with Two Process Variables	31
4.5	Example 4: Estimate a Mixture Experiment with a 3-Level Process Variable	33
4.6	Summary	35
5	Optimal Proportions of Mixture Components	36
5.1	Motivation	37
5.2	Methodology of Finding Optimal Mixture Proportions	37
5.2.1	Models Used in the Simulation Study	37
5.2.2	Simulation Setup	38
5.3	Optimal Mixture Proportions for a 3-Component Experiment	41
5.3.1	Summary	48
5.4	Optimal Mixture Proportions for a 4-Component Experiment	49
5.4.1	Summary	55
5.5	Optimal Mixture Proportions for a 3-Component Experiment with One Process Variable	57
5.5.1	Summary	61
5.6	Optimal Mixture Proportions for a 3-Component Experiment with Two Process Variables	64
5.6.1	Summary	69
5.7	Overall Summary	72
6	Designing Experiments for CMFP Models	74
6.1	Introduction	74
6.2	Optimal Continuous Designs for CMFP Models	88
6.2.1	Designs for First-Degree CMFP Models with a Single Power Parameter . . .	88
6.2.2	Designs for First-Degree CMFP Models with Two Power Parameters	92
6.2.3	Designs for Second-Order CMFP Models with One Power Parameter	95
6.2.4	Designs for Second-Order CMFP Models with Two Power Parameters	98
6.2.5	The CMFP Models with Misspecified Terms.	101
6.2.6	Designs for CMFP models with 4-Mixture Components	104
6.3	Strategies for Finding Optimal Exact Designs	106
6.3.1	Comparison Between Exact Designs and Rounded Continuous Designs	108
6.4	Designs when Considering a Process Variable	129
6.4.1	Example 1: MPV Designs for the Opacity of Printable Coating Material Experiment with a 2-level Process Variable	131

6.4.2	Example 2: MPV Designs for the Opacity of Printable Coating Material Experiment with a 3-level Process Variable	136
6.4.3	Example 3: MPV Designs for Oil-Water Separation Experiment with a 3-level Process Variable	141
7	Conclusion and Some Further Recommendations	147
7.1	Brief Review	147
7.2	Suggested Points for Future Work	149
8	Appendix	151
	Bibliography	159

List of Figures

2.1	Simplex-lattice design for three components	14
2.2	Simplex-Centroid design for three components	15
4.1	The contour plots of the response surface of models (3.13), (3.14), and (3.18), respectively, at both levels of the process variable	28
4.2	The contour plots of the response surface of models (3.13), (3.14), and (3.18), respectively, in all levels of z	30
4.3	The contour plots of the response surface of models (3.13), (3.14), and (3.17), respectively, in all combinations of levels of the two process variables, z_1 and z_2	32
4.4	The contour plots of the response surface of models (3.13), (3.14), and (3.18), respectively, at all levels of the process variable	34
5.1	The difference between TM and EM	41
5.2	The contour plots of the response surfaces of the true Scheffé's model, fitted Scheffé's model, and the CMFP model, respectively	63
5.3	The contour plots of the response surfaces of three different cases of the MFP model: true, good, and bad models, respectively	71
6.1	A restricted experimental region	83
6.2	a. The initial design, and b. The near-optimal design	85
6.3	Optimized designs for four different scenarios of a first-order CMFP model with a single power parameter	91
6.4	Optimized designs for four different scenarios of first-order CMFP models with two power parameters.	94
6.5	Optimized designs for four different scenarios of quadratic CMFP models with one power parameter.	97
6.6	Optimized designs for four different scenarios of second-order CMFP models with two power parameters	100

6.7	Optimal designs for a. x_1x_2 , b. x_1x_3 , and c. x_2x_3	103
6.8	The optimal support points and their replication for a first-order CMFP model with one power parameter when all parameters have the estimated values (Scenario a in Section 6.2.1)	110
6.9	The optimal support points and their replication for a first-order CMFP model with one power parameter when all parameters have the estimated values but with opposite signs (Scenario b in Section 6.2.1)	111
6.10	The optimal support points and their replication for a first-order CMFP model with one power parameter when $\alpha = -1.5$ (Scenario c in Section 6.2.1)	112
6.11	The optimal support points and their replication for a first-order CMFP model with one power parameter when $\alpha = 1.2$ (Scenario d in Section 6.2.1)	113
6.12	The optimal support points and their replication for a first-order CMFP model with two power parameters when parameters have the estimated values (Scenario a in Section 6.2.2)	115
6.13	The optimal support points and their replication for a first-order CMFP model with two power parameters when parameters have the estimated values but with opposite signs (Scenario b in Section 6.2.2)	116
6.14	The optimal support points and their replication for a first-order CMFP model with two power parameters when $\alpha_1 = 0.1$, $\alpha_2 = 0.39$ (Scenario c in Section 6.2.2)	117
6.15	The optimal support points and their replication for a first-order CMFP model with two power parameters when $\alpha_1 = -0.1$, $\alpha_2 = -0.9$ (Scenario d in Section 6.2.2)	118
6.16	The design points and their replication in the exact design and the rounded continuous design when all parameter values have the estimated values (Scenario a in Section 6.2.3)	120
6.17	The design points and their replication in the exact design and the rounded continuous design when all parameter values have the estimated values but with opposite signs (Scenario b in Section 6.2.3)	121
6.18	The design points and their replication in the exact design and the rounded continuous design when $\alpha = -1.5$ (Scenario c in Section 6.2.3)	122
6.19	The design points and their replication in the exact design and the rounded continuous design when $\alpha = 1.2$ (Scenario d in Section 6.2.3)	123
6.20	The design points and their replication in the exact design and the rounded continuous design when all parameter values have the estimated values (Scenario a in Section 6.2.4)	125

6.21	The design points and their replication in the exact design and the rounded continuous design when all parameter values have the estimated values but with opposite signs (Scenario b in Section 6.2.4)	126
6.22	The design points and their replication in the exact design and the rounded continuous design when $\alpha_1 = 0.1$, $\alpha_2 = 0.6$ (Scenario c in Section 6.2.4)	127
6.23	The design points and their replication in the exact design and the rounded continuous design when $\alpha_1 = -0.1$, $\alpha_2 = -0.9$ (Scenario d in Section 6.2.4)	128
6.24	MVP designs for CMFP models with a single power parameter for the four studied scenarios	133
6.25	MVP designs for CMFP models with two power parameters for the four studied scenarios	135
6.26	MVP designs for CMFP models with a single power parameter for the four studied scenarios	138
6.27	MVP designs for CMFP models with two power parameters for the four studied scenarios	140
6.28	MVP designs for CMFP models with one power parameter for the four studied scenarios	143
6.29	MVP designs for CMFP models with two power parameters for the four studied scenarios	146

List of Tables

2.1	The most important model classes in mixture experiments	7
3.1	Summary of models	23
4.1	Summary Statistics for competing models	26
4.2	Summary Statistics for competing models	29
4.3	Summary Statistics for competing models	31
4.4	Summary Statistics for competing models	33
5.1	The outcome measures for all fitted models when the Ratio model is the true model and $s = 0.5$	42
5.2	The outcome measures for all fitted models when the Ratio model is the true model and $s = 8.924$	43
5.3	The outcome measures for all fitted models when Scheffé's model is the true model and $s = 0.5$	44
5.4	The outcome measures for all fitted models when Scheffé's model is the true model and $s = 7.135$	44
5.5	The outcome measures for all fitted models when the GBM model is the true model and $s = 0.5$	45
5.6	The outcome measures for all fitted models when the GBM model is the true model and $s = 6.688$	45
5.7	The outcome measures for all fitted models when the MFP model is the true model and $s = 0.5$	46
5.8	The outcome measures for all fitted models when the MFP model is the true model and $s = 7.901$	46
5.9	The outcome measures for all fitted models when the CMFP model is the true model and $s = 0.5$	47

5.10	The outcome measures for all fitted models when the CMFP model is the true model and $s = 8.467$	47
5.11	The models' ranks when the standard errors equal 0.5	48
5.12	The models' ranks when the standard errors have realistic values	48
5.13	The outcome measures for all fitted models when the Ratio model is the true model and $s = 0.5$	49
5.14	The outcome measures for all fitted models when the Ratio model is the true model and $s = 84.94$	50
5.15	The outcome measures for all fitted models when Scheffé's model is the true model and $s = 0.5$	51
5.16	The outcome measures for all fitted models when Scheffé's model is the true model and $s = 59.55$	51
5.17	The outcome measures for all fitted models when the GBM model is the true model and $s = 0.5$	52
5.18	The outcome measures for all fitted models when the GBM model is the true model and $s = 32.45$	52
5.19	The outcome measures for all fitted models when the MFP model is the true model and $s = 0.5$	53
5.20	The outcome measures for all fitted models when the MFP model is the true model and $s = 33.66$	53
5.21	The outcome measures for all fitted models when the CMFP model is the true model and $s = 0.5$	54
5.22	The outcome measures for all fitted models when CMFP model is the true model and $s = 43.53$	54
5.23	The models' ranks when the standard errors equal 0.5	55
5.24	The models' ranks when the standard errors have realistic values	56
5.25	Outcome measures for all models when simulating data using the Ratio model . . .	58
5.26	Outcome measures for all models when simulating data using Scheffé's model . . .	59
5.27	Outcome measures for all models when simulating data using the GBM model . . .	59
5.28	Outcome measures for all models when simulating data using the MFP model . . .	60
5.29	Outcome measures for all models when simulating data by the CMFP model . . .	61
5.30	The ranks of the fitted models	61
5.31	Outcome measures for all models when simulating data from the Ratio model, $s=0.5$	65
5.32	Outcome measures for all models when simulating data using the Ratio model, $s=25.37$	65
5.33	Outcome measures for all models when simulating data using Scheffé's model, $s=0.5$	65

5.34	Outcome measures for all models when simulating data using Scheffé's model, $s=44.79$	66
5.35	Outcome measures for all models when simulating data using the GBM model, $s=0.5$	66
5.36	Outcome measures for all models when simulating data using the GBM model, $s=29.59$	67
5.37	Outcome measures for all models when simulating data using the MFP model, $s=0.5$	67
5.38	Outcome measures for all models when simulating data using the MFP model, $s=47.3$	67
5.39	Outcome measures for all models when simulating data using the CMFP model, $s=0.5$	68
5.40	Outcome measures for all models when simulating data using the CMFP model, $s=19.33$	68
5.41	The models' ranks when the standard errors equal 0.5	69
5.42	The models' ranks when the standard errors have realistic values	69
5.43	Overall distribution of ranks of all models	72
6.2	D-optimal 4-point design for a first-degree CMFP model	78
6.3	Initial Design and Optimal Design for the example	84
6.1	Constraint matrix \mathbf{u}_i of four support points design	87
6.4	The optimized design when all model parameters have the estimated values	89
6.5	The optimized design when all parameters have the estimated values but with op- posite signs	89
6.6	The optimized design when $\alpha = -1.5$ and $\beta's=1$	90
6.7	The optimized design when $\alpha = 1.2$ and $\beta's=1$	90
6.8	The optimized design when all parameter values have the estimated values	93
6.9	The optimized design when all parameters have the estimated values but with op- posite signs	93
6.10	The optimized design when $\alpha_1 = 0.1$, $\alpha_2 = 0.39$ and $\beta's=1$	93
6.11	The optimized design when $\alpha_1 = -0.1$, $\alpha_2 = -0.9$ and $\beta's=1$	93
6.12	The optimized design when all parameter values have the estimated values	95
6.13	The optimized design when all parameters values have the estimated values but with opposite signs	96
6.14	The optimized design when $\alpha = -1.5$ and $\beta's=1$	96
6.15	The optimized design when $\alpha = 1.2$ and $\beta's=-1$	96
6.16	The optimized design when all parameter values have the estimated values	99
6.17	The optimized design when all parameters values have the estimated values but with opposite signs	99
6.18	The optimized design when $\alpha_1 = 0.1$, $\alpha_2 = 0.6$, $\beta_0 = 300$, $\beta_1=\beta_2=\beta_3=\beta_4=-1$, and $\beta_5=10$	99
6.19	The optimized design when $\alpha_1 = -0.1$, $\alpha_2 = -0.9$ and $\beta's=1$	99

6.20	D-efficiencies for optimal designs for the misspecified models relative to the optimal designs for the correct model	102
6.21	The optimized design when the parameter values have the estimated values	105
6.22	The optimized design when the parameter values have the estimated values but with opposite signs	105
6.23	The MPV design when all parameter values have the estimated values	131
6.24	The MPV design when all parameter values have the estimated values but with opposite signs	131
6.25	The MPV design when $\alpha = 0.88$ and $\beta's=-1$	132
6.26	The MPV design when $\alpha = -0.93$ and $\beta's=1$	132
6.27	The MPV design when all parameter values have the estimated values	134
6.28	The MPV design when all parameters values have the estimated values but with opposite signs	134
6.29	The MPV design when $\alpha_1 = -0.50$, $\alpha_2 = 0.77$ and $\beta's=-1$	134
6.30	The MPV design when $\alpha_1 = 0.85$, $\alpha_2 = -0.60$ and $\beta's=1$	135
6.31	The MPV design when all parameter values have the estimated values	136
6.32	The MPV design when all parameter values have the estimated values but with opposite signs	137
6.33	The MPV design when $\alpha = 0.88$ and $\beta's=-1$	137
6.34	The MPV design when $\alpha = -0.93$ and $\beta's=1$	137
6.35	The MPV design when all parameter values have the estimated values	139
6.36	The MPV design when all parameter values have the estimated values but with opposite signs	139
6.37	The MPV design when $\alpha_1 = -0.50$, $\alpha_2 = 0.77$ and $\beta's=-1$	139
6.38	The MPV design when $\alpha_1 = 0.85$, $\alpha_2 = -0.60$ and $\beta's=1$	140
6.39	The MPV design when all parameter values have the estimated values	142
6.40	The MPV design when all parameter values have the estimated values but with opposite signs	142
6.41	The MPV design when $\alpha = 0.88$ and $\beta's=-1$	142
6.42	The MPV design when $\alpha = -0.93$ and $\beta's=1$	143
6.43	The MPV design when all parameter values have the estimated values	144
6.44	The MPV design when all parameter values have the estimated values but with opposite signs	144
6.45	The MPV design when $\alpha_1 = -0.50$, $\alpha_2 = 0.77$ and $\beta's=-1$	145
6.46	The MPV design when $\alpha_1 = 0.85$, $\alpha_2 = -0.60$ and $\beta's=1$	145

8.1	Experimental data of the opacity of printable coating material with a 2-level process variable	151
8.2	Experimental data of the opacity of printable coating material with a 3-level process variable	152
8.3	Homemade bubble solution experimental data	153
8.4	Experimental data of oil separation ratio	154
8.5	The chick feeding experimental data	155
8.6	The illumination candle experimental data	156
8.7	The soap processing experimental data	156
8.8	Constraint matrix u_i of 6 support points design	157
8.9	Constraint matrix u_i of 7 support points design	158

Declaration of Authorship

I, Shroug Alzahrani, declare that the thesis entitled "Nonlinear Models for Mixture Experiments Including Process Variables" and the work presented in the dissertation are my work and were created by me as a result of my original research.

I confirm that:

- This work was done wholly or mainly while in candidature for a research degree at this University;
- Should any part of this dissertation have been previously submitted for a degree or other qualification at this university or other institution, this has been clearly stated;
- When I have consulted the published work of others, this is always clearly attributed;
- Where I have quoted from the work of others, the source is always given. Except for these quotations, this thesis is entirely my work;
- I have acknowledged all major sources of assistance;
- Where the thesis is based on work done by myself jointly with others, I have made clear exactly what was done by others and what I have contributed myself;
- None of this work has been published prior to submission;

Signed:

Date:

Acknowledgments

Praise be to Allah, God of everything, as much as his mercy.

Then, pleased to express my deep gratitude to my supervisor, Prof. Stefanie Biedermann, who always had a willingness to motivate and help me. Great thanks to her encouragement and guidance during the Ph.D. research from the start. It has been a great honor to work with her. Prof. Stefanie's knowledge and experiences that benefited me are invaluable.

Thanks to my husband, sons, and parents.

Finally, all thanks and respect to my country, which gave me this scholarship opportunity.

Chapter 1

Introduction

1.1 Mixture Experiments

Many industrial products and scientific experiments involve mixing or blending more than one ingredient. In such experiments, changing the proportions of components of the mixture affects the resulting product that the experimenter is interested in measuring. These experiments are called mixture experiments. For example, concrete in building construction consists of mixing cement, sand, and water in certain proportions. Indeed, mixture experiments are widely applied in almost all fields and are commonly encountered in industrial product formulations, such as food processing, chemical engineering, and improving the quality of a product by identifying the optimal formulation as described by Chu and Resurreccion (2004), Akalin et al. (2010), and Bello and Vieira (2011), respectively. The measured response (the properties of interest) is a function of the proportions of the mixture components (factor levels) instead of being a function of the total amount of the mixture. Therefore, mixture experiments are considered an effective tool for exploring and adjusting the effects on the response of the proportions of each component in the mixture. Such relationships can be represented as

$$\text{Measured response} = f(\text{The mixture components' proportions})$$

The proportions of the components present in the mixture can be expressed by weight, fraction, volume, etc. These proportions are subject to two basic restrictions known as natural constraints for mixture experiments. The first one is the sum of the proportions of the mixture components is equal to one. The second constraint is that each proportion must be greater than or equal to zero. Often, there are lower and upper limits on component proportions as additional restrictions. To clarify this, assume that q denotes the number of mixture components, and the proportions of the components are represented by x_r , for $r = 1, \dots, q$, where the two natural constraints for mixtures

are as follows:

$$0 \leq x_r \leq 1, \quad r = 1, \dots, q \quad (1.1)$$

and

$$\sum_{r=1}^q x_r = x_1 + x_2 + \dots + x_q = 1 \quad (1.2)$$

Often, there are lower and upper limits to ingredient proportions as additional restrictions, which can be expressed as

$$l_r \leq x_r \leq u_r \quad (1.3)$$

where $l_r > 0$ and $u_r < 1$, $r = 1, \dots, q$

In some mixture experiments, the properties of the product are affected by the processing conditions, in addition to the proportions of the ingredients in the mixture. Such experiments are known as mixture experiments with process variables. For example, baking conditions, such as time and temperature (process variables), are important concerns in developing cake textures besides the cake mix (proportions of the mixture components). The experimenter needs to consider process variables when conducting a mixture experiment in order to find the best settings of process variables by studying their effect on the final product. This topic has become more prevalent in recent research, for example, in pharmaceutical development (Anderson-Cook et al., 2004). Bello and Vieira (2011) present a case study of optimizing a chemical compound consisting of a three-component mixture where they consider two process variables to improve rocket engine performance.

There are many models in the literature that are used to fit data from mixture experiments, but most of these models are either inflexible, as in the case of traditional models, or very complex, in the case of newer models. Therefore, we develop a new class of models that balance flexibility and complexity. These proposed models fit data from mixture experiments with restricted design regions. We also develop the extended forms of these models to fit data from mixture-process variables experiments as well. We evaluate this class of models in estimation situations by fitting them to several real datasets to demonstrate their good fit and compare the performance of the new models with other statistical models from the literature.

Often, the purpose of a mixture experiment is to find the optimal combination of the mixture proportions where the optimal response is obtained. Therefore, we want to establish how our proposed models perform in this task. We assess our models by comparing them to several common models from the literature. In particular, a simulation study was done based on five mixture models. We consider five scenarios of the true model used to generate data. We use a small standard

error and a realistic standard error to generate two new datasets from the true model to check if the variability of the random error affects the performance of the models. How close the optimal proportions values of the mixture component of each fitted model are to those obtained from the true model is a benchmark of the models' performance evaluation. Furthermore, it is also of interest to assess the most recent models in the literature, such as the modified fractional polynomials (Khashab, 2018) and general blending models (Brown et al., 2015), which have limited assessment.

1.2 Design of Experiments

Experimental designs are tools to plan an experiment in order to achieve particular objectives and answer research questions as clearly and efficiently as possible. So, designing an experiment statistically is a powerful tool to improve scientific experimentation by collecting the maximum information from the data with the least potential waste of resources. The design and the analysis of an experiment go hand in hand, and therefore we will not only investigate modelling strategies for mixture experiments (with and without process variables), but will also consider how to design such experiments.

The design of experiments is an important statistical method that has become the cornerstone of modern scientific research in many fields. Evaluating strategies to find optimal designs for these new models is another purpose of this work. Thus, we intend to find efficient designs for these models. First, we find locally optimal designs and then assess their robustness with respect to the model parameter and/or model misspecification. In our study, we construct exact designs by using the exchange algorithm (Meyer & Nachtsheim, 1995) and optimize the continuous designs using constrained optimization functions in R such as `constrOptim`, `solnp`, and `nloptr` under the D-optimality criterion. It should be noted that optimal design search for mixture experiments is challenging because of the non-standard experimental regions, in particular when additional constraints of the form 1.3 are encountered. Little attention has been paid in the literature to find exact optimal designs. Algorithms to find exact designs directly are often based on candidate sets, and while a large candidate set slows down the optimization, a small set may not contain points that are close to the optimal ones. Therefore, often continuous designs are found, and then their weights are rounded to make them exact. We evaluate the merits of each of these strategies in the framework of mixture experiments.

In summary, our novel contributions to the literature are:

- A new class of models to fit data from mixture and mixture process variable experiments.
- Extensive model comparisons between our proposed class of models and common models from the literature. Here, we not only compare the models with respect to their fit to the data (Chapter 4) but also with respect to their ability to find the optimal proportions of a mixture (Chapter 5), which is of interest to practitioners in the area.
- In our comparisons, we also include the most recent models proposed in the literature, modified fractional polynomials and general blending models, for which only limited assessment is available.
- Finally, we found locally D-optimal designs for our new class of models and assessed their robustness. We further evaluated different strategies for finding exact optimal designs.

1.3 Organization of the Work

This present work is concerned with modeling mixture experiments and mixture process variables experiments in restricted experimental regions. So, we proposed a new class of models that can fit experimental data from mixture and mixture process variables experiments. These new models are called complement mixture fractional polynomials models (CMFP). The CMFP models will be evaluated and compared with other models from the literature by statistical criteria such as Akaike Information Criterion and Bayesian Information Criterion, as will be seen in Chapter 3 and Chapter 4. A literature review of modeling mixture experiments and mixture process variables experiments will be provided in Chapter 2. In many areas of experimentation, one of the research aims is to maximize the response by finding the optimal values of the mixture proportions. Therefore, we did a simulation study based on five different models. The simulation setup, models used in the simulation, and the assessment measures that are used in the simulation study will be presented in detail in Chapter 5.

Chapter 6 is dedicated to the designs of the CMFP models. First, we search for the optimum continuous designs of four types of CMFP models, which are first-order CMFP and second-order CMFP models with one power parameter and two power parameters in four different scenarios of model parameter values. Also, comparisons are made between rounded continuous designs and exact designs generated from an exchange algorithm for each scenario of parameter values. Moreover, we search for optimal design in case of mixture experiments that include a process variable. All optimal designs we obtained and their plots, accompanied by the results of the robustness study of the designs will be shown in Chapter 6. Chapter 7 contains our main conclusions and suggestions for future work.

Chapter 2

Literature Review and Background

The wide range of applications for mixture experiments in various fields makes the mixture experiments an essential research area in statistics. For example, they have numerous applications in chemical engineering, pharmaceutical fields, materials science, and food science. Although mixture experiments were first discussed by Quenouille et al. (1953), pioneering work on experiments with mixtures was published by Scheffé (1958), and then Scheffé (1963). This literature review provides a comprehensive overview of models that fit data from mixture experiments and mixture-process variables experiments, finding optimal proportions of mixture components and optimal designs of mixture experiments if process variables are included.

2.1 Modelling of Mixture Experiments

Polynomial models introduced by Box and Wilson (1951) are regression models appropriate to represent mixture components through their polynomial terms. Ordinary polynomial models were applied before Scheffé's work and were commonly used in mixture experiments, for example, Clar- ingbold (1955) and Hackler et al. (1956). Scheffé (1958) introduced a linear regression model called the simplex-centroid model and the extension of the simplex-centroid model, which includes quadratic terms. Despite the availability of sophisticated models of mixture experiments in today's literature, Scheffé's canonical polynomial is still widely applied to analyze mixture experiments. Scheffé's canonical polynomials are obtained by modifying standard polynomial models considering the natural constraints (1.1) and (1.2) of mixture experiments as shown in more detail in Section 3.1. The canonical polynomial model contains only a small number of terms and requires few ob-

servations to estimate parameters, which makes it easy to interpret the effects of the components in mixture experiments. Nevertheless, Scheffé's models were criticized by Quenouillé (1963) who stated a weak point of Scheffé's polynomials, as these models cannot incorporate the common linear blending when one component of the mixture has an excessive portion in the mixture. Kenworthy (1963) introduced useful models for mixture data analysis, ratio models, distinct from traditional regression models focusing on the absolute quantities of variables. These models were among the early attempts to address the primary challenges posed by experiments involving mixtures, where the components of the mixture sum up to one. Becker (1968, 1978) explained the creation of alternative models that allow additive components or inactive ingredients and can determine the effect of a specific component. In addition, he added improvements that exceeded those previously considered by inserting terms that could describe a broader range of effects.

However, the utility of Scheffé's polynomial has been expanded by some researchers who have developed Scheffé's models in several ways. For example, the inverse of Scheffé's polynomials was suggested by Draper and St.John (1977), while Chen et al. (1985) proposed using logarithmic terms of such models. Moreover, other researchers presented beneficial parameterizations, such as Draper and Pukelsheim (1998) and Cornell (2000). Even though Scheffé's models have a good ability to analyze data from mixture data experiments, Cox (1971) criticized the lack of the direction and magnitude of the curvature of the response in Scheffé's quadratic polynomial models due to the lack of the squared terms in these models and suggested several alternative models address this obstacle. In addition, polynomial models include various formulations proposed by Cornell (1990) using transformations and diagnostic tools to accommodate more complex and nonlinear relationships in mixture experiments. However, statistical models that are nonlinear in their parameters have been applied to data from mixture experiments on a small scale. Such models were proposed by Focke et al. (2007). These models are applied to a few components of mixture experiments and assume linear blending of one or more mixture components.

Brown et al. (2015) integrated existing statistical models, which have been proposed in Scheffé (1958), Scheffé (1963) and Becker (1968), to introduce a new class of models to analyze data from mixture experiments, known as general blending models. Although general blending models expanded the description of effects of a broader range of mixture components, these models may make an accurate interpretation of the response surface difficult due to a considerable number of parameters in these models.

A new class of nonlinear models proposed by Khashab (2018), based on fractional polynomial

models, has been shown to outperform common models from the literature in many examples. These models are simple but flexible and fit experimental data from restricted regions. However, these modified fractional polynomial (MFP) models require that all mixture proportions are bounded away from zero, which is not always realistic in applications. Therefore, we propose a different transformation to the fractional polynomial, which is less restrictive. This proposed new class of models provides a good explanation for the experimental response mechanism and fits data from mixture experiments similarly well as the MFP models, which we will demonstrate in Chapter 4. The advantages and disadvantages that mixture experiment models offer depend on the nature of the experimental data and the complexity of the models. Table 2.1 outlines the widely used models for mixture experiments and an overview of their advantages and disadvantages.

Table 2.1: The most important model classes in mixture experiments

Mixture experiments models	Advantages	Disadvantages
Canonical Polynomial Models (Scheffé, 1958)	Widely used for their simplicity and general applicability in mixture experiments and can be adapted to different levels of complexity.	Potential limitations in modeling complex interactions. Potentially large numbers of terms in complex situations.
Becker Models (Becker, 1968)	Have polynomial terms different from Scheffé's models to capture certain nuances in the data.	Their applicability is limited to specific types of problems and potentially requires more sophisticated statistical analysis.
Cornell Models (Cornell, 1990)	Focused on practical applications and use transformation techniques to accommodate more complex relationships.	Complexity and computational demands for proper application and interpretation.
Weighted Power Mean Mixture Model (Focke et al., 2007)	Adaptability to different types of mixtures and accuracy in predicting overall properties.	Requires a solid background in the relevant chemistry and mathematics to implement and understand.
General Blending Models (Brown et al., 2015)	High flexibility makes them fit a more comprehensive range of experimental data with varying blending behaviors well.	Implementation and interpretation may be challenging due to their sophisticated nature.
Modified Fractional Polynomial Models (Khashab, 2018)	Show a good fit for several real datasets from mixture experiments.	Quite restrictive if some proportions may be zero.

2.2 Modelling of Mixture-Process Variables Experiments

In some mixture experiments, the properties of the product are affected by the processing conditions in addition to being affected by the proportions of the ingredients in the mixture. Such experiments are known as mixture experiments with process variables (MPV). So, these types of experiments aim to find the best conditions of processes simultaneously with the best blending formulas to produce the desired result. The mixture experiment problem involving process variables was first introduced by Scheffé (1963), who fitted the m^{th} degree polynomial to the q,m

simplex-lattice design (see Section 2.5.1) and used a q^{th} degree polynomial to include process variables. Subsequently, Cornell (1973) discussed including process variables and fitting the full model form of the traditional Scheffé's model but found that cross products between process variables and mixture components did not provide any comprehensive measurement of the main effects and interactions of process variables themselves. Gorman and Cornell (1982) managed this issue by separating the effects of the process variables and the mixture components. They used a subset selection procedure to introduce a reparametrized model form that reduced the canonical model.

Piepel and Cornell (1985) introduced a modeling approach to unrestricted and restricted mixture amount experiments, but it was also applicable to mixture-process variable experiments involving one process variable. They wrote the parameters of the mixture model as functions of the total amount variable, and any mixture model form can be used as a base with the parameters of a mixture model in it, such as Scheffé's canonical polynomials in Scheffé (1958) or Becker's models in Becker (1968, 1978). Moreover, experiments with mixtures in the presence of process variables were also considered by Czitrom (1988, 1989). She used Scheffé's quadratic models for the expected response of mixture components run in blocks or complete replicas in different combinations of process variables. Cornell (1988, 1990) suggested models that contain mixture components and process variables where blending properties of mixture components are expressed by Scheffé's polynomial, while the main effects and interaction effects of process variables are defined using the standard polynomial model. The required information determines the combined form of the model that contains the mixture components and the process variables.

Chitra and Ekong (1993) address a three-component mixture problem related to product development in constrained region mixture experiments when three process variables are present. A reduced form of the six-term quadratic Scheffé's model was used at each combination of levels of the three process variables. However, Cornell (1995) questioned the validity of this reduced combined model and suggested some general recommendations and strategies for model fitting. For example, he suggested a sufficient number of mixture blends must be performed to support the fitting of Scheffé's quadratic model to model the nonlinear blending properties of monomers.

Thereafter, a study was presented by Næs et al. (1998) in experimental data with a three-component mixture and two process variables, which provided an equation of a combined model representing the blending properties and the effects of the process variables. This model is a product of the two separated polynomial models where the blending properties are represented by the three components full cubic Scheffé's model minus the three components interaction, and a 2nd-degree

polynomial represents the effects of the process variables. Although they attempted to exclude all unimportant terms from this combined model using specific regression analysis accompanied by t-tests of parameter estimates, this reduced model is still very complex in nature and is not easy to explain. However, a combined model, which is based on Taylor series approximation, was proposed by Kowalski et al. (2000). This model provides valuable insights into the experiment under study because the interaction between the specific mixture component and the specific process variable can be seen directly through this proposed model.

There are different ways to combine mixture models with process variable models. To accommodate mixture components and process variable interactions, multiplying the mixture model and the process variable model to produce a combined model is the method adopted by many authors, such as Cornell (2011), who provided a combined mixture process variables model by crossing a special cubic model in mixture components with a quadratic process variables model. In addition, another combined model obtained by crossing a quadratic mixture model with a quadratic process variables model has been proposed by Prescott (2004) and Måge and Næs (2005). These kinds of combined models are called interaction Mixture Process variables models, and they usually have a large number of terms, some of which may not be necessary.

The simplicity of the model and its validity for interpretation is an important characteristic to consider in any model. Therefore, variable selection techniques are usually used to reduce the terms in Mixture-Process variable models without losing their predictive power. Sahni et al. (2009) determined the complexity of the models needed to form a combined MPV model as a first step by fitting separate Scheffé's quadratic models for each combination of the process variables, and separate process variables quadratic polynomial models at each combination of the mixture components. Then, they removed the insignificant terms from each model before multiplying them to produce the combined mixture process variables model. Strategies for formulations development by Snee and Hoerl (2016) provided reasonable models that significantly reduced the number of terms required by considering hybrid models with non-linear parameters.

In this work, we used the same combining idea proposed in Kowalski et al. (2000). In this combining approach, only the primary interaction between each process variable and each mixture component is considered. Therefore, we obtained a parsimonious model that is often adequate to fit data from mixture process variables experiments, as will be seen in Chapter 3 (the model) and Chapter 4 (the results).

2.3 Finding Optimal Proportions of Mixture Components

Finding the optimal proportions of mixture components in order to optimize (maximize or minimize) the experimental response is of great practical significance in many industries. However, the choice of approach for finding the optimal components' proportions of a mixture depends on the given resources and the particular implementation. So, there is no specified method to do it. The classical optimization technique to find the optimal proportion of mixture components is the simplex method (Nelder & Mead, 1965) and is widely used in fields such as engineering and chemistry. The simplex method is operated by replacing the vertex with the highest value with another vertex point of a general simplex, searching for the minimum function value. Another approach is a computational procedure called Monte Carlo simulation (see Fishman (1996) for a review). Monte Carlo Simulation starts with generating a large number of random samples from the probability distribution of each mixture component for the purpose of optimizing the mixture components' proportions. Then, the sample with the highest calculated response determines the optimal proportions of the mixture components.

Moreover, Bayesian methods have been used to optimize the formation of the oil mixture in the oil industry (Gelfand & Ghosh, 1998). These methods build on a prior distribution over the model parameters and then use data obtained from the mixture experiments to update this distribution. Pal and Mandal (2006) and Pal and Mandal (2008) considered finding optimal designs for estimating the optimal proportion of mixture components. Thus, Pal and Mandal (2006) suggested a pseudo-Bayesian approach, which does not assume any specific form of the prior distribution, to estimate the optimum mixture combination, and they have assumed the response function can be approximated by a quadratic concave function in the mixture components over the simplex region. They minimized the expected trace of the mean square error of the estimated optimum mixture combination to get the optimum design. However, the resulting optimum design is a non-linear function of the unknown parameters in the response function. Pal and Mandal (2008) solve this problem by utilizing the minimax criterion in estimating the optimal proportion of the mixture components, in the case of only two and three components when mixing ingredients subject to restrictions. Furthermore, Sinha et al. (2014) discussed determining optimal designs to address the problem of determining the optimum proportions of mixture components when one of the proportions is bounded above. Response Surface Methodology by Khuri and Cornell (2018) builds on analyzing the relationship between the response variable and the independent variables to optimize the proportions of mixture components. This optimization technique can maximize or minimize the response by fitting a mathematical model to the response surface data, which is used to predict

the optimal proportions of the mixture variables. This method is widely used, especially in food science and chemistry.

The desired properties of a mixture are yielded by determining the optimal combination of the proportions of a mixture. The common approaches that have been used to find the optimal proportions of mixture components often use Scheffé's quadratic model besides various optimization criteria to optimize the interesting properties of a mixture. This present work uses an optimization approach based on a simulation study to find the Maximum response in constrained mixture experiments and mixture experiments that include process variables. The Simulation setup will be explained in detail in Chapter 5. This approach uses five models from the literature to simulate data from mixture experiments, and their performances are evaluated through three selected criteria that measure our interests.

2.4 Optimal Design of Mixture Experiments

The scientific community and the relevant research world that relies on real experiments to produce reliable results need optimal experimental designs. Therefore, recently optimal designs have been used to maximize the chances of success in an experiment to reach the desired results with less resource consumption. The comparison of designs using the values of non-centrality parameters was initiated by Wald (1943) in linear normal regression. Chernoff (1953) was interested in optimal designs, whether in the case of the traditional fixed-sample size or sequential settings. He estimated parameters using the novel concept of locally optimal designs and gave several novel and practical solutions for the sequential design of experiments. Next, research on finding the optimal designs for the experiments appeared consecutively. Kiefer (1959, 1961) explored D-optimal designs for various problems in the setting of simplex designs of the models proposed in Scheffé (1958) and found the $\{q, 2\}$ simplex lattice design; see also Section 2.5. Box and Lucas (1959) found locally D-optimum designs for nonlinear models arising in chemical kinetics. Thus, they select the design points by maximizing the determinant of Fisher information or by minimizing the asymptotic formula for the generalized variance of the maximum likelihood of the parameter estimates. Following that, several works that had previously been done on experiments for nonlinear functions were reviewed by Cochran (1973). Also, he stated that before finding the design points to estimate model parameters, we should know the values of the parameters previously, which is the weakness of locally optimal designs.

John and Draper (1975) provided a review of general findings on optimal design theory and de-

sign criteria in the case of nonlinear models as well as the construction of D-optimal designs by algorithms. Some significant findings on the theory of design and design criteria were reviewed by Draper and St.John (1977) in the case of nonlinear models. The development of designs for nonlinear models is summarized by Atkinson (1982). Also, he highlighted developments in experimental designs based on previous research. Ford et al. (1989) described some design methods and their application, such as a sequential and static design with models in nonlinear parameters. Besides, in their articles, they show that a reliable design of a nonlinear model can be obtained if we have prior information about the parameters and by using the sequential design technique. In the nineties, Atkinson and Donev (1992) presented statistical approaches to the design of experiments and provided primary results on the theory of optimal design with a discussion of some design aspects and pointed out the difficulty of estimating good design structure in constrained regions.

Subsequently, constructing and optimizing designs with several constraints on experiments was a popular topic discussed in many publications, such as Pukelsheim (1993) and Cook and Fedorov (1995). Moreover, to search for design points that help us to estimate the parameters correctly in non-linear models, Chaudhuri and Mykland (1993) continued to search for models with non-linear parameters with the aim of searching for design points that help us estimate the parameters correctly. They build asymptotically D-optimal designs using their approach to select design points sequentially. Also, optimizing various product formulations through D-optimal designs is presented by Jones (2011) through case studies. Furthermore, Fedorov (2013) presents the essential properties of continuous optimal design for various optimality criteria. He uses statistical methods to make a sequential experimental design by supposing an initial experimental design and the values of the variables in the design can be chosen in the planning stages, taking into account one or more measurements in each sequential step to find the correct model and design.

In general, the literature on experiment design has evolved significantly over time, while there are only a few contributions that look at mixture experiments. Moreover, Cornell (1990) and Cornell (2011) made significant contributions to compiling and describing previous work on mixture experiment designs comprehensively. Brown (2014) represented a new method of building optimal designs for mixture experiments using general blending models. These designs are robust against model uncertainty and possess good properties with respect to the D-optimality criterion. Furthermore, Atkinson (2014) solved problems by optimal experimental design methods and provides an overview of D-optimal designs in mixture experiments over irregular design regions for several nonlinear models, such as the exponential and Weibull models.

Moreover, Anderson and Whitcomb (2016) provides a simplified way of response surface methods which is an advanced tool for optimizing experimental design. Optimal designs for mixture experiments, including D-optimal designs have been discussed in this book. Montgomery (2017) provides a comprehensive overview of the design and analysis of the experiments and also includes discussions of D-optimal designs for mixture experiments and mixture process variables experiments. Coetzer and Haines (2017) presented a new approach for creating D- and I-optimal designs for constrained mixture experiments using Scheffé's models as the most common models used in designs' generating. Khashab (2018) found the continuous optimal designs with respect to the D-optimality criterion of modified fractional polynomial models for constrained mixture experiments. In the present work, we encounter experimental regions with limitations and find D-optimal designs using the proposed CMFP models in the case of mixture experiments and mixture-process variables experiments, as will be seen in Chapter 6.

2.5 Mixture Designs Settings

In this section, we will briefly describe and explain the shape of experimental regions in mixture experiments. We will also introduce the most commonly used designs in this area. The constraints on the proportions of components define the region shape of mixture designs. So, when the components are subject to the natural restrictions that are given in 1.1 and 1.2, there are mixture designs known as Simplex-Lattice designs and Simplex-Centroid designs, which are particularly important designs and are often used as standard designs as they allow efficient estimation of Scheffé's models. These designs can be described as follows.

2.5.1 Simplex-Lattice Design

This design was introduced by Scheffé (1958), Which allows the experimenter to search the response surface throughout the whole design simplex. A $\{q, m\}$ simplex-lattice design for an m -degree polynomial model is to fit the response surface of blends consisting of q mixture components with proportions $x_r = 0, \frac{1}{m}, \frac{2}{m}, \dots, 1$ for $r = 1, 2, \dots, q$. All possible proportions combinations of a mixture are used from the above formula. The number of points for $\{q, m\}$ Simplex-Lattice design is $\binom{q+m-1}{m}$ according to Scheffé (1958). To illustrate, a $\{3, 2\}$ Simplex-Lattice design will contains $\binom{3+2-1}{2} = 6$ points, and the values of x_r are $0, \frac{1}{2}, 1$, for $r = 1, 2, 3$. The design points are $(1, 0, 0), (0, 1, 0), (0, 0, 1), (\frac{1}{2}, \frac{1}{2}, 0), (0, \frac{1}{2}, \frac{1}{2}), (\frac{1}{2}, 0, \frac{1}{2})$. Figure 2.1 shows the simplex-shaped design region for the $\{3, 2\}$ simplex-lattice design.

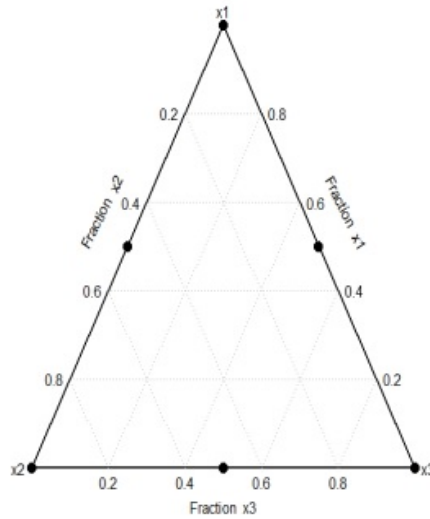


Figure 2.1: Simplex-lattice design for three components

We note that in the case of no additional constraints, the design region is an equilateral triangle, or 2-dimensional simplex, which is formed by incorporating the natural constraints. The vertices correspond to so-called pure mixtures, which consist of only one ingredient. The edges correspond to mixtures of two ingredients, and the interior points correspond to mixtures of all 3 ingredients.

2.5.2 Simplex-Centroid Design

Scheffé (1963) proposed this mixture design in which all design points are equally weighted mixtures of 1 to q components. It consists of $\binom{q}{1}$ permutations of pure blends: $(1, 0, \dots, 0)$, $\binom{q}{2}$ permutations of binary blends: $(\frac{1}{2}, \frac{1}{2}, 0, \dots, 0)$, $\binom{q}{3}$ permutations of tertiary blends: $(\frac{1}{3}, \frac{1}{3}, \frac{1}{3}, 0, \dots, 0)$, and so on to the overall centroid $(\frac{1}{q}, \frac{1}{q}, \dots, \frac{1}{q})$ with $\binom{q}{q}$ permutations. So, the number of points in a Simplex-centroid design is $2^q - 1$. To illustrate, in the case of $q = 3$, the design points are $(1, 0, 0)$, $(0, 1, 0)$, $(0, 0, 1)$, $(\frac{1}{2}, \frac{1}{2}, 0)$, $(\frac{1}{2}, 0, \frac{1}{2})$, $(0, \frac{1}{2}, \frac{1}{2})$, and one centroid point $(\frac{1}{3}, \frac{1}{3}, \frac{1}{3})$. Thus, the total points in the design are $2^3 - 1 = 7$ points. Figure 2.2 shows the Simplex-Centroid design in the case of three mixture components.

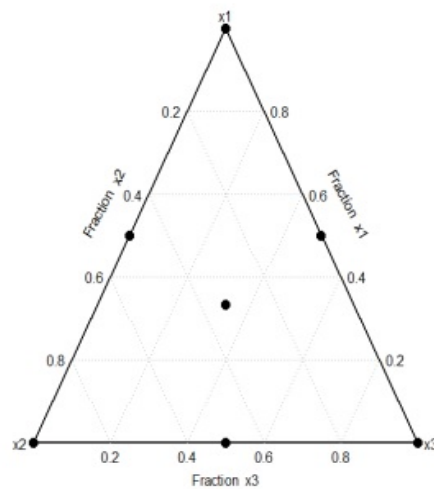


Figure 2.2: Simplex-Centroid design for three components

We note that:

- For irregularly shaped design regions with additional constraints, these constructions may no longer be meaningful or feasible, in particular, if the constrained design region is not a triangle.
- Both simplex-lattice and simplex-centroid designs have been shown to be efficient for estimating Scheffé's models. However, it is not clear if they can usefully be employed to estimate more recent models for mixture experiments.

Therefore, there is a gap in the literature, which we will address in Chapter 6.

Chapter 3

Models for MPV Experiments

The objective of performing experiments involving mixtures is to discover the relationship between the measured response and the proportions of the mixture components. While modeling data from mixture experiments, the natural constraints (1.1) and (1.2) must be taken into account in the modeling process. Pioneering work on modeling the data from experiments involving mixtures was published by Scheffé (1958) and Scheffé (1963), who introduced the so-called canonical polynomial models. The canonical polynomial models became the recourse for most practitioners since, although alternative models appeared. These models are specifically developed to handle the natural constraints of mixture data. Let us briefly illustrate modifying standard polynomial models to incorporate the natural constraints. For example, to get Scheffé's first-degree polynomial model, β_0 in an ordinary first-degree polynomial, $\beta_0 + \sum_{r=1}^q \beta_r x_r$, is replaced with $\beta_0 \times \sum_{r=1}^q x_r$ using that $\sum_{r=1}^q x_r = 1$. Hence,

$$\begin{aligned} E[y] &= \beta_0 + \sum_{r=1}^q \beta_r x_r \\ &= \beta_0 \times 1 + \sum_{r=1}^q \beta_r x_r \\ &= \beta_0 \times \left(\sum_{r=1}^q x_r \right) + \sum_{r=1}^q \beta_r x_r \quad \text{as} \quad \sum_{r=1}^q x_r = 1 \\ &= \sum_{r=1}^q (\beta_0 + \beta_r) x_r \\ &= \sum_{r=1}^q \beta_r^* x_r \end{aligned}$$

where $\beta_r^* = \beta_0 + \beta_r$, for all $r = 1, 2, \dots, q$.

The literature review of mixture experiments shows that canonical polynomial models are still widely used in experiments with mixtures. In this chapter, first, we present the most common models used in mixture experiments, such as the canonical polynomial models, in addition to more recent models. Next, we motivate and propose a new class of nonlinear models known as CMFP models. Then we introduce models that are often used to describe the effects of two or more process variables. In the final section of this chapter, we describe methods that can be used to incorporate process variables into mixture models.

3.1 Models for Mixture Experiments

Scheffé (1958) and Scheffé (1963) suggested canonical polynomial models traditionally used in mixture experiments. Scheffé's first-order polynomial model is the linear model for a q -component mixture that has the following form:

$$E(y) = \sum_{r=1}^q \beta_r x_r \quad (3.1)$$

Here, $E(y)$ means the expectation of the response y , and it is usually assumed that the responses are independent with mean $E(y)$ and constant variance. Scheffé's quadratic polynomial model is the quadratic model for a q -component mixture and has the following form:

$$E(y) = \sum_{r=1}^q \beta_r x_r + \sum_{r=1}^{q-1} \sum_{j=r+1}^q \beta_{rj} x_r x_j \quad (3.2)$$

The full cubic model is as follows:

$$\begin{aligned} E(y) = & \sum_{r=1}^q \beta_r x_r + \sum_{r=1}^{q-1} \sum_{j=r+1}^q \beta_{rj} x_r x_j + \sum_{r=1}^{q-1} \sum_{j=r+1}^q \delta_{rj} x_r x_j (x_r - x_j) \\ & + \sum_{r=1}^{q-2} \sum_{j=r+1}^{q-1} \sum_{k=j+1}^q \beta_{rjk} x_r x_j x_k \end{aligned} \quad (3.3)$$

An alternative to the full cubic model with fewer parameters is the special cubic polynomial model, which results from excluding the terms $\sum_{r=1}^{q-1} \sum_{j=r+1}^q \delta_{rj} x_r x_j (x_r - x_j)$ from the full cubic model. The full cubic and special-cubic models are popular alternatives to the quadratic models. The special cubic polynomial model is as follows:

$$E(y) = \sum_{r=1}^q \beta_r x_r + \sum_{r=1}^{q-1} \sum_{j=r+1}^q \beta_{rj} x_r x_j + \sum_{r=1}^{q-2} \sum_{j=r+1}^{q-1} \sum_{k=j+1}^q \beta_{rjk} x_r x_j x_k \quad (3.4)$$

However, increasing the degree of a polynomial does not sufficiently increase its flexibility. To continue the mixture models list that we are going through, we should mention the fractional polynomial models proposed by Royston and Altman (1994). This is because these fractional polynomial models have been modified by Khashab (2018) to fit data from mixture experiments. The modified fractional polynomial models are an important class of models that we consider in our study. Perhaps even more importantly, the new class of models we propose in this work is also based on fractional polynomials. The first-degree fractional polynomial (FP1) and the second-degree fractional polynomial (FP2) are written as

$$E(y) = \beta_0 + \sum_{r=1}^q \beta_r x_r^{(\alpha_r)}, \quad (3.5)$$

and

$$E(y) = \beta_0 + \sum_{r=1}^q \beta_r x_r^{(\alpha_r)} + \sum_{r=1}^q \beta_{rr} x_r^{2(\alpha_r)} + \sum_{r=1}^{q-1} \sum_{s=r+1}^q \beta_{rs} x_r^{(\alpha_r)} x_s^{(\alpha_s)}, \quad (3.6)$$

where $x_r^{(\alpha_r)} = x_r^{\alpha_r}$ when $\alpha_r \neq 0$ and $\log(x_r)$ otherwise.

These models have been shown to fit well in many non-mixture applications and often gave a more reasonable interpretation than polynomial models (Gilmour & Trinca, 2005). Although these parameters can take any real values, Royston and Altman (1994) limit the values of powers α to a set of integer and non-integer values such as $\{-3, -2, -1, -\frac{1}{2}, -\frac{1}{3}, 0, \frac{1}{3}, \frac{1}{2}, 1, 2, 3\}$ to avoid having vast powers in these models, whether positive or negative, and to obtain a meaningful understanding of them. However, fitting the models FP1 and FP2 described in (3.5) and (3.6) to mixture experiments is not straightforward due to the natural restrictions that should be satisfied in the proportions of components.

Subsequently, the fractional polynomial models have been modified by Khashab (2018) to satisfy the natural constraints on mixture components' proportions to fit the data from mixture experiments. This class of modified fractional polynomial nonlinear models (MFP) exploits similarities of this type of data with compositional data (Atchison & Shen, 1980). The MFP1 and MFP2 models, respectively, are as follows:

$$E(y) = \beta_0 + \sum_{r=1}^{q-1} \beta_r \left(\frac{x_r}{x_q} \right)^{(\alpha_r)}, \quad (3.7)$$

and

$$E(y) = \beta_0 + \sum_{r=1}^{q-1} \beta_r \left(\frac{x_r}{x_q} \right)^{(\alpha_r)} + \sum_{r=1}^{q-1} \beta_{rr} \left(\frac{x_r}{x_q} \right)^{2(\alpha_r)} + \sum_{r=1}^{q-2} \sum_{s=r+1}^{q-1} \beta_{rs} \left(\frac{x_r}{x_q} \right)^{(\alpha_r)} \left(\frac{x_s}{x_q} \right)^{(\alpha_s)}, \quad (3.8)$$

where

$$x^{(\alpha)} = \begin{cases} x^\alpha & \text{if } \alpha \neq 0 \\ \log(x) & \text{if } \alpha = 0 \end{cases}$$

The choice of denominators in the MFP models is a significant issue. Thus, the best fitting model is chosen by their residual standard error (RSE), trying to compare every possible denominator of x_r , for $r = 1, \dots, q$, in turn. Khashab (2018) showed that the MFP models fit several real data sets well when the data come from constrained mixture experiments (i.e., where all proportions x_r are bounded away from 0). Nevertheless, these models are quite restrictive if some proportions may be zero.

Therefore, we propose a different transformation of fractional polynomials, which is less restrictive. We call the new proposed class of nonlinear models the complement mixture fractional polynomial (CMFP) models. In these models, for any proportion of the mixture component selected in the numerator, the numerator's complement is in the denominator. This makes it impossible for the denominator to be zero unless the numerator is 1, which is unrealistic in most applications as this would correspond to a mixture that consists of only one component. In addition, these new models may avoid a high correlation between parameter estimates due to the repetition of the same mixture component proportion in the denominator of all model terms. These CMFP models can be considered competitors to many recent and common models from the literature. The first and second-order CMFP models, respectively, are as follows:

$$E(y) = \beta_0 + \sum_{r=1}^{q-1} \beta_r \left(\frac{x_r}{1-x_r} \right)^{(\alpha_r)}, \quad (3.9)$$

and

$$E(y) = \beta_0 + \sum_{r=1}^{q-1} \beta_r \left(\frac{x_r}{1-x_r} \right)^{(\alpha_r)} + \sum_{r=1}^{q-1} \beta_{rr} \left(\frac{x_r}{1-x_r} \right)^{2(\alpha_r)} + \sum_{r=1}^{q-2} \sum_{s=r+1}^{q-1} \beta_{rs} \left(\frac{x_r}{1-x_r} \right)^{(\alpha_r)} \left(\frac{x_s}{1-x_s} \right)^{(\alpha_s)}, \quad (3.10)$$

where $x^{(\alpha)}$ is defined as above.

As mentioned earlier, these models have the advantage that not all x_r have to be bounded away from 0 to appear in the denominator. However, for all x_r that may be 0, we still have to restrict

the corresponding exponent α_r to be positive. We also need to select which $q - 1$ proportions explicitly appear in the model. Choosing this combination is based on what best fits the data under consideration according to residual standard error (RSE).

To estimate the nonlinear parameters in the new models, we used nonlinear least squares (nls). The function `nls` in R uses the values that minimize the residual sum of squares to estimate the parameters. The main procedure for nonlinear least squares is to use a partial linear algorithm such as the Golub-Pereyra algorithm proposed by Golub and Pereyra (1973). The algorithm seeks to minimize the residual sum of squares as follows. If the residual sum of squares at parameter J is smaller than the residual sum of squares at parameter $J - 1$, the counter J is increased by 1, and this step is repeated. Otherwise, parameter $J - 1$ is taken as an estimator for the parameters if no such improvement is possible.

3.2 Models for Process Variables

Some common models are often used to describe process variables, such as a two-factor interaction model (Cornell, 2011). This model is as follows:

$$E(y) = \gamma_0 + \gamma_1 z_1 + \gamma_2 z_2 + \gamma_{12} z_1 z_2 \quad (3.11)$$

This form can extend to p process variables z_1, z_2, \dots, z_p , and may also contain quadratic terms.

$$E(y) = \gamma_0 + \sum_{l=1}^p \gamma_l z_l + \sum_{l=1}^{p-1} \sum_{m=l+1}^p \gamma_{lm} z_l z_m \quad (3.12)$$

3.3 Mixture Model Including Process Variables

When the experimentation process is influenced by mixture components and process variables, we need a model that can describe both the effect of mixture components and process variables and their relationship to the response. Therefore, we need to combine a mixture model and a process variables model to obtain a mixture process variables model (MPV model). There are various ways to combine a mixture model and a process variable model to consider the effects of both types of variables simultaneously. It is not uncommon to suggest adding a process variable model to a mixture model, supposing that the blending properties of the mixture components are not affected by the levels of the process variables. For example, Prescott (2004) considered that the additive model is the simplest way to combine models of mixture and process variables. Then the additive MPV model is (Mixture model)+(Process variable model). However, the additive mixture process

variables model is often unrealistic even though it is easy to produce.

More realistic composite models are needed to describe data from experiments with mixture process variables. Cornell (2011) relied on another way to produce a mixture process variables model: multiplying a mixture model by a process variable model. The interaction MPV model is (Mixture model) * (Process variable model). The interaction models suppose that the levels of the process variables affect the blending properties of the mixture and are, therefore, more realistic. However, the number of terms in such models is much higher than in the additive MPV models. Still, the combined models that fit data from mixture process variables experiments are traditionally created by multiplying a mixture model and a standard linear model of process variables. Model (3.13) is generated by multiplying model (3.2), which is Scheffé's quadratic model, with model (3.12), which is the process variables model. However, in such combined models, the number of coefficients increases rapidly with the number of components in the mixture and levels of the process variables.

$$\begin{aligned}
 E(y) = & \sum_{r=1}^q \beta_r^{(0)} x_r + \sum_{r=1}^{q-1} \sum_{s=r+1}^q \beta_{rs}^{(0)} x_r x_s + \sum_{r=1}^q \sum_{l=1}^p \beta_{rl}^{(1)} x_r z_l + \sum_{r=1}^{q-1} \sum_{s=r+1}^q \sum_{l=1}^p \beta_{rsl}^{(1)} x_r x_s z_l \\
 & + \sum_{r=1}^q \sum_{l=1}^{p-1} \sum_{m=l+1}^p \beta_{rlm}^{(2)} x_r z_l z_m + \sum_{r=1}^{q-1} \sum_{s=r+1}^q \sum_{l=1}^{p-1} \sum_{m=l+1}^p \beta_{rslm}^{(2)} x_r x_s z_l z_m
 \end{aligned} \tag{3.13}$$

Thus, more parsimonious models for mixture process variable experiments are in demand. Therefore, Kowalski et al. (2000) introduced a quadratic MPV model, which assumed that there is no linear effect of the process variables on the nonlinear mixture component blending. This model is more parsimonious and frequently adequate for mixture process variables experiments. Some compromise was made between the interaction and additive models to create model (3.14). Therefore, this model combines the general second-order polynomial in q mixture components with a second-order model of p process variables.

$$E(y) = \sum_{r=1}^q \beta_r^{(0)} x_r + \sum_{r=1}^{q-1} \sum_{s=r+1}^q \beta_{rs}^{(0)} x_r x_s + \sum_{l=1}^p \left[\sum_{r=1}^q \beta_{rl}^{(1)} x_r \right] z_l + \sum_{l=1}^{p-1} \sum_{m=l+1}^p \gamma_{lm} z_l z_m + \sum_{l=1}^p \gamma_{ll} z_l^2 \tag{3.14}$$

The MFP models (3.7) and (3.8) are recent and strong competitors to the established mixture models from the literature. Therefore, we expanded one of them in two ways to fit the data from the mixture process variables experiments. The first way we used the traditional method that was used in model (3.13). It is obtained by multiplying model (3.8) by model (3.12). Thus, the extended form of the first MFP model is as follows:

$$\begin{aligned}
E(y) = & \beta_0 + \sum_{r=1}^{q-1} \beta_r^{(0)} \left(\frac{x_r}{x_q} \right)^{(\alpha_r)} + \sum_{r=1}^{q-1} \beta_{rr}^{(0)} \left(\frac{x_r}{x_q} \right)^{2(\alpha_r)} + \sum_{r=1}^{q-2} \sum_{s=r+1}^{q-1} \beta_{rs}^{(0)} \left(\frac{x_r}{x_q} \right)^{(\alpha_r)} \left(\frac{x_s}{x_q} \right)^{(\alpha_s)} \\
& + \sum_{r=1}^{q-1} \sum_{l=1}^p \beta_{rl}^{(1)} \left(\frac{x_r}{x_q} \right)^{(\alpha_r)} z_l + \sum_{r=1}^{q-1} \sum_{l=1}^p \beta_{rrl}^{(1)} \left(\frac{x_r}{x_q} \right)^{2(\alpha_r)} z_l + \sum_{r=1}^{q-2} \sum_{s=r+1}^{q-1} \sum_{l=1}^p \beta_{rsl}^{(1)} \left(\frac{x_r}{x_q} \right)^{(\alpha_r)} \left(\frac{x_s}{x_q} \right)^{(\alpha_s)} z_l \\
& + \sum_{r=1}^{q-1} \sum_{l=1}^{p-1} \sum_{m=l+1}^p \beta_{rlm}^{(2)} \left(\frac{x_r}{x_q} \right)^{(\alpha_r)} z_l z_m + \sum_{r=1}^{q-1} \sum_{l=1}^{p-1} \sum_{m=l+1}^p \beta_{rrlm}^{(2)} \left(\frac{x_r}{x_q} \right)^{2(\alpha_r)} z_l z_m + \sum_{r=1}^{q-2} \sum_{s=r+1}^{q-1} \sum_{l=1}^{p-1} \\
& \sum_{m=l+1}^p \beta_{rslm}^{(2)} \left(\frac{x_r}{x_q} \right)^{(\alpha_r)} \left(\frac{x_s}{x_q} \right)^{(\alpha_s)} z_l z_m
\end{aligned} \tag{3.15}$$

The second way to extend the MFP model is the method used in model (3.14). Therefore, we added the interaction effect of each mixture component with each level of the process variables plus the pure quadratic term of each process variable to model (3.8).

$$\begin{aligned}
E(y) = & \beta_0 + \sum_{r=1}^{q-1} \beta_r \left(\frac{x_r}{x_q} \right)^{(\alpha_r)} + \sum_{r=1}^{q-1} \beta_{rr} \left(\frac{x_r}{x_q} \right)^{2(\alpha_r)} + \sum_{r=1}^{q-2} \sum_{s=r+1}^{q-1} \beta_{rs} \left(\frac{x_r}{x_q} \right)^{(\alpha_r)} \left(\frac{x_s}{x_q} \right)^{(\alpha_s)} \\
& + \sum_{r=1}^{q-1} \sum_{l=1}^p \beta_{rl}^{(1)} \left(\frac{x_r}{x_q} \right)^{(\alpha_r)} z_l + \sum_{l=1}^p \gamma_l z_l^2
\end{aligned} \tag{3.16}$$

Likewise, the same two ways that are used to expand the MFP models to fit data from mixture process variable experiments are applied to the CMFP models. The extended forms of (3.10) model that incorporate process variables are as follows:

$$\begin{aligned}
E(y) = & \beta_0 + \sum_{r=1}^{q-1} \beta_r^{(0)} \left(\frac{x_r}{1-x_r} \right)^{(\alpha_r)} + \sum_{r=1}^{q-1} \beta_{rr}^{(0)} \left(\frac{x_r}{1-x_r} \right)^{2(\alpha_r)} + \sum_{r=1}^{q-2} \sum_{s=r+1}^{q-1} \beta_{rs}^{(0)} \left(\frac{x_r}{1-x_r} \right)^{(\alpha_r)} \\
& \left(\frac{x_s}{1-x_s} \right)^{(\alpha_s)} + \sum_{r=1}^{q-1} \sum_{l=1}^p \beta_{rl}^{(1)} \left(\frac{x_r}{1-x_r} \right)^{(\alpha_r)} z_l + \sum_{r=1}^{q-1} \sum_{l=1}^p \beta_{rrl}^{(1)} \left(\frac{x_r}{1-x_r} \right)^{2(\alpha_r)} z_l + \sum_{r=1}^{q-2} \sum_{s=r+1}^{q-1} \\
& \sum_{l=1}^p \beta_{rsl}^{(1)} \left(\frac{x_r}{1-x_r} \right)^{(\alpha_r)} \left(\frac{x_s}{1-x_s} \right)^{(\alpha_s)} z_l + \sum_{r=1}^{q-1} \sum_{l=1}^{p-1} \sum_{m=l+1}^p \beta_{rlm}^{(2)} \left(\frac{x_r}{1-x_r} \right)^{(\alpha_r)} z_l z_m + \sum_{r=1}^{q-1} \\
& \sum_{l=1}^{p-1} \sum_{m=l+1}^p \beta_{rrlm}^{(2)} \left(\frac{x_r}{1-x_r} \right)^{2(\alpha_r)} z_l z_m + \sum_{r=1}^{q-2} \sum_{s=r+1}^{q-1} \sum_{l=1}^{p-1} \sum_{m=l+1}^p \beta_{rslm}^{(2)} \left(\frac{x_r}{1-x_r} \right)^{(\alpha_r)} \left(\frac{x_s}{1-x_s} \right)^{(\alpha_s)} z_l z_m
\end{aligned} \tag{3.17}$$

and

$$\begin{aligned}
E(y) = & \beta_0 + \sum_{r=1}^{q-1} \beta_r \left(\frac{x_r}{1-x_r} \right)^{(\alpha_r)} + \sum_{r=1}^{q-1} \beta_{rr} \left(\frac{x_r}{1-x_r} \right)^{2(\alpha_r)} + \sum_{r=1}^{q-2} \sum_{s=r+1}^{q-1} \beta_{rs} \left(\frac{x_r}{1-x_r} \right)^{(\alpha_r)} \left(\frac{x_s}{1-x_s} \right)^{(\alpha_s)} \\
& + \sum_{r=1}^{q-1} \sum_{l=1}^p \beta_{rl}^{(1)} \left(\frac{x_r}{1-x_r} \right)^{(\alpha_r)} z_l + \sum_{l=1}^p \gamma_l z_l^2
\end{aligned} \tag{3.18}$$

Model (3.18) includes CMFP model terms plus the interaction terms for each mixture component with each process variable and the pure quadratic term of each process variable. Model (3.17) and model (3.18) are flexible and comprehensive models because any term can be kept or deleted depending on the data under study. As will be seen in the next chapter, we will fit MPV models from model (3.13) to model (3.18) to several real empirical datasets to compare and evaluate their performance.

All competing models that fit data of mixture process variables experiments consist of the mixture model terms besides interaction terms between mixture components and process variables. The extended form of Scheffé's quadratic model (3.13) has terms of all possible interactions between mixture components and process variables. Model (3.14) consists of terms of Scheffé's quadratic model, which represent the mixture components, and has interaction terms of mixture components with each level of the individual process variables besides the terms that represent the process variables only. We use the same way to consider the interaction between mixture components and process variables in (3.13) and (3.14) models to extend MFP and CMFP models. Model (3.15) and model (3.17) have the second-order of MFP and CMFP models, respectively, and used the same traditional way that was used in model (3.13). Also, Model (3.16) and model (3.18) have the second-order of MFP and CMFP models, respectively, and used the same way that was used in model (3.14). For convenience, the models (3.13) to (3.18) are summarised in Table 3.1 below.

Table 3.1: Summary of models

Model name	Model type/combination
Model (3.13)	Scheffé's quadratic/Full interaction MPV (Traditional)
Model (3.14)	Scheffé's quadratic/Individual main interaction MPV (Kowalski)
Model (3.15)	2nd order MFP/Traditional
Model (3.16)	2nd order MFP/Kowalski
Model (3.17)	2nd order CMFP/Traditional
Model (3.18)	2nd order CMFP/Kowalski

Chapter 4

Estimation in MPV Experiments

As estimation is the main objective of this chapter, we use several statistical criteria to assess the quality of models to fit a dataset. In this chapter, we will first introduce criteria commonly used in model selection to compare CMFP models with other competing models from the literature. In particular, we will consider residual standard error, Akaike information criterion, and Bayesian information criterion. Then, we will look at the performance of the models under comparison when fitted to datasets from mixture process variables experiments in four examples. Moreover, the contour plots of response surfaces are used for further comparison between the competing MPV models.

4.1 Statistical Criteria for Model Comparison

We use the residual standard error (RSE) to assess the quality of an estimator to obtain an accurate estimate of the model parameters (see, e.g., Baty and Delignette-Muller (2004) and Khudri and Sadia (2013)). RSE is calculated from the data to measure the discrepancy between the fitted model predictions and the observed data, and it can be expressed as

$$\text{RSE} = \sqrt{\sum_{e=1}^n (y_e - \hat{y}_e)^2 / \text{df}}$$

where n is the sample size, y is the observed value, \hat{y} is the predicted value, and df is the degrees of freedom which is calculated by subtracting the total number of model parameters from the total number of observations. Thus, the model that provides the best fit to a dataset is the one with the smallest RSE. In addition, we use further statistical criteria such as the Akaike Information Criterion (AIC) and Bayesian Information Criterion (BIC) to make more significant comparisons

between competing models. The AIC and BIC are common model selection criteria that balance parsimony with a good fit; see, for example, Schwarz (1978) and Tong (2010). AIC is defined as

$$\text{AIC} = 2k - 2\ell$$

where k is the number of parameters in the model, and ℓ is the natural logarithm of the likelihood of the fitted model (the likelihood of a model is usually determined automatically by statistical software). BIC can be calculated with the following mathematical equation

$$\text{BIC} = k \log(n) - 2\ell$$

A minimum value of these criteria is desired and indicates the optimum model that best fits the experimental data because it means the model is closer to the truth while also not being unnecessarily complicated.

In addition to using these criteria for comparing the different models introduced in Chapter 3, we also used them to remove insignificant terms from the models. To illustrate the process of selecting the best-fit model for each dataset under study, we demonstrate this process using the CMFP model as an example. To select the best-fit CMFP models for a dataset, we fitted both models (3.17) and (3.18), which include all terms, to the dataset. Then, one of these two models is selected according to the statistical criteria that we are considering here. After that, each term in the selected model is removed individually, and the statistical criteria are checked. If the statistical criteria are improved by removing this term, then this term is deemed insignificant, and it is removed from the model. Otherwise, we return this term back to the model and try to check the removal of another term. This process continues until the model only contains the significant terms.

4.2 Example 1: Estimate a Mixture Experiment with a 2-Level Process Variable

The opacity of a printable coating material used for tags and identification labels was studied by Chau and Kelley (1993). In this formulation, there were three mixture components: two pigments, x_1 and x_2 , and a polymeric binder x_3 . The constraints on the component proportions were $0.13 \leq x_1 \leq 0.45$, $0.21 \leq x_2 \leq 0.67$, $0.20 \leq x_3 \leq 0.34$. The response of interest was the opacity of the coating influenced by the two levels (low = -1 and high = $+1$) of the thickness of the coating

(a process variable) besides the mixture of the three components. The opacity of printable coating material, with two levels of the thickness of the coating, was investigated, and the data of the experiment are given in Table 8.1. The original experiment was designed using the D-optimality criterion (which will be introduced in Chapter 6), and polynomial models were fitted to the data to approximate coating properties.

Model (3.18) showed the best results compared to the other models according to RSE, AIC, and BIC criteria. Moreover, in terms of the complexity of the models, the number of parameters is small in the models (3.18) and (3.16), which makes them simpler than the other models under comparison, which is an extra advantage. Model (3.13) has the largest number of parameters (12) as expected, followed by model (3.14) with ten parameters, while model (3.18) and model (3.16) have the same number of parameters (7 parameters), which is the fewest among the competing models. The results are as in Table 4.1:

Table 4.1: Summary Statistics for competing models

Models	RSE	AIC	BIC
Model (3.13)	0.0148	-93.11	-83.32
Model (3.14)	0.0143	-94.28	-85.38
Model (3.16)	0.0135	-96.73	-89.61
Model (3.18)	0.0129	-98.35	-91.22

According to criteria RSE, AIC, and BIC, model (3.18) best fits the experimental dataset of the first example among all other competing models. It has the following form after removing insignificant terms:

$$\hat{y} = 0.846 - 0.034 \left(\frac{x_1}{1-x_1} \right)^{(-0.52)} + 0.059 \left(\frac{x_2}{1-x_2} \right)^{(-0.35)} + 0.027 \left(\frac{x_1}{1-x_1} \right)^{(-0.52)} z + 0.037 \left(\frac{x_2}{1-x_2} \right)^{(-0.35)} z$$

The contour plots of the response surface are provided for the models that differ from CMFP models the most, as shown in Figure 4.1. The models (3.13), (3.14), and (3.18) are shown respectively at both coating thickness levels $z = -1$ and $z = 1$. By looking at the contour plots of the response surface of model (3.13), model (3.14), and model (3.18), the surface of each model clearly differs. At the lower level of the process variable, $z = -1$, the fitted surfaces seem to be generally lower than at the higher level, $z = 1$. However, we can clearly see the differences between the models, for example, when we consider the value of the estimated maximum response in the experimental region for each model. The same values of cuts are used for all models under comparison, whether the value of z is -1 or 1 .

The left side of Figure 4.1 represents the surface plots of the models when $z = 1$. In this status, both model (3.13) and model (3.18) can reach their maximum responses at 0.99 or above, while the maximum point that model (3.14) can reach is between 0.90 and 0.99. At the low level of the process variables, which the right side of Figure 4.1 shows, the contour plot of the surface shows more colors for model (3.13). In this case, model (3.13) can again reach a maximum of more than 0.99, as in the case of the high level of the process variable. However, the maximum response that model (3.14) reaches is between 0.80 and 0.85, which is less than its maximum in the high level of the process variable. Model (3.18) also has its maximum value (within the experimental region) between 0.8 and 0.85.

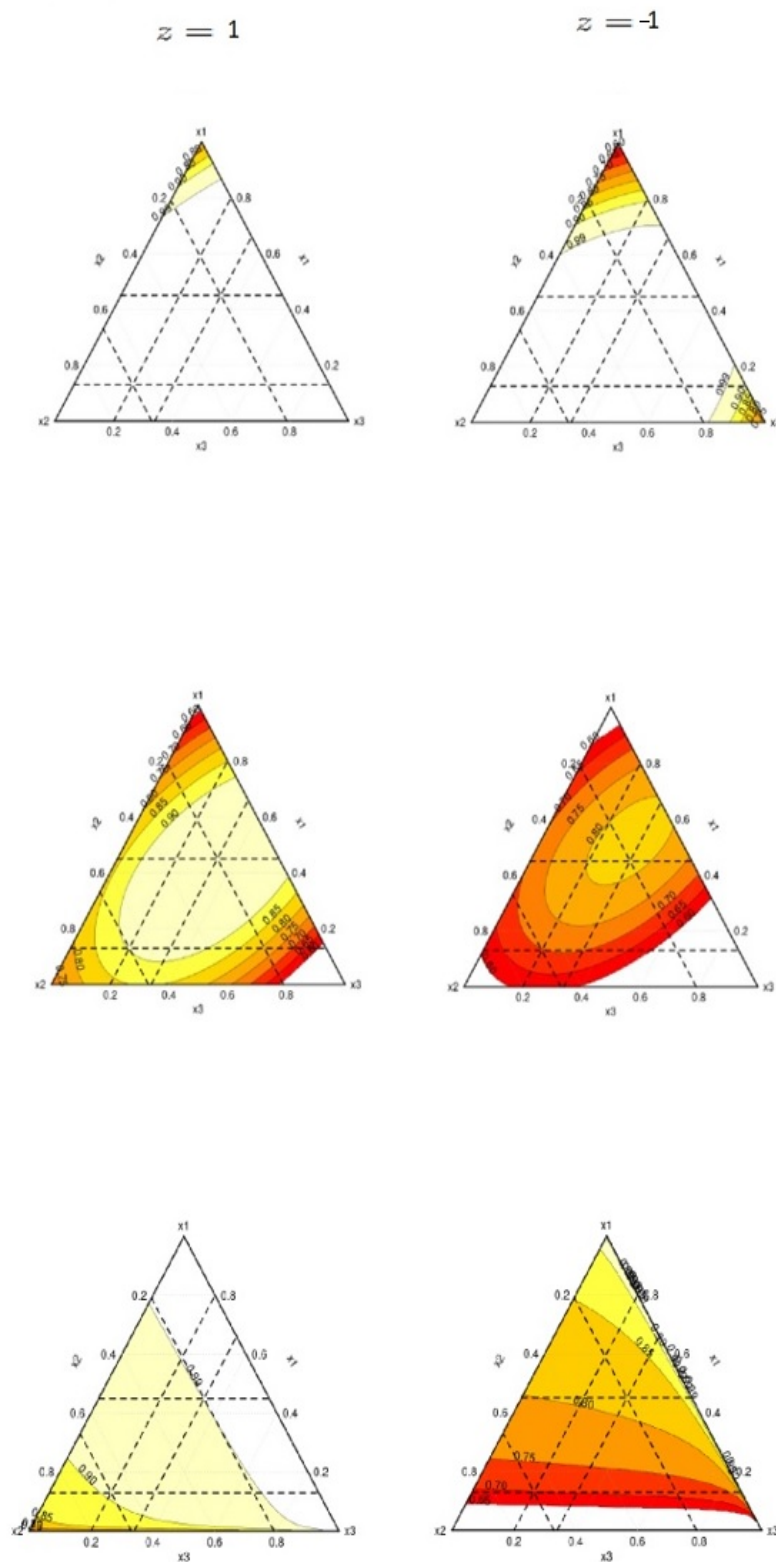


Figure 4.1: The contour plots of the response surface of models (3.13), (3.14), and (3.18), respectively, at both levels of the process variable

4.3 Example 2: Estimate a Mixture Experiment with a 3-Level Process Variable

A further mixture process variable experiment, this time with three levels of coating thickness, was conducted by Chau and Kelley (1993) as well. The response of interest was influenced by changing the selected level of coating thickness, where the levels of this process variable z are 10, 19, and 28, corresponding to 0, 1, and 2, respectively. The components of the mixture have the following constraints on their proportions: $0.13 \leq x_1 \leq 0.45$, $0.21 \leq x_2 \leq 0.67$, $0.20 \leq x_3 \leq 0.34$. The experimental data of the opacity of printable coating material with three coating thickness levels are given in Table 8.2. When the competing models of mixture process variables were applied to the second experimental dataset, model (3.18) was shown to be the best fit for this data among all other competing models according to the RSE, AIC, and BIC criteria. The results are given in Table 4.2.

Table 4.2: Summary Statistics for competing models

Models	RSE	AIC	BIC
Model (3.13)	0.0157	-116.66	-103.03
Model (3.14)	0.0134	-124.31	-111.82
Model (3.16)	0.0137	-124.05	-113.83
Model (3.18)	0.0130	-126.26	-116.04

Regarding the complexity of the models, model (3.13) has the largest number of parameters (12) followed by model (3.14) with ten parameters. While both models (3.16) and (3.18) have 8 parameters. However, the comparison criteria show that the model (3.18) is the best fit to this experimental data among all other competing models and has the following form:

$$\hat{y} = 0.874 - 0.061 \left(\frac{x_1}{1-x_1} \right)^{(-0.6)} - 0.005 \left(\frac{x_2}{1-x_2} \right)^{(-0.6)} + 0.007 \left(\frac{x_1}{1-x_1} \right)^{(-0.6)} \left(\frac{x_2}{1-x_2} \right)^{(-0.6)} \\ + 0.021 \left(\frac{x_1}{1-x_1} \right)^{(-0.6)} z + 0.017 \left(\frac{x_2}{1-x_2} \right)^{(-0.6)} z + 0.014(z)^2$$

The contour plots of the response surface of the models (3.13), (3.14), and (3.18) are shown in Figure 4.2 from top to bottom, respectively, at the three levels of the process variable. The surface contours of each model are distinctly different, even for the same level of the process variable. Model (3.13) generally seems to have higher fitted values, whereas model (3.14) and model (3.18) show similar values within the experimental region.

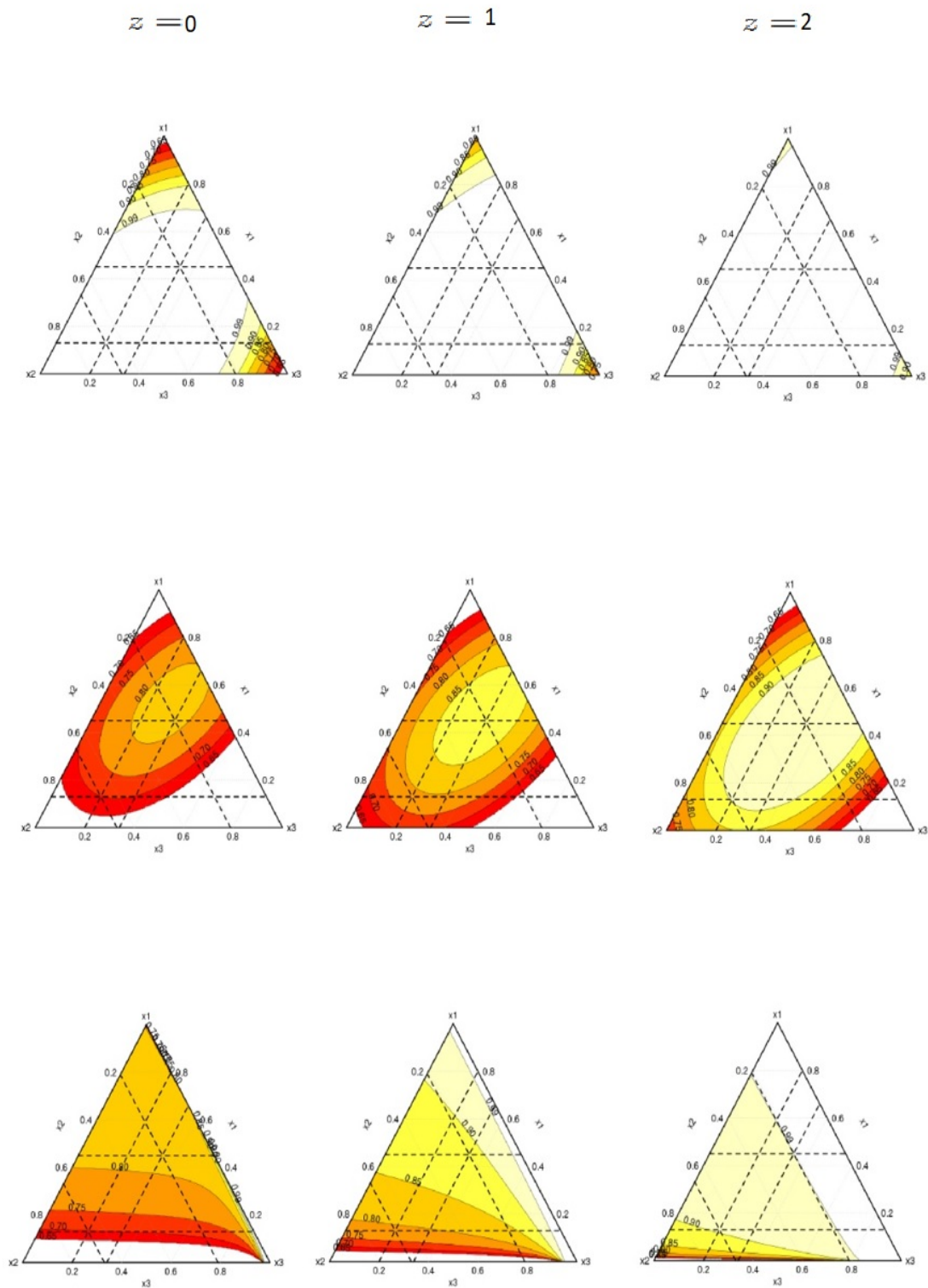


Figure 4.2: The contour plots of the response surface of models (3.13), (3.14), and (3.18), respectively, in all levels of z

4.4 Example 3: Estimate a Mixture Experiment with Two Process Variables

Steiner et al. (2007) described an experiment aiming to find a good mixture of water, soap, and glycerin for making a homemade bubble solution. Students conducted this experiment to find an optimal mixture of these three mixture components. Realistic constraints considered in their project were time and cost based on recipes in children's books, leading to the following constraints on the proportions: $0.04 \leq x_1 \leq 0.35$, $0.60 \leq x_2 \leq 0.98$, $0.03 \leq x_3 \leq 0.15$. To analyse the data, they extended the quadratic model (Cornell, 1990) by adding the process variables combinations, then reduced the quadratic model by removing insignificant terms. The original design of this experiment was constructed to be distance-based (not model dependent). That means the design points were spread uniformly over the feasible region (Johnson et al., 1990). The response of interest was the number of bubbles, and the attribute was the average number of bubbles across all conditions in the population. Soap type and water type were also included in the experiment. Each of these process variables has two levels, which were z_1 : brand of soap (Joy = -1, Ivory = +1) and z_2 : type of water (spring water = -1, tap water = +1). The dataset of the experiment is given in Table 8.3. Since we only fit one extended form of MFP and CMFP models to each dataset under study, we chose models (3.15) and (3.17), which fitted the data better than models (3.16) and models (3.18) in the case of two process variables. Model (3.17) showed the best results among all other models. The results are as in Table 4.3.

Table 4.3: Summary Statistics for competing models

Models	RSE	AIC	BIC
Model (3.13)	1.349	134.14	173.73
Model (3.14)	1.867	159.39	183.14
Model (3.15)	1.594	148.77	178.86
Model (3.17)	1.095	121.74	151.82

More process variables and mixture components will produce a higher number of model parameters. Model (3.13) has 24 parameters, the biggest number of parameters. Also, models (3.17) and (3.15) both have 16 parameters, while model (3.14) has 15 parameters, which is the smallest number of parameters. According to residual standard error in addition to the AIC and BIC criteria, model (3.17) is the best among all other competing models. In the case of the experiment affected by two process variables, we consider four statuses of levels combinations of the process variables, as shown in Figure 4.3. Model (3.13) has a distinct surface at each status of level combinations. Here, we are plotting only a subregion of the regular simplex to show the (relatively small) experimental region more clearly.

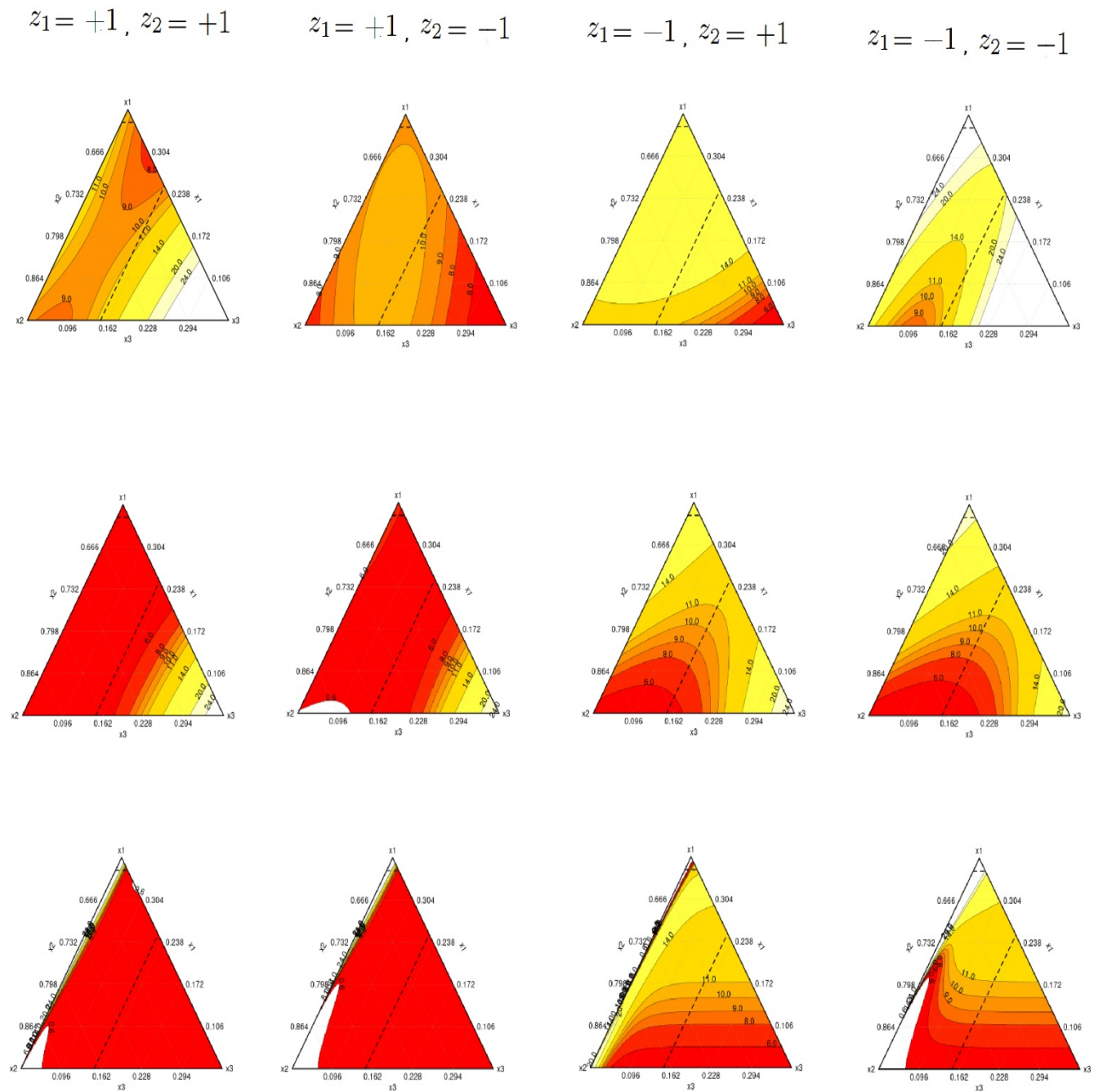


Figure 4.3: The contour plots of the response surface of models (3.13), (3.14), and (3.17), respectively, in all combinations of levels of the two process variables, z_1 and z_2

4.5 Example 4: Estimate a Mixture Experiment with a 3-Level Process Variable

Hare (1979) designed an experimental study using three mixture variables: water (x_1), oil (x_2), and emulsifier (x_3) to determine the effectiveness of the unsaturated fatty acid esters of corn oil. The following constraints were considered:

$$0.430 \leq x_1 \leq 0.645, 0.350 \leq x_2 \leq 0.550, 0.005 \leq x_3 \leq 0.020$$

The oil separation ratio of water a week after storage at room temperature was the response of interest in this experiment, which was also influenced by the agitation time in minutes as a three-level process variable ($z = 2, 3, \text{ and } 4$, corresponding to 0, 1, and 2, respectively). They performed a similar transformation to that of Thompson and Myers (1968) (mixture components transformed to pseudo-components) for quadratic Scheffé's model for the combined mixture-process variable exploration. To collect the data, a three-level factorial design was used in the process and mixture-related variables. The experimental dataset of this example is given in Table 8.4, and the results when the competing models of mixture process variables were applied to this experimental data set are given in Table 4.4:

Table 4.4: Summary Statistics for competing models

Models	RSE	AIC	BIC
Model (3.13)	1.258	99.16	116.00
Model (3.14)	1.057	89.13	103.38
Model (3.16)	1.097	89.51	99.88
Model (3.18)	0.969	82.86	93.22

In the case of this example that is affected by three mixture components besides a three-level process variable, model (3.13) has the biggest number of parameters, 12. There are 10 parameters in the model (3.14), while models (3.16) and (3.18) have the smallest number of parameters, i.e.7. According to the residual standard error in addition to AIC and BIC, model (3.18) is the best among all other competing models and has the following form:

$$\hat{y} = -23.21 - 13.55 \left(\frac{x_3}{1-x_3} \right)^{(-0.15)} - 0.00008 \left(\frac{x_2}{1-x_2} \right)^{(48.11)} z + 1.39 \left(\frac{x_3}{1-x_3} \right)^{(-0.15)} z - 0.93(z)^2$$

Figure 4.4 illustrates the surface plots of the response of model (3.13), model (3.14), and model (3.18) from top to bottom, respectively, at all levels of the process variable $z = 0, z = 1, \text{ and } z = 2$. However, the surface plot of the models in this example is challenging because the constrained region of this experiment is too small.

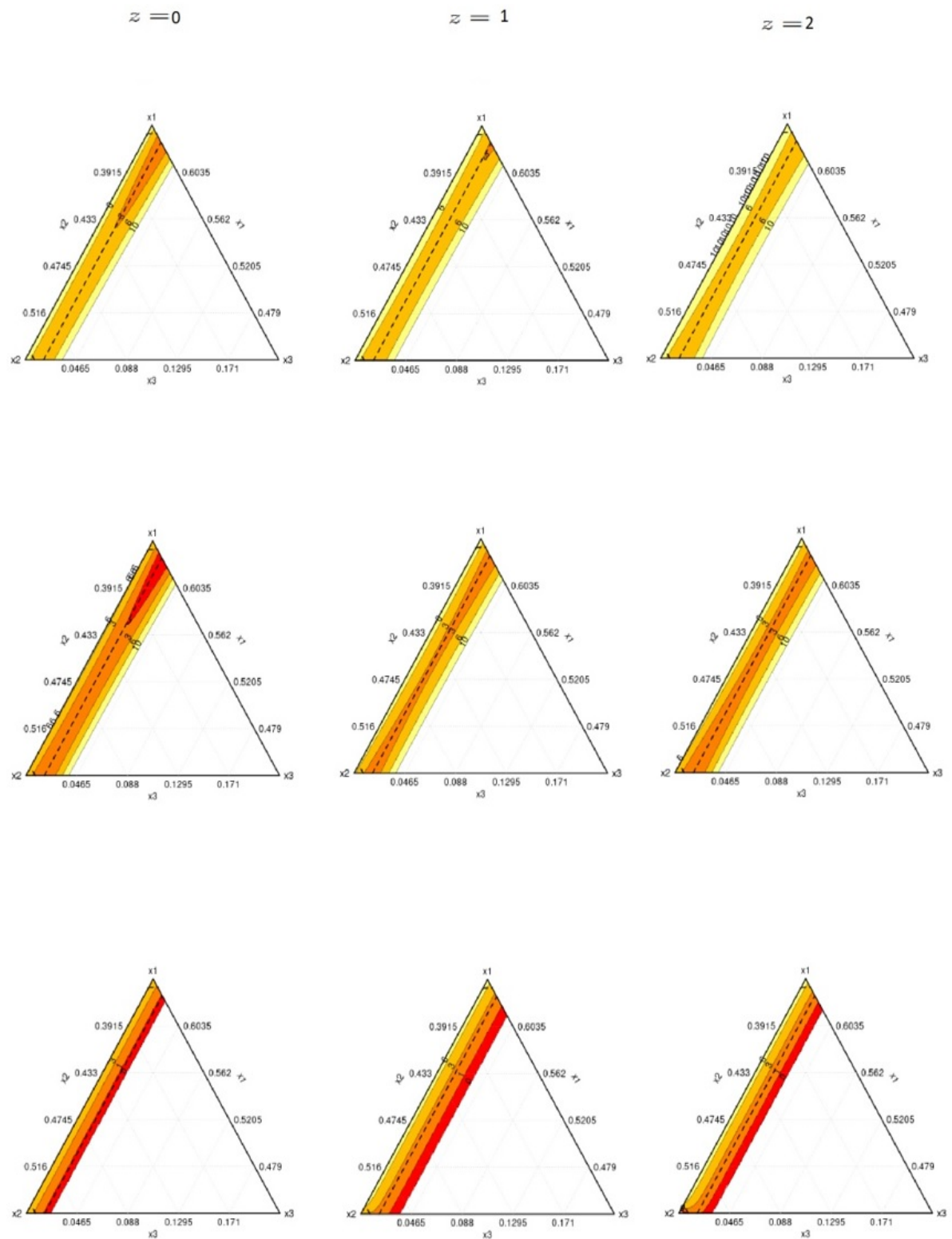


Figure 4.4: The contour plots of the response surface of models (3.13), (3.14), and (3.18), respectively, at all levels of the process variable

4.6 Summary

According to the statistical criteria RSE, AIC, and BIC, the extended forms of the CMFP models that incorporate process variables perform best in all 4 examples. Model (3.17) provides the best fit for the datasets when the experimental datasets are affected by two process variables in addition to the proportions of the mixture components, as shown in Example 4.4. Moreover, in cases of a three-level process variable experiment, as in Examples 4.3 and 4.5, model (3.18) fits the experimental dataset better than any of the other competing models. When looking at the surface plots, we noticed that these could look quite different, even for models that provide a similar overall fit. For example, the value and the positions of local and global maxima/minima in the fitted surfaces can be quite different. As we don't know where exactly the extrema are in these real datasets, we will use simulated data, which are based on real datasets to make them realistic, in the following chapter.

Chapter 5

Optimal Proportions of Mixture Components

A statistical model is a mathematical equation that describes the relationship between explanatory variables and one or more response variables. In mixture experiments, the explanatory variables are the proportions of the mixture components and potentially one or more process variables, and the response is a function of these explanatory variables. There are various purposes for defining mixture models. One of them is to estimate the optimal proportions of mixture components to optimize the measured response. In this chapter, we assess our proposed CMFP models with respect to finding the optimal proportions of mixture components. This is done through a simulation study that generates simulated data based on four real datasets using five different models. The datasets we generated simulate mixture experiments and mixture-process variables experiments. First, we will introduce the models that are used in the simulation study. Then, we will demonstrate the whole process of this simulation study, including the outcome measures that have been used to evaluate the models under study.

5.1 Motivation

Often, an experimenter needs to determine the optimal combination of mixture proportions in order to optimize the experimental response, as optimization (maximization or minimization) problems appear in many areas of mixture experiments. Many research studies have been devoted to experimental optimization, such as Li et al. (2021). For example, cement-based materials are prepared using different types and proportions of individual ingredients. These mixture proportions play a significant role in performing the fresh and hardened state, such as fluidity, development of strength, and durability. Therefore, finding the maximum response and determining the proportions of the mixture components that achieved this maximization is one of the main objectives of this chapter. In particular, we want to compare standard models from the literature used in mixture experiments with the CMFP models in optimization situations.

5.2 Methodology of Finding Optimal Mixture Proportions

5.2.1 Models Used in the Simulation Study

This study is based on simulated data from five models, which can represent data from mixture experiments. So, we considered Scheffé's quadratic model, MFP model, and CMFP model, which are model (3.2), model (3.8), and model (3.10) in Section 3.1. They are shown again for convenience.

Scheffé's quadratic model:

$$E(y) = \sum_{r=1}^q \beta_r x_r + \sum_{r=1}^{q-1} \sum_{j=r+1}^q \beta_{rj} x_r x_j$$

MFP model:

$$E(y) = \beta_0 + \sum_{r=1}^{q-1} \beta_r \left(\frac{x_r}{x_q} \right)^{(\alpha_r)} + \sum_{r=1}^{q-1} \beta_{rr} \left(\frac{x_r}{x_q} \right)^{2(\alpha_r)} + \sum_{r=1}^{q-2} \sum_{s=r+1}^{q-1} \beta_{rs} \left(\frac{x_r}{x_q} \right)^{(\alpha_r)} \left(\frac{x_s}{x_q} \right)^{(\alpha_s)}$$

CMFP model:

$$E(y) = \beta_0 + \sum_{r=1}^{q-1} \beta_r \left(\frac{x_r}{1-x_r} \right)^{(\alpha_r)} + \sum_{r=1}^{q-1} \beta_{rr} \left(\frac{x_r}{1-x_r} \right)^{2(\alpha_r)} + \sum_{r=1}^{q-2} \sum_{s=r+1}^{q-1} \beta_{rs} \left(\frac{x_r}{1-x_r} \right)^{(\alpha_r)} \left(\frac{x_s}{1-x_s} \right)^{(\alpha_s)},$$

where

$$x^{(\alpha)} = \begin{cases} x^\alpha & \text{if } \alpha \neq 0 \\ \log(x) & \text{if } \alpha = 0 \end{cases}$$

In addition, we consider two additional classes of models from the literature. One of these is a flexible class of models called General Blending Models (GBM) proposed by Brown et al. (2015).

The second-order GBM:

$$E(y) = \sum_{r=1}^q \beta_r x_r + \sum_{r=1}^{q-1} \sum_{s=r+1}^q \beta_{rs} \left(\frac{x_r}{x_r + x_s} \right)^{v_{rs}} \left(\frac{x_s}{x_r + x_s} \right)^{v_{sr}} (x_r + x_s)^{w_{rs}}, \quad (5.1)$$

where each v_{rs} and v_{sr} should be chosen from the values [0.5, 1, 1.5, 2, 2.5, 3], while w_{rs} should be chosen from the values [0, 1, 2, 3].

Besides, we used the second-order Ratio model suggested by Cornell (1990). The second-order Ratio model can be represented as follows.

$$E(y) = \beta_0 + \sum_{r=1}^{q-1} \beta_r \left(\frac{x_r}{x_q} \right) + \sum_{r=1}^{q-1} \beta_{rr} \left(\frac{x_r}{x_q} \right)^2 + \sum_{r=1}^{q-2} \sum_{s=r+1}^{q-1} \beta_{rs} \left(\frac{x_r}{x_q} \right) \left(\frac{x_s}{x_q} \right), \quad (5.2)$$

where the proportion x_q that has the smallest range is usually chosen for the denominator.

In addition, the expanded form of each competing model was also used in this study to simulate data from mixture-process variable experiments. The extended forms of the MFP and CMFP models are introduced in Section 3.3 as model (3.16) and model (3.18), respectively, which are used in mixture-process variable experiments that include one process variable, whereas models (3.15) and (3.17) are used in experiments that are affected by two process variables. Applying the mixture-process variable models in Chapter 4, in which we conducted the study on four different experimental datasets, provided us with a predictive viewpoint, enabling us to select the appropriate model for each experimental dataset.

5.2.2 Simulation Setup

- For each experimental dataset under consideration, we chose a ‘true model’ for the simulation process based on a real dataset. Each competing model was fitted to the experimental dataset with different scenarios to decide which form and terms would be in the true model. To

illustrate the step of the choice of the true model, all different forms of each model under consideration were fitted to the experimental dataset, and the model's form with the smallest residual standard error (RSE) will be chosen.

- This true model with chosen values of parameters was used to create two new datasets. These new datasets were generated by adding errors from a normal distribution to the true model. Here, we wanted to check if the variability of the random error affects the performance of the models. Therefore, we use a small standard error and a realistic standard error to generate the new datasets. The normal distribution with a mean of zero and a standard deviation equal to 0.5 was used to generate data in the first simulation. Next, generate the second datasets by adding errors generated from a normal distribution with a mean of zero and a standard deviation equal to RSE obtained in the previous step when the true model is fitted to the real experimental dataset.
- All different forms of each competitor model were fitted to these two new datasets that have been created. For example, to select an appropriate Ratio model, we tried to fit each x_r , for $r = 1, \dots, q$ in the denominator to determine the best value of x_r in the denominator. Likewise, for MFP and CMFP models, we need to select the model form that has the best fit depending on the status of exponents (for instance, the same exponent or different exponents). Also, try different combinations of mixture proportions (x_1, x_2, \dots, x_q) to determine which form of the CMFP model is the best. To select an appropriate GBM model, we need to compare all possible model forms that can be obtained by trying different exponent values for each model term and so on.
- Next, we search for the maximum value from the true model (TM) and corresponding values of x_1, x_2, \dots, x_q (where the TM is obtained). Thus, optimization in R is needed to find TM. The `solnp` function solves nonlinear optimization problems with both equality and inequality constraints by providing sequential quadratic programming (SQP) algorithms, which is an iterative method combining ideas from quadratic programming and Newton's method.
- We fitted the chosen form of each competing model to the datasets generated by the simulation process using the true model and found the optimum values of x_1, x_2, \dots, x_q (where

the maximum is reached). Then, we enter the optimal values of the component proportions we just got into the true model to obtain the estimated maximum (EM).

- We repeated this step 10,000 times in each standard error case for each true model scenario (there are five scenarios in this study). So, we have 10,000 values of EM and optimal proportions for each model we want to compare. This allows us to produce three different outcome measures to evaluate the performance of the five competing models. Determining the optimal proportions' values of the mixture components (where the maximum is attained) for each fitted model close to the optimal proportions' values obtained from the true model (which is used to simulate data) is our main concern. Therefore, three different methods were used to assess the proportions of the mixture components that resulted from each competing model.

Suppose x_1, \dots, x_q are the optimal proportions of the mixture components obtained from the true model, f , and $\hat{x}_1, \dots, \hat{x}_q$ are the optimal proportions of the mixture components obtained from another model (not the true model). Then

$$TM = f(x_1, \dots, x_q)$$

and

$$EM = f(\hat{x}_1, \dots, \hat{x}_q)$$

We considered two ways to make a comparison using the values of TM and EM. One way is by finding the average difference (AD) between TM and EM. This difference measures how much (in terms of the maximum response) we are losing if we recommend optimal x values from a possibly incorrect model. The following formula can express it

$$AD = Mean[TM - EM]$$

Figure 5.1 illustrates the meaning of true maximum and estimated maximum and magnitude of the term AD as the average of the difference between TM and EM .

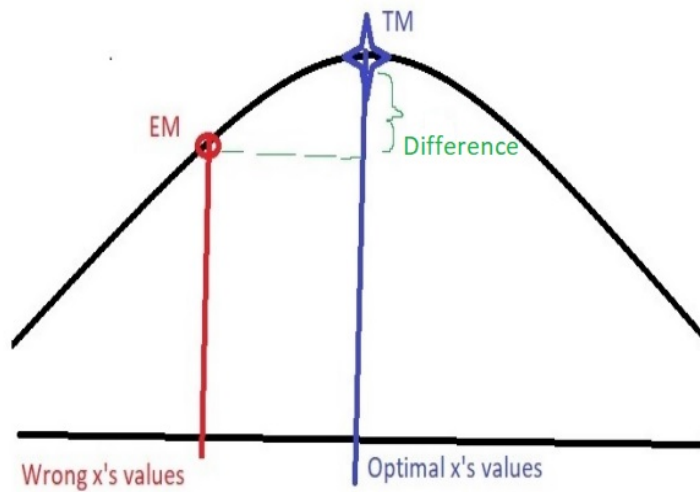


Figure 5.1: The difference between TM and EM

Another way for comparison could be a standardized measure which can be produced by dividing the average of EM by TM. Such a measure can be viewed as some form of efficiency of a model for finding the maximum response, and we denote it by EFF. Its formula can be expressed as follows:

$$EFF = \text{Mean}[EM]/TM$$

In addition, we find the mean of the optimal x -values for each model in every single replay of the last step of the simulation study on average as a further measure of outcome. We will denote these averages of the estimated optimal proportions by $\text{Mean}[x_1]$, $\text{Mean}[x_2]$, \dots , $\text{Mean}[x_q]$.

5.3 Optimal Mixture Proportions for a 3-Component Experiment

Our approach will first be illustrated using the chick-feeding experiment example. Cornell (1990) provided experimental data which involved three mixture components with restricted proportions. Restrictions on the proportions of the components of the mixture are $0.05 \leq x_1 \leq 0.40$,

$0.02 \leq x_2 \leq 0.89$, $0.06 \leq x_3 \leq 0.86$. The data were on thirty groups, all of similar weight and size. Chicks in the experiment were fed for ten days, three times a day. These chicks were fed refined diets of fats, proteins, and carbohydrates as energy supplements. The weight y was measured for all chicks at the end of this time. The data from the chick feeding experiment are listed in Table 8.5. Five different true models (CMFP model, Ratio Model, General Blending Model, Scheffé's Second-Degree Model, and Modified Fractional Polynomial Model) were used to simulate the data of this experimental dataset. The Ratio model when the denominator is x_1 (the component with the smallest range), was the first chosen true model that simulated data of the chick feeding experiment. We found the optimal proportions of the mixture component values for each fitted model at each simulation replay.

To make the comparison, all five competing models were fitted to the two datasets generated by the true Ratio model where the standard deviation of the random error is equal to 0.5 and 8.924. The optimum proportions values for x_1 , x_2 , and x_3 (where the maximum is attained for the true model) are 0.4, 0.54, and 0.06, respectively. Table 5.1 shows the outcome measures for all fitted models when the Ratio model is the true model and $s = 0.5$.

Table 5.1: The outcome measures for all fitted models when the Ratio model is the true model and $s = 0.5$

Models	AD	EFF	Mean[x_1]	Mean[x_2]	Mean[x_3]
Scheffé's	2.014098	0.98821	0.39996	0.23977	0.36016
MFP	0.015099	0.99990	0.39996	0.53994	0.05999
CMFP	0.015099	0.99990	0.39996	0.53994	0.05999
GBM	1.014998	0.99114	0.39996	0.31246	0.28747
Ratio	0.015099	0.99990	0.39996	0.53994	0.05999

According to the first outcome measure, the MFP and CMFP models produce the optimum proportions of the mixture component values identical to that resulting from the Ratio model (AD close to zero) and the same as for the Ratio model. The desired result that we want to achieve is determining the model form that has been used to simulate datasets under study. Because of that, we try every possible form of each model. Consequently, the MFP and CMFP models that were fitted to these datasets have no squared terms and have a single exponential value. The MFP model has denominator x_1 , and the chosen combination of the fitted CMFP model was x_2 and x_3

in this scenario. At the same time, Scheffé's model produces the worst estimated maximum among all the competing models according to the AD measure.

For the second outcome measure, the closer to 1, the better the model finds the maximum. So again, it is evident that the MFP and CMFP models achieved the best result in this outcome measure. Moreover, the last three columns in this table show the mean of the optimal mixture proportions we get in each replay of the simulation as a third outcome measure. Scheffé's and GBM models cannot get the correct values of the mixture proportions (same as those from the true ratio model). In contrast, the MFP model and CMFP model can find the correct values of optimal mixture proportions. Likewise, we fitted all five competing models to 10,000 datasets where the standard deviation of the random error is equal to 8.924. Table 5.2 shows the outcome measures for all fitted models when $s = 8.924$.

Table 5.2: The outcome measures for all fitted models when the Ratio model is the true model and $s = 8.924$

Models	AD	EFF	Mean[x_1]	Mean[x_2]	Mean[x_3]
Scheffé's	1.97591	0.98747	0.39832	0.25689	0.34469
MFP	0.17849	0.99878	0.39996	0.51207	0.08787
CMFP	0.25076	0.99832	0.39996	0.50079	0.09915
GBM	1.43366	0.99088	0.39996	0.30671	0.29323
Ratio	0.28190	0.99813	0.39996	0.49566	0.10428

The same five competing models we fitted to the previous datasets were also fitted to these simulated datasets. As a result of simulating larger standard errors, the first and second outcome measures get worse than the outcome measures of the previous scenario (when $s = 0.5$) for the MFP, CMFP, and Ratio models. However, there is no significant change in the outcome measures of Scheffé's and GBM models. Almost all models can get the correct x_1 proportion. But again, Scheffé's and GBM models cannot get the correct proportion values for x_2 and x_3 .

Scheffé's quadratic polynomial model was the second true model from which we simulated data of the chick feeding experiment. To make the comparison, all five competing models were fitted to 10,000 versions of two datasets generated from Scheffé's quadratic polynomial model where the standard deviation of the random error is equal to 0.5 and 7.135. The optimum values of the pro-

portions for x_1 , x_2 , and x_3 are 0.40, 0.29, 0.30 respectively. Table 5.3 shows the outcome measures for all fitted models when Scheffé's model is the true model and $s = 0.5$.

Table 5.3: The outcome measures for all fitted models when Scheffé's model is the true model and $s = 0.5$

Models	AD	EFF	Mean[x_1]	Mean[x_2]	Mean[x_3]
Scheffé's	0.02126	0.99977	0.39996	0.30283	0.29711
MFP	2.79045	0.98285	0.39996	0.47495	0.12499
CMFP	3.91567	0.97597	0.39996	0.50745	0.09249
GBM	0.02464	0.99975	0.39996	0.29582	0.30412
Ratio	2.96295	0.98179	0.39996	0.11749	0.48245

According to the first and second outcome measures, the GBM model produces the best values of the mixture proportions among all the other models, whilst the CMFP model produces the worst values of the mixture proportions among all the other models. The MFP models used here have denominator x_3 and have no squared terms and a single exponential value. The CMFP models have no interaction terms, and the terms are based on proportions x_2 and x_3 . The Ratio model with a denominator x_2 was chosen to fit the generated datasets. All models can find the right optimal proportions of x_1 . However, only the GBM model can get the right optimal proportions of x_2 and x_3 . Likewise, we fitted all five competing models to the second generated 10,000 datasets. Table 5.4 shows the outcome measures for all fitted models when $s = 7.135$.

Table 5.4: The outcome measures for all fitted models when Scheffé's model is the true model and $s = 7.135$

Models	AD	EFF	Mean[x_1]	Mean[x_2]	Mean[x_3]
Scheffé's	0.63014	0.99605	0.39993	0.29816	0.30182
MFP	3.72495	0.97713	0.39996	0.36054	0.23940
CMFP	3.91567	0.97597	0.39996	0.50745	0.09249
GBM	0.93056	0.99421	0.39712	0.28959	0.31318
Ratio	3.20968	0.98028	0.39996	0.11056	0.48938

The outcome measures are slightly different from the previous outcome measures (a little worse) for all models except the CMFP model, which remains stable.

The GBM model was the third true model that we used to simulate the chick feeding experiment data. To make the comparison, all five competing models were fitted to the datasets generated from

the GBM model, where the standard deviation of the random error is equal to 0.5 and 6.688. The optimum values for x_1 , x_2 , and x_3 are 0.40, 0.34, 0.26 respectively. Table 5.5 shows the outcome measures for all fitted models when the GBM model is the true model and $s = 0.5$.

Table 5.5: The outcome measures for all fitted models when the GBM model is the true model and $s = 0.5$

Models	AD	EFF	Mean[x_1]	Mean[x_2]	Mean[x_3]
Scheffé's	1.46280	0.99294	0.39996	0.37746	0.22248
MFP	11.8424	0.94364	0.39996	0.40996	0.18998
CMFP	1.46281	0.99294	0.39996	0.37746	0.22248
GBM	0.04714	0.99968	0.39996	0.34497	0.25497
Ratio	24.3061	0.88422	0.39996	0.50745	0.09249

Scheffé's and CMFP models produce the best values of the mixture proportion according to the first and second outcome measures, whilst the Ratio model outputs the worst outcome measures. The MFP and CMFP models that were fitted to these datasets are full models (all terms are included), and both have a single exponential value. The MFP and Ratio models with a denominator x_3 were fitted to these simulated datasets, while the chosen combination of the fitted CMFP model was x_2 and x_3 in this scenario. All models can find the right optimal proportion of x_1 . However, Scheffé's and CMFP models get the same optimal proportions of x_2 and x_3 , which are slightly different from the true model. The values of x_2 and x_3 from the Ratio model are farther from the ones from the true model. Likewise, we fitted all five competing models to the datasets of the second simulation.

Table 5.6 shows the outcome measures for all fitted models when $s = 6.688$.

Table 5.6: The outcome measures for all fitted models when the GBM model is the true model and $s = 6.688$

Models	AD	EFF	Mean[x_1]	Mean[x_2]	Mean[x_3]
Scheffé's	1.56309	0.99246	0.39986	0.37530	0.22474
MFP	13.3259	0.93656	0.39996	0.41835	0.18159
CMFP	2.33459	0.98879	0.39996	0.38595	0.21399
GBM	0.09186	0.99946	0.39990	0.34275	0.25725
Ratio	23.8002	0.88663	0.39996	0.50535	0.09459

In the GBM true model scenario, there is no significant difference between the results when changing the value of the standard error ($s = 6.688$, $s = 0.5$), as shown in Table 5.5 and Table 5.6. So when the same model forms are fitted to these datasets, Scheffé's and CMFP models achieve the best outcome measures among the other models.

The MFP model was the fourth chosen true model that was used to simulate data based on

the chick feeding experiment. To make the comparison, all five competing models were fitted to the datasets generated from the MFP model where the standard deviation of the random error is equal to 0.5 and 7.901. The optimum values of x_1, x_2 , and x_3 for this true model are 0.40, 0.46, and 0.14, respectively. Table 5.7 shows the outcome measures for all fitted models when the MFP model is the true model and $s = 0.5$.

Table 5.7: The outcome measures for all fitted models when the MFP model is the true model and $s = 0.5$

Models	AD	EFF	Mean[x_1]	Mean[x_2]	Mean[x_3]
Scheffé's	7.54098	0.95677	0.39996	0.29618	0.30376
MFP	0.19300	0.99790	0.39996	0.44414	0.15526
CMFP	0.25416	0.99845	0.39996	0.47495	0.12499
GBM	6.63702	0.96194	0.39996	0.31247	0.28747
Ratio	3.32090	0.98091	0.39996	0.50745	0.09249

The CMFP model is the closest model to the MFP true model, and this was proven by outcome measures shown in Table 5.7. On the contrary, we find that the outcome measures of Scheffé's and GBM models are similar, and both are far from the true model compared with the other models. The CMFP model fitted to these datasets has no intercept and interaction terms and has a single exponential value. The chosen combination of the fitted CMFP model was x_2 and x_3 , and the denominator was x_3 in the fitted Ratio model in this scenario. Then, all five competing models were fitted to the second generated datasets. Table 5.8 shows the outcome measures for all fitted models when $s = 7.901$.

Table 5.8: The outcome measures for all fitted models when the MFP model is the true model and $s = 7.901$

Models	AD	EFF	Mean[x_1]	Mean[x_2]	Mean[x_3]
Scheffé's	8.43729	0.95165	0.39994	0.29625	0.30372
MFP	0.70785	0.99587	0.39997	0.47960	0.12034
CMFP	0.53164	0.99686	0.39912	0.47626	0.12452
GBM	6.73489	0.96138	0.39996	0.31001	0.28993
Ratio	2.91147	0.98325	0.39996	0.50311	0.09683

There is no significant difference in the outcome measures for all models between Table 5.7 and Table 5.8, except for the slight difference in outcome measures for the CMFP and MFP models. However, it is important to mention that the outcome measures of the CMFP model became closer to the true model than the fitted MFP model, even though the true model was the MFP model. This is because the intercept in the fitted MFP model is removed to avoid the convergence problem that occurred.

The CMFP model was the fifth chosen true model that was used to simulate data based on the chick feeding experiment. To make the comparison, all five competing models were fitted to the datasets generated from the CMFP model, where the standard deviation of the random error is equal to 0.5 and 8.467. The optimum values for x_1 , x_2 , and x_3 are 0.40, 0.54, and 0.06, respectively, for the fifth chosen true model. Table 5.9 shows the outcome measures for all fitted models when the MFP model is the true model and $s = 0.5$.

Table 5.9: The outcome measures for all fitted models when the CMFP model is the true model and $s = 0.5$

Models	AD	EFF	Mean[x_1]	Mean[x_2]	Mean[x_3]
Scheffé's	1.16250	0.99289	0.39996	0.34284	0.25710
MFP	0.01356	0.99982	0.39996	0.53995	0.05999
CMFP	0.01356	0.99982	0.39996	0.53995	0.05999
GBM	1.14655	0.99298	0.39996	0.34497	0.25498
Ratio	0.01356	0.99982	0.39996	0.53995	0.05999

According to the outcome measures, it is clear that the MFP and Ratio models can get the correct optimum values for x_1 , x_2 , and x_3 , the same as the true model itself. The Ratio and the MFP models have x_1 in the denominator. Also, the MFP model has a single exponential value, while the CMFP model has two different exponential values. Likewise, all five competing models were fitted to the generated datasets when the standard deviation of the random error was equal to 8.467. Table 5.10 shows the outcome measures for all fitted models when $s = 8.467$.

Table 5.10: The outcome measures for all fitted models when the CMFP model is the true model and $s = 8.467$

Models	AD	EFF	Mean[x_1]	Mean[x_2]	Mean[x_3]
Scheffé's	1.51988	0.99073	0.39993	0.33168	0.26829
MFP	0.26959	0.99827	0.39996	0.51353	0.08641
CMFP	0.03473	0.99969	0.39996	0.53776	0.06218
GBM	1.19395	0.99270	0.39996	0.34273	0.25721
Ratio	0.08817	0.99937	0.39996	0.53154	0.06841

There is no significant difference in the outcome measures for all models between Table 5.9 and Table 5.10. So, the MFP and Ratio models still have the best outcome measures among all competing models.

5.3.1 Summary

- The outcome measures of all competing models are close to each other and close to the values of the mixture components obtained from the true model in case the true model is a CMFP model, whatever the standard error value used to simulate the experimental dataset.
- For all models, there are no better outcome measures than outcome measures for the model that is the same type as the true model used to simulate the dataset when the standard error equals 0.5.
- In this experimental dataset, the x_1 component has the smallest range among the other mixture components according to the restrictions on the proportions of the components. Then, all true models can obtain the same value for the optimal proportion of the component x_1 , which is equal to the upper bound of x_1 . But at the same time, all models got various values of the optimal proportion of other mixture components.

Table 5.11: The models' ranks when the standard errors equal 0.5

The true model					
Models	CMFP	MFP	GBM	Scheffé's	Ratio
CMFP	2	2	2.5	5	2
MFP	2	1	4	3	2
GBM	4	4	1	2	4
Scheffé's	5	5	2.5	1	5
Ratio	2	3	5	4	2

Table 5.12: The models' ranks when the standard errors have realistic values

The true model					
Models	CMFP	MFP	GBM	Scheffé's	Ratio
CMFP	1	1	3	5	2
MFP	3	2	4	4	1
GBM	4	4	1	2	4
Scheffé's	5	5	2	1	5
Ratio	2	3	5	3	3

Table 5.11 and Table 5.12 show the ranks of all competing models in each scenario according to their performance when generating datasets by adding a small standard error and a realistic standard error, respectively. The first rank indicates the best performance according to AD and is often for the fitted model with the same type as the true model. When two or more fitted models have the same performance, we give them the average of their joint rank and the next rank.

The lowest two ranks (4 and 5) are the same for the above tables in almost all scenarios. Every fitted model except the Ratio model can get the first and second places at least once for each scenario when the standard error value is realistic. Moreover, Scheffé's model is ranked 5th (worst) three times, while the CMFP model is ranked 1st twice. When the true model was an MFP model or a Ratio model, adding a larger standard error to generate the second datasets affected the performance of the fitted model that was of the same type as the true model negatively, as shown in Table 5.2 and Table 5.8. As a result, it is not ranked first and is outperformed by the outcome measures of other models.

5.4 Optimal Mixture Proportions for a 4-Component Experiment

A dataset where the response is the illumination of candles and which includes four components with specified proportions above and below is presented by Box and Draper (2007). The constraints on the proportions are $0.4 \leq x_1 \leq 0.6$, $0.10 \leq x_2, x_3 \leq 0.47$, $0.03 \leq x_4 \leq 0.08$. The illumination candle experimental data is given in Table 8.6. The process used in the previous example, which contained three components of a mixture, will also be used in this example of four mixture components.

The Ratio model has the denominator x_4 is the first chosen true model that was used to simulate data based on the illumination candle experiment. To make the comparison, all five competing models fitted to the datasets generated by the true Ratio model where the standard deviation of the random error is equal to 0.5 and 84.94. The optimum proportions values for x_1, x_2, x_3 , and x_4 where the true maximum is attained are 0.60, 0.22, 0.10, and 0.08, respectively. Table 5.13 shows the outcome measures for all fitted models when the Ratio model is the true model and $s = 0.5$.

Table 5.13: The outcome measures for all fitted models when the Ratio model is the true model and $s = 0.5$

Models	AD	EFF	Mean[x_1]	Mean[x_2]	Mean[x_3]	Mean[x_4]
Scheffé's	10.9746	0.96946	0.57221	0.22363	0.12407	0.07999
MFP	5.89e-05	0.99990	0.59994	0.21998	0.09999	0.07999
CMFP	5.89e-05	0.99990	0.59994	0.21998	0.09999	0.07999
GBM	7.57e-05	0.99990	0.59994	0.21998	0.09999	0.07999
Ratio	4.92e - 05	0.99990	0.59994	0.21998	0.09999	0.07999

Obviously, the MFP, CMFP, and GBM models can get the correct optimum values for x_1 , x_2 , x_3 and x_4 which are close to the optimum proportions that were obtained from the true Ratio model, while Scheffé's model can get the correct proportion only for x_4 . As for the fitted models, x_4 is the denominator in the Ratio model, while the MFP model has a denominator x_3 . Also, both the MFP and the CMFP models have a single exponential value. The CMFP model has the mixture combination of x_1 , x_2 , and x_4 and only contains pairwise interaction terms. However, the MFP model contains only first-order terms with no intercept. Likewise, we fitted all five competing models to the datasets of the second simulation. Table 5.14 shows the outcome measures for all fitted models when $s = 84.94$.

Table 5.14: The outcome measures for all fitted models when the Ratio model is the true model and $s = 84.94$

Models	AD	EFF	Mean[x_1]	Mean[x_2]	Mean[x_3]	Mean[x_4]
Scheffé's	29.1233	0.91908	0.55839	0.20783	0.15803	0.07564
MFP	9.60268	0.97317	0.58672	0.22836	0.10554	0.07929
CMFP	9.03718	0.97442	0.59281	0.20391	0.12378	0.07940
GBM	18.2006	0.94940	0.58398	0.19854	0.14237	0.07500
Ratio	37.6286	0.89553	0.56653	0.22718	0.14264	0.06356

Adding such a significant error to the true model has a negative effect on all outcome measures for all fitted models, but the Ratio model was shown to be the most sensitive, while the CMFP and MFP models were the least affected. For accuracy and clarification, we find that using a small sample size ($n = 15$) to simulate data causes a convergence problem in approximately 1 in 1000 replications of the simulation when fitting the MFP model.

Furthermore, Scheffé's model was the second true model that was used to simulate data based on the illumination candle experiment. To make the comparison, all five competing models were fitted to the two datasets generated by Scheffé's model with a standard deviation of the random error equal to 0.5 and 59.55. The optimum values for x_1 , x_2 , x_3 , and x_4 are 0.52, 0.23, 0.17, and 0.08, respectively. Table 5.15 shows the result of all competing models fitted to the first generated dataset.

Table 5.15: The outcome measures for all fitted models when Scheffé's model is the true model and $s = 0.5$

Models	AD	EFF	Mean[x_1]	Mean[x_2]	Mean[x_3]	Mean[x_4]
Scheffé's	0.00080	0.99990	0.52293	0.22927	0.16771	0.07999
MFP	3.48036	0.99134	0.50146	0.23933	0.17912	0.07999
CMFP	0.44552	0.99881	0.52960	0.22038	0.16993	0.07999
GBM	3.04502	0.99241	0.50477	0.22472	0.19042	0.07999
Ratio	7.95465	0.98034	0.49049	0.24660	0.18282	0.07999

The outcome measures of the CMFP model show that the correct optimum proportions for the mixture components can be obtained. Furthermore, the outcome measures of the MFP and GBM models are very close to each other and better than the outcome measures of the Ratio model. As for the fitted models, the MFP and CMFP models that were fitted to these datasets are full models (all terms are included), and both have a single exponential value. Also, x_1 is the denominator in the Ratio and MFP models, while the proportions x_1 , x_2 , and x_4 are used in the CMFP model. In the same way, we fitted all five competing models to the second generated datasets. The outcome measures are shown in Table 5.16.

Table 5.16: The outcome measures for all fitted models when Scheffé's model is the true model and $s = 59.55$

Models	AD	EFF	Mean[x_1]	Mean[x_2]	Mean[x_3]	Mean[x_4]
Scheffé's	19.8527	0.95088	0.52864	0.22605	0.16632	0.07868
MFP	54.1417	0.86658	0.58998	0.20827	0.12167	0.07977
CMFP	51.2465	0.87388	0.59761	0.20934	0.11286	0.07990
GBM	35.4251	0.91260	0.52230	0.20363	0.19664	0.07712
Ratio	30.9485	0.92360	0.49682	0.24602	0.17891	0.07794

Adding such a significant error to the true model has a negative effect on the outcome measures for all fitted models. However, the outcome measures for the GBM model and the Ratio model are close to each other and better than the outcome measures for both the MFP and the CMFP models.

The GBM model was the third true model that was used to simulate data based on the illumination candle experiment. To make the comparison, all five competing models were fitted to the datasets generated from the true GBM model where the standard deviation of the random error is equal to 0.5 and 32.45. The optimum proportions for x_1 , x_2 , x_3 , and x_4 are 0.53, 0.18, 0.21, 0.08 respectively. Table 5.17 shows the outcome measures for all fitted models when the GBM model is the true model and $s = 0.5$.

Table 5.17: The outcome measures for all fitted models when the GBM model is the true model and $s = 0.5$

Models	AD	EFF	Mean[x_1]	Mean[x_2]	Mean[x_3]	Mean[x_4]
Scheffé's	20.3176	0.95361	0.52790	0.22528	0.16673	0.07999
MFP	13.1638	0.96999	0.55387	0.19321	0.17283	0.07999
CMFP	12.0337	0.97248	0.55233	0.19396	0.17363	0.07999
GBM	0.00086	0.99990	0.52739	0.18116	0.21136	0.07999
Ratio	26.9633	0.93846	0.51969	0.13825	0.26197	0.07999

The outcome measures of the MFP model and the CMFP model are the best among all other models' outcome measures. But, the outcome measures of the Ratio model are the worst. As for the chosen fitted models, both the MFP model and the CMFP model are full models (all terms are included), and each has one exponential value. Moreover, x_1 is the denominator in the MFP model, and x_2 is the denominator in the Ratio model, while the mixture combination was x_2 , x_3 , and x_4 for the CMFP model. To fit the CMFP and MFP models to the second generated datasets. Some changes in the fitted CMFP and MFP models are needed to avoid convergence issues. Therefore, the intercept has been removed from both models. The outcome measures are in Table 5.18.

Table 5.18: The outcome measures for all fitted models when the GBM model is the true model and $s = 32.45$

Models	AD	EFF	Mean[x_1]	Mean[x_2]	Mean[x_3]	Mean[x_4]
Scheffé's	33.1967	0.92427	0.53219	0.22513	0.16261	0.07999
MFP	55.8407	0.87276	0.59515	0.16942	0.15616	0.07918
CMFP	41.6814	0.90495	0.58018	0.17887	0.16099	0.07986
GBM	3.77244	0.99131	0.52799	0.18228	0.20964	0.07999
Ratio	36.7770	0.91611	0.52330	0.13789	0.25875	0.07996

Adding such a significant error to the true model has affected the outcome measures for all fitted models. Thus, the optimum proportions of mixture components that result from the fitted models are inaccurate. However, the worst outcome measure is for the MFP model, and the best is for Scheffé's model. Moreover, there was the occasional convergence problem (in 5 of the 10,000 replications of the simulation) when fitting the MFP model to these datasets and in 7 of the 10,000 replications when fitting the CMFP model.

The MFP model was the fourth true model that was used to simulate data based on the illumination candle experiment. To make the comparison, all five competing models were fitted to the datasets generated from the true MFP model where the standard deviation of the random

error is equal to 0.5 and 33.66. The optimum values for x_1, x_2, x_3 , and x_4 are 0.54, 0.20, 0.18, and 0.08, respectively. Table 5.19 shows the result of fitting all competing models to the first generated datasets.

Table 5.19: The outcome measures for all fitted models when the MFP model is the true model and $s = 0.5$

Models	AD	EFF	Mean[x_1]	Mean[x_2]	Mean[x_3]	Mean[x_4]
Scheffé's	6.74991	0.98439	0.52683	0.23379	0.15928	0.07999
MFP	0.00028	0.99990	0.53924	0.20190	0.17877	0.07999
CMFP	6.10063	0.98589	0.51675	0.23004	0.17312	0.07999
GBM	4.79060	0.98890	0.52334	0.22891	0.16766	0.07999
Ratio	21.1087	0.95142	0.50307	0.26193	0.15491	0.07999

The GBM model produced the values of the mixture proportions, which are the closest to the ones obtained from the true MFP model, while the values of the mixture proportions produced by the Ratio model are the furthest away. The outcome measures for the CMFP model and Scheffé's model are almost the same, and they range between the outcome measures of the GBM and the Ratio models but closer to the results of the GBM model. Regarding the chosen forms of the fitted models, x_1 is the denominator in the Ratio model, and the CMFP model has no squared and interaction terms and includes mixture proportions x_1, x_2 , and x_3 . In the same way, we fitted all five competing models to the datasets of the second simulation. The result is shown in Table 5.20.

Table 5.20: The outcome measures for all fitted models when the MFP model is the true model and $s = 33.66$

Models	AD	EFF	Mean[x_1]	Mean[x_2]	Mean[x_3]	Mean[x_4]
Scheffé's	26.4582	0.93913	0.53194	0.23404	0.15395	0.07996
MFP	1.42399	0.99663	0.54049	0.20158	0.17784	0.07999
CMFP	18.4686	0.95749	0.51851	0.23346	0.16793	0.07999
GBM	26.7765	0.93840	0.52962	0.23161	0.16009	0.07858
Ratio	45.2929	0.89587	0.50635	0.26210	0.15155	0.07991

The CMFP model is closest to the true model according to the outcome measures, while the Ratio model is furthest away again.

Then, the CMFP model was the fifth chosen true model that was used to simulate data based on the illumination candle experiment. To make the comparison, all five competing models were fitted to the datasets generated from the true CMFP model, where the standard deviation of the random error is equal to 0.5 and 43.53. The optimum values for x_1, x_2, x_3 , and x_4 are 0.51, 0.18,

0.23, and 0.08, respectively, for the fifth chosen true model. Table 5.21 shows the result of fitting all competing models to the first generated datasets.

Table 5.21: The outcome measures for all fitted models when the CMFP model is the true model and $s = 0.5$

Models	AD	EFF	Mean[x_1]	Mean[x_2]	Mean[x_3]	Mean[x_4]
Scheffé's	17.1570	0.95793	0.53064	0.25988	0.12938	0.07999
MFP	4.00125	0.99011	0.53963	0.17899	0.20129	0.07999
CMFP	0.00083	0.99990	0.51333	0.18148	0.22509	0.07999
GBM	0.88197	0.99774	0.52529	0.17926	0.21536	0.07999
Ratio	24.2241	0.94065	0.50677	0.28888	0.12425	0.07999

The GBM model produced the values of the mixture proportions, which are the closest to the ones obtained from the true model, while the values of the mixture proportions produced by the Ratio model are the furthest away. Also, the outcome measures for the MFP model are considered good compared to the outcome measures of Scheffé's and Ratio models. Here, the full MFP model with a single exponential value and x_2 in the denominator was fitted to these datasets. But, the Ratio model fitted to these datasets has x_1 in the denominator. Likewise, we fitted all five competing models to the datasets generated by the second simulation. The result is shown in Table 5.22.

Table 5.22: The outcome measures for all fitted models when CMFP model is the true model and $s = 43.53$

Models	AD	EFF	Mean[x_1]	Mean[x_2]	Mean[x_3]	Mean[x_4]
Scheffé's	19.9232	0.95117	0.53171	0.25226	0.13609	0.07984
MFP	47.5019	0.88371	0.51817	0.12459	0.27727	0.07987
CMFP	10.3471	0.97456	0.51775	0.19496	0.20782	0.07937
GBM	14.1030	0.96541	0.52949	0.18998	0.20153	0.07889
Ratio	26.2095	0.93579	0.50447	0.27655	0.13917	0.07971

The values of the mixture proportions of all models became far from the values of the true optimal proportions when fitted to the second datasets. For clarification, there is the occasional convergence problem when fitting the CMFP and MFP models to these datasets in proportions 0.0026 and 0.0004, respectively. However, removing the intercept from the MFP model reduced the convergence problem but made the outcome measures for the MFP model the worst among all fitted models, as shown in Table 5.22, while the outcome measures for the GBM model were the closest to the true ones.

5.4.1 Summary

- The estimated standard error value for each true model used to generate the second simulation datasets became significantly larger compared to the example of the three mixture components.
- The outcome measures of all competing models are close to each other; simultaneously, they are close to the optimal proportions obtained from the true model in the case of true Scheffé's model when generating the first datasets by adding a standard error equal to 0.5. In contrast, the outcome measures for all competing models are the furthest from the optimal values obtained from the true Scheffé's model when adding a realistic standard error to generate the second datasets.
- In each true model scenario, there are no better outcome measures than those for the model that resembles the true model when the standard error equals 0.5. However, adding a large standard error to generate the second simulated datasets usually has a bad impact on the outcome measures for all models, especially in the case of the true Ratio model, in which the fitted Ratio model is most affected and produces the worst outcome measures among all models. As a result, the CMFP model outcome measures outperformed the Ratio model outcome measures in the true Ratio model scenario.
- In this experimental dataset, the proportion x_4 has the smallest range among the other mixture proportions according to the restrictions. Then, all true models can obtain the same value for the optimal proportion x_4 , equal to the upper bound of this proportion. But at the same time, all models got various values of the optimal proportion of other mixture components.

Table 5.23: The models' ranks when the standard errors equal 0.5

The true model					
Models	CMFP	MFP	GBM	Scheffé's	Ratio
CMFP	1	3	2	2	2.5
MFP	3	1	3	4	2.5
GBM	2	2	1	3	4
Scheffé's	4	4	4	1	5
Ratio	5	5	5	5	1

Table 5.24: The models' ranks when the standard errors have realistic values

The true model					
Models	CMFP	MFP	GBM	Scheffé's	Ratio
CMFP	1	2	4	4	1
MFP	5	1	5	5	2
GBM	2	4	1	3	3
Scheffé's	3	3	2	1	4
Ratio	4	5	3	2	5

The ranks of all fitted models in each scenario are shown in Table 5.23 and Table 5.24 when datasets were generated by adding a small standard error and a large standard error, respectively. The first rank is often for a fitted model whose type is the same as the true model. The first ranks are almost the same in both tables in all scenarios, in contrast to the lowest ranks, which are often different when comparing the two tables. The Ratio model has most of the fifth ranks in Table 5.23. Also, every fitted model except the Ratio model can get the first and second places at least once for each scenario when the standard error value used in the simulation process is realistic, as shown in Table 5.24. Moreover, in Table 5.24, the MFP and the Ratio models were ranked 5 (worst) at least twice, while the CMFP model was ranked 1st twice. Referring to Table 5.24, it is clear that the outcome measures of the MFP model and CMFP model are better than the outcome measures of the fitted Ratio model, which are surprising results as the true model in this scenario was the Ratio model.

These surprising results of the Ratio model appeared after adding a significant standard error ($s=84.94$) to the true Ratio model to generate the second datasets. This obviously had a negative impact on all competing models except MFP and CMFP models, which are the least affected by adding such significant errors to simulate the data. Such unexpected results deserve more investigation to find out their causes. A similar issue appeared when applying Example 5.5. Again, the outcome measures of the MFP and CMFP models exceed the outcome measures of the fitted model, whose type is the same as the true model in two different scenarios. For more clarification, we investigate the logical reasons behind the results for such cases, which are provided in the last paragraph of Section 5.5.

5.5 Optimal Mixture Proportions for a 3-Component Experiment with One Process Variable

In some mixture experiments, the response is dependent on the processing conditions as well as the proportion of the mixture components. This example, which has been introduced in Section 4.2, represents the opacity of a printable coating material used for tags and identification labels as the response, and this mixture-process variable experiment was studied by Chau and Kelley (1993). This formulation contained three mixture components, two pigments, x_1 and x_2 , and a polymeric binder (x_3). The constraints on the component proportions were

$$0.13 \leq x_1 \leq 0.45, 0.21 \leq x_2 \leq 0.67, 0.20 \leq x_3 \leq 0.34$$

The response of interest was the opacity of the coating, which was influenced by the thickness of the coating (z) as a process variable besides the mixture of the three components. The opacity of printable coating material, with two levels of the thickness of the coating, was investigated, and the experiment data are given in Table 8.1. To fit all competing models under study to the data from a mixture-process variable experiment, the interaction terms between the individual main effects of mixture components with each process variable are added to each competing mixture model to simulate data of mixture-process variable experiments. So, the extended forms of the models are used in this experimental data that includes a process variable. Using the same method as the previous examples, each model was fitted to the real dataset in turn to decide which form and terms would be in the respective true models. Besides, the values of the parameters and the values of RSE will be used in the true models to simulate the datasets. So, we tried all different forms for each of the models by fitting them to the real experimental dataset, and the model's form with the smallest RSE was chosen to be the true model. Since the realistic standard errors for this example were small (about 0.015) in all scenarios, we will not simulate the data with $s = 0.5$.

Moreover, each form of the competing model was fitted to the simulated datasets generated by the true model to choose the form with the minimum standard error and find the optimum setting of

the process variable of this model using an optimization function called `solnp`. Then, we optimized the values of the proportions of the mixture components and the level of the process variable for all fitted models in each round of the simulation procedure. So, this step was repeated 10,000 times for each true model scenario.

The Ratio model with denominator x_3 was the first chosen true model to simulate data based on the experimental data provided by Chau and Kelley (1993). In this scenario, we obtained the true optimal values for x_1 , x_2 , x_3 when $z = 1$, which are 0.35, 0.45, and 0.20, respectively. Table 5.25 shows the outcome measures for all five competing models when simulating the mixture-process variable experiment data using the Ratio model. In addition, the correct value of the process variable was identified by all models in all simulation runs.

Table 5.25: Outcome measures for all models when simulating data using the Ratio model

Models	AD	EFF	Mean[x_1]	Mean[x_2]	Mean[x_3]
Scheffé's	0.00858	0.99128	0.38951	0.40647	0.20393
MFP	0.00583	0.99404	0.39461	0.40530	0.19999
CMFP	0.01042	0.98943	0.41350	0.37988	0.20653
GBM	0.00776	0.99210	0.38883	0.40815	0.20293
Ratio	0.00572	0.99415	0.36251	0.42944	0.20795

According to the outcome measures, the Ratio and MFP models can produce accurate optimum values of the mixture proportions. The MFP model that was fitted to these simulated datasets has $n = 18$ denominator x_1 and a single exponent value. As a result, a proportion of 0.006 of the runs have convergence issues that occurred when fitting the MFP model to the simulated datasets in this scenario. Outcome measures are not counted if any convergence issue occurs when fitting the models to generated datasets. This is because the simulation process has a loop with 10,000 repeats, which stops in such a situation. In general, all fitted models have good outcome measures close to the optimal ones, which result from the true Ratio model. The CMFP model that was fitted to these datasets has a single exponent value, and the terms are based on proportions x_2 and x_3 .

Scheffé's quadratic model was the second chosen true model that was used to simulate data. In this scenario, we obtained the true optimal proportions values for x_1 , x_2 , x_3 when $z = 1$, which

are 0.43, 0.23, and 0.34, respectively. The outcome measures for all five competing models when simulating the mixture-process variable experiment data using Scheffé's model are shown in Table 5.26. In addition, the correct value of the process variable was identified by all models in all simulation runs.

Table 5.26: Outcome measures for all models when simulating data using Scheffé's model

Models	AD	EFF	Mean[x_1]	Mean[x_2]	Mean[x_3]
Scheffé's	0.00253	0.99734	0.41481	0.26302	0.32207
MFP	0.00041	0.99949	0.44996	0.20998	0.33997
CMFP	0.00042	0.99947	0.44996	0.21005	0.33991
GBM	0.00238	0.99749	0.41476	0.25781	0.32734
Ratio	0.02258	0.97705	0.38344	0.38157	0.23489

The outcome measures of the CMFP model and MFP model are very close to each other and show that they can get accurate optimum values for x_1 , x_2 , and x_3 . Both the CMFP model and MFP model have a single exponent value here. The MFP model has denominator x_2 , and the CMFP model is based on proportions x_1 , x_3 . In contrast, the Ratio model produced values of the mixture proportions that are the furthest from the optimal ones. However, all other models produced values of the proportions of the mixture components close to that produced by the true model according to their outcome measures.

The GBM model was the third true model chosen to simulate data of the mixture-process variable experiment. In this scenario, we obtained the true optimal proportions values for x_1 , x_2 , x_3 when $z = 1$, which are 0.43, 0.24, and 0.34, respectively. Table 5.27 shows the outcome measures for all fitted models when a GBM model is the true model.

Table 5.27: Outcome measures for all models when simulating data using the GBM model

Models	AD	EFF	Mean[x_1]	Mean[x_2]	Mean[x_3]
Scheffé's	0.00343	0.99734	0.41537	0.26443	0.32010
MFP	0.00066	0.99643	0.44996	0.20998	0.33997
CMFP	0.00067	0.99923	0.44996	0.21000	0.33994
GBM	0.00298	0.99688	0.42018	0.25749	0.32223
Ratio	0.03122	0.96832	0.36587	0.43381	0.20023

The outcome measures of the CMFP model and MFP model are very close to each other and show that they can get accurate optimum values for x_1 , x_2 , and x_3 . Both the CMFP model and MFP

model have a single exponent value. The MFP model has denominator x_2 , and the CMFP model is based on proportions x_1, x_3 . In contrast, the Ratio model has denominator x_3 and produced the furthest values of the mixture components proportions among all models according to its outcome measures.

Furthermore, the MFP model was the fourth true model chosen to simulate data from a mixture-process variable experiment. In this scenario, we obtained the true optimal proportions values for x_1, x_2, x_3 when $z = 1$, which are 0.45, 0.21, and 0.34, respectively. Table 5.28 shows the outcome measures for all fitted models when the MFP model is the true model. In addition, the correct value of the process variable was identified by all models in all simulation runs.

Table 5.28: Outcome measures for all models when simulating data using the MFP model

Models	AD	EFF	Mean[x_1]	Mean[x_2]	Mean[x_3]
Scheffé's	0.00287	0.99703	0.44373	0.22039	0.33577
MFP	3.21e - 08	0.99990	0.44996	0.20998	0.33997
CMFP	3.76e-06	0.99990	0.44996	0.20999	0.33995
GBM	0.00262	0.99728	0.44440	0.21952	0.33598
Ratio	0.00547	0.99441	0.44996	0.22977	0.32018

The outcome measures indicate that the CMFP model yields optimal values of the mixture proportions that are the closest to the ones from the MFP model. The CMFP model is based on proportions x_1, x_3 , and the MFP model has denominator x_2 . Both the CMFP model and MFP model have a single power value. It is clear that the Ratio model has the worst outcome measures among all competing models.

Thereafter, the CMFP model was the fifth true model that was used to simulate data of the mixture-process variable experiment. In this scenario, we obtained the true optimal proportions values for x_1, x_2, x_3 when $z = 1$, which are 0.45, 0.21, and 0.34, respectively. Table 5.29 shows the outcome measures for all five competing models when simulating the mixture-process variable experiment data by the CMFP model. In addition, the correct value of the process variable was identified by all models in all simulation runs.

Table 5.29: Outcome measures for all models when simulating data by the CMFP model

Models	AD	EFF	Mean[x_1]	Mean[x_2]	Mean[x_3]
Scheffé's	0.00250	0.99806	0.43989	0.22254	0.33747
MFP	$5.36e - 07$	0.99990	0.44996	0.20998	0.33997
CMFP	$5.40e - 07$	0.99990	0.44996	0.20998	0.33997
GBM	0.00181	0.99856	0.44258	0.21912	0.33820
Ratio	0.00025	0.99972	0.44996	0.21067	0.33927

All five fitted models produced optimal values of the mixture proportions close to the optimal values of the true model. To be more detailed, the MFP and the CMFP models produced almost identical values of the optimal proportions of the mixture components. Thus, the AD measure for the MFP and the CMFP models is nearly equal to zero. The Ratio used here has denominator x_1 and produced AD measure equal to 0.0002, which is better than the GBM and Scheffé's models. However, the GBM and Scheffé's models produce values of mixture proportions that are similar to each other and very close to the optimal values of the true model.

5.5.1 Summary

- Generally, for all scenarios, each competing model can produce accurate values of the optimal mixture proportions like those obtained from the true model.
- The outcome measures of the MFP model and the CMFP model surpassed the outcome measures of all other models for all scenarios except when the true model is the Ratio model.
- The model form for the CMFP and the MFP models was model (3.16) and model (3.18), respectively (but without square terms) in all scenarios, except when the Ratio model is the true model, a square term are included in the CMFP models.

Table 5.30: The ranks of the fitted models

		The true model				
Models	CMFP	MFP	GBM	Scheffé's	Ratio	
CMFP	1.5	2	1.5	1.5	5	
MFP	1.5	1	1.5	1.5	2	
GBM	4	3	3	3	3	
Scheffé's	5	4	4	4	4	
Ratio	3	5	5	5	1	

The Table of the ranks 5.30 shows the performance for each competing model of each true model scenario. 1st place indicates the best performance, but 1.5 is the average of 1st and 2nd place,

which is used when two models have the best performance. So, the CMFP and MFP models have the highest rank most often, while the GBM model is the most ranked third, which means it has moderate performance when fitted to the different true models. However, the Ratio model has the highest number of the fifth rank, which indicates it has the worst performance among all models. What is unexpected in Table 5.30 is that the CMFP model and the MFP model have better ranks than the fitted model whose type is the same as the true model in two scenarios, when the true model is Scheffé's model and when the true model is the GBM model.

To find a logical explanation for the above finding, Scheffé's model has been further investigated. We generated several samples (from Scheffé's model in this case). Then, Scheffé's and CMFP models were fitted to such samples to observe the optimal values of the mixture proportions produced from each model. The result is that the CMFP model is more stable in producing the optimal proportions of the mixture components $(\hat{x}_1, \dots, \hat{x}_q)$, which are close to the optimal ones, while Scheffé's model is inconsistent in producing these values. So, produced values from Scheffé's model are sometimes identical to those from the true model and other times clearly far from the true model's values. Furthermore, we investigated the scenario of the true GBM model, which has similar results to the true Scheffé's model scenario. Likewise, we found that the GBM model produced dissimilar proportions of the mixture components, which are sometimes identical to the true optimal ones and other times far from the optimal values of the true model. Figure 5.2 depicts an example of the magnitude of the difference between true Scheffé's, fitted Scheffé's, and CMFP models by providing the contour plots of the response surfaces of the true Scheffé's model, fitted Scheffé's model, and the CMFP model, respectively. Here, the last two plots were generated by fitting the respective models to a simulated dataset where the estimated optimal proportions are different from the true optimal proportions for Scheffé's model. We can see from Figure 5.2 that for this dataset, Scheffé's model estimates the maximum to occur in the interior of the experimental region, whereas it is close to the boundary.

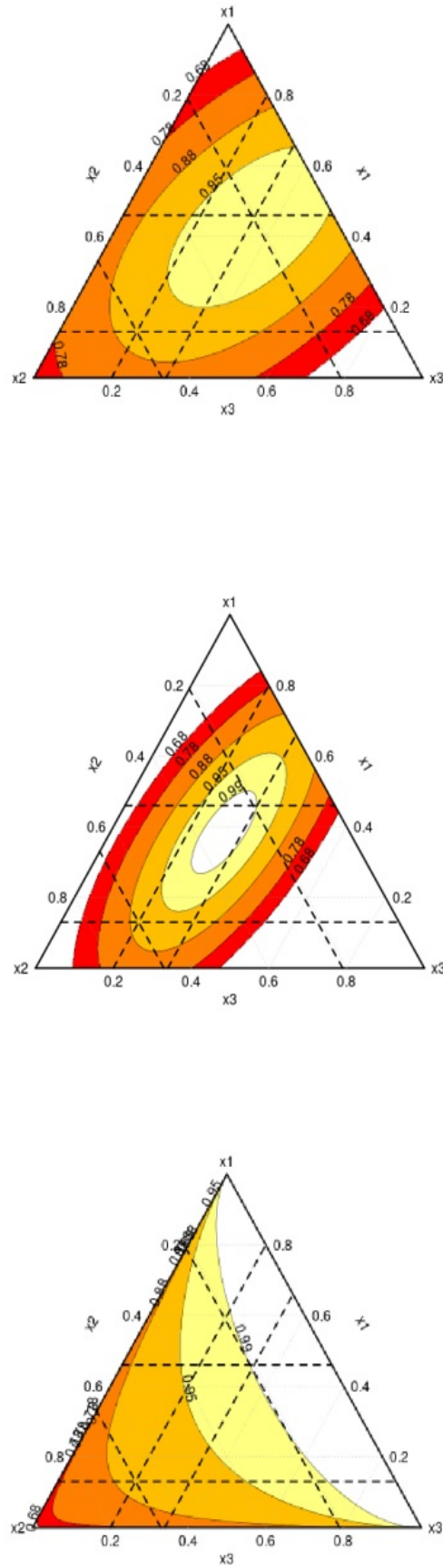


Figure 5.2: The contour plots of the response surfaces of the true Scheffé's model, fitted Scheffé's model, and the CMFP model, respectively

5.6 Optimal Mixture Proportions for a 3-Component Experiment with Two Process Variables

Goldfarb et al. (2003) studied throughput in a soap processing plant application where the amount of soap the process yields (in pounds per hour) is this experiment's primary interest. This soap blend consists of three mixture components (soap = x_1 , co-surfactant = x_2 , and filler = x_3). However, the proportions of these mixture components are subject to the following restrictions:

$$0.20 \leq x_1 \leq 0.80$$

$$0.15 \leq x_2 \leq 0.50$$

$$0.05 \leq x_3 \leq 0.30$$

Moreover, there are two process variables of interest in manufacturing mixture blends: plodder temperature (z_1) and mixing time (z_2). Low and high levels of plodder temperature will be considered in the experiment, as well as mixing time run at two levels, 0.5 hours and 1 hour, corresponding to -1 and 1, respectively. The soap processing experimental data is given in Table 8.7. To fit the competing models to the data of mixture experiments affected by two process variables, the extended forms of the models that include the terms of the process variables are used. Each type of model was fitted to this experimental dataset, and then the model with the smallest RSE was chosen. The realistic standard error that results when fitting the true models to this experimental dataset is big. For this reason, two different new datasets were generated by each true model by adding a big realistic standard error and a standard error equal to 0.5.

The Ratio model with denominator x_1 was the first chosen true model used to simulate data based on the soap processing experiment. The optimum values of the mixture proportions in the true model are given when $z_1 = -1$ and $z_2 = -1$, and they are 0.55, 0.15, and 0.30, respectively. Table 5.31 shows the outcome measures for all five competing models when simulating the mixture-process variables experiment data using the Ratio model when the error standard deviation equals 0.5.

Table 5.31: Outcome measures for all models when simulating data from the Ratio model, $s=0.5$

Models	AD	EFF	Mean $[x_1]$	Mean $[x_2]$	Mean $[x_3]$
Scheffé's	$4.69e - 05$	0.99989	0.54995	0.14998	0.29997
MFP	29.6864	0.93355	0.62423	0.14998	0.22568
CMFP	0.00023	0.99989	0.54995	0.14998	0.29997
GBM	0.00022	0.99989	0.54995	0.14999	0.29997
Ratio	$4.48e - 05$	0.99989	0.54995	0.14999	0.29990

The outcome measures of Scheffé's model are closest to the outcome measures of the Ratio model, and both can produce accurate optimal values of the mixture proportions. The MFP model has the furthest values of mixture proportions, but it got the proportion values of x_2 correctly as all other models did. However, Table 5.32 shows the effect on the outcome measures when data is generated with the realistic standard error.

Table 5.32: Outcome measures for all models when simulating data using the Ratio model, $s=25.37$

Models	AD	EFF	Mean $[x_1]$	Mean $[x_2]$	Mean $[x_3]$
Scheffé's	0.11602	0.99964	0.55052	0.14999	0.29940
MFP	25.7098	0.94240	0.62286	0.14999	0.22706
CMFP	0.42503	0.99895	0.55204	0.14999	0.29787
GBM	5.91609	0.98668	0.57479	0.14999	0.27512
Ratio	0.32022	0.99918	0.55091	0.14999	0.29900

According to the outcome measures, the proportion values of the mixture components became slightly further from the true optimal values for all fitted models except the MFP model. Nevertheless, Scheffé's model has the best outcome measures, and the MFP model still has the worst.

Scheffé's model was the second true model used to simulate data based on the soap processing experiment. The optimal proportion values of the true Scheffé's model are given when $z_1 = 1$, and $z_2 = -1$ for x_1 , x_2 , and x_3 and they are 0.799, 0.15, and 0.05 respectively. Table 5.33 shows the outcome measures for all five competing models when the true model is Scheffé's model, and the standard deviation is equal to 0.5.

Table 5.33: Outcome measures for all models when simulating data using Scheffé's model, $s=0.5$

Models	AD	EFF	Mean $[x_1]$	Mean $[x_2]$	Mean $[x_3]$
Scheffé's	0.0	0.99999	0.79992	0.149985	0.049995
MFP	0.0	0.99989	0.79992	0.149985	0.049995
CMFP	0.0	0.99989	0.79992	0.149985	0.049995
GBM	$4.34e - 05$	0.99989	0.79992	0.149985	0.049995
Ratio	0.0	0.99999	0.79992	0.149985	0.049995

It is obvious that all fitted models got the optimal values of the mixture proportions accurately. Table 5.34 demonstrates outcome measures for all five competing models when each fitted to the new datasets generated by adding the realistic standard error.

Table 5.34: Outcome measures for all models when simulating data using Scheffé's model, $s=44.79$

Models	AD	EFF	Mean [x_1]	Mean [x_2]	Mean [x_3]
Scheffé's	0.33473	0.99920	0.79927	0.14999	0.05065
MFP	20.8496	0.95563	0.76321	0.14999	0.08670
CMFP	0.03184	0.99983	0.79986	0.14999	0.05005
GBM	1.75339	0.99623	0.79775	0.14999	0.05216
Ratio	1.95102	0.99581	0.79648	0.14999	0.05343

The CMFP model has the best outcome measures, indicating that it produced accurate values for the mixture proportions. In contrast, the MFP model had the worst outcome measures among all models.

The third true model from which we simulated the data was the GBM model. The optimal proportion values of the true GBM model are given when $z_1 = -1$ and $z_2 = 1$, and they are 0.55, 0.15, and 0.30, respectively. Table 5.35 shows the outcome measures for all five competing models when the true model is the GBM model and the error standard deviation is equal to 0.5.

Table 5.35: Outcome measures for all models when simulating data using the GBM model, $s=0.5$

Models	AD	EFF	Mean [x_1]	Mean [x_2]	Mean [x_3]
Scheffé's	0.0	0.99899	0.54995	0.14999	0.29997
MFP	0.07	0.99976	0.55015	0.14999	0.29977
CMFP	0.0	0.99989	0.54995	0.14999	0.29997
GBM	0.0	0.99899	0.54995	0.14999	0.29997
Ratio	0.0	0.99899	0.54995	0.14999	0.29997

Although the outcome measures of the MFP model indicate that it produced values slightly different from the true optimal proportions, in general, all fitted models can have accurate optimal values for the mixture proportions, as is evident in Table 5.35. However, Table 5.36 shows changes in outcome measures for all five competing models when each was fitted to the new datasets generated by adding the realistic standard error.

Table 5.36: Outcome measures for all models when simulating data using the GBM model, $s=29.59$

Models	AD	EFF	Mean $[x_1]$	Mean $[x_2]$	Mean $[x_3]$
Scheffé's	0.04616	0.99979	0.55012	0.14999	0.29979
MFP	18.0120	0.96081	0.61069	0.14999	0.23922
CMFP	6.27417	0.98627	0.56939	0.15139	0.27913
GBM	1.00149	0.99773	0.55371	0.14999	0.29621
Ratio	0.00452	0.99989	0.54996	0.14999	0.29996

According to the outcome measures of the Ratio model, it has the best outcome measures among all models, while the MFP model has the worst outcome measures among all models.

Likewise, the MFP model was the fourth true model used to simulate this data. The optimal proportion values of the true MFP model are given when $z_1 = -1$ and $z_2 = 1$, and they are 0.76, 0.15, and 0.089, respectively. Table 5.37 shows the outcome measures for all five competing models when the true model is the MFP model, and the standard error is equal to 0.5.

Table 5.37: Outcome measures for all models when simulating data using the MFP model, $s=0.5$

Models	AD	EFF	Mean $[x_1]$	Mean $[x_2]$	Mean $[x_3]$
Scheffé's	2.21989	0.99473	0.79991	0.14999	0.04999
MFP	0.00132	0.99989	0.76111	0.14999	0.08880
CMFP	2.21989	0.99473	0.79991	0.14999	0.04999
GBM	2.21989	0.99473	0.79991	0.14999	0.04999
Ratio	0.88873	0.99783	0.72799	0.14999	0.12192

The outcome measures for Scheffé's model, CMFP model, and GBM model have similar results, but the Ratio model has the outcome measures that are closest to those of the MFP model. When each competing model was fitted to the new datasets generated by adding the realistic standard error, the outcome measures changed for all models, which indicates that all models produce values for the mixture proportions different from the optimal true proportions. Table 5.38 demonstrates outcome measures for all five competing models.

Table 5.38: Outcome measures for all models when simulating data using the MFP model, $s=47.3$

Models	AD	EFF	Mean $[x_1]$	Mean $[x_2]$	Mean $[x_3]$
Scheffé's	8.23815	0.98073	0.71311	0.15039	0.13639
MFP	3.16541	0.99253	0.74109	0.14998	0.10883
CMFP	7.38619	0.98271	0.72126	0.15037	0.12827
GBM	9.72349	0.97727	0.69135	0.15030	0.15825
Ratio	7.12503	0.98332	0.72005	0.15316	0.12669

According to the outcome measures of all fitted models, all models obtain values slightly different from the optimal values of the mixture proportions. In comparison, the Ratio and CMFP models have close outcome measures and are better than the outcomes measures of the GBM model and Scheffé's model.

The CMFP model was the fifth true model used to simulate this data. The optimal proportion values of the true CMFP model are given when $z_1 = -1$ and $z_2 = 1$, and they are 0.55, 0.15, and 0.299, respectively. Table 5.39 shows the outcome measures for all five competing models when the true model is the CMFP model, and the standard error equals 0.5. All fitted models except the MFP model can produce accurate values of the mixture proportions identical to the true values of mixture proportions from the true model.

Table 5.39: Outcome measures for all models when simulating data using the CMFP model, $s=0.5$

Models	AD	EFF	Mean $[x_1]$	Mean $[x_2]$	Mean $[x_3]$
Scheffé's	0.0	0.99989	0.54995	0.14999	0.29997
MFP	8.13	0.98131	0.62066	0.14999	0.22925
CMFP	0.0	0.99989	0.54995	0.14999	0.29997
GBM	0.0	0.99989	0.54995	0.14999	0.29997
Ratio	0.0	0.99989	0.54995	0.14999	0.29997

Also, the changes in outcome measures for all five competing models when each was fitted to the new datasets generated using the realistic standard error are shown in Table 5.40.

Table 5.40: Outcome measures for all models when simulating data using the CMFP model, $s=19.33$

Models	AD	EFF	Mean $[x_1]$	Mean $[x_2]$	Mean $[x_3]$
Scheffé's	0.01875	0.99986	0.55012	0.14999	0.29979
MFP	9.40702	0.97840	0.63519	0.14999	0.21473
CMFP	4e - 08	0.99989	0.54995	0.14999	0.29997
GBM	0.46096	0.99885	0.55424	0.14999	0.29568
Ratio	0.45294	0.99887	0.55330	0.15005	0.29655

The outcome measures of Scheffé's model are closest to the outcome measures of the true CMFP model, while the MFP model has the worst outcome measures among all models.

5.6.1 Summary

- When generating data from a true model by adding a standard error of 0.5, all competing models except the MFP model have similar outcome measures and can produce accurate optimal proportion values for mixture components like those obtained from the true model.
- When generating data from a true model by adding a realistic standard error, the fitted model, whose type is the same as the true model, can produce values that are closest to the true optimal values of mixture proportion, often in only two scenarios: the true CMFP model and the true MFP model.
- Each true model has the same optimal proportion of x_2 . Thus, all fitted models can find the optimal proportion values of component x_2 in all scenarios.
- Overall, the MFP model has the worst outcome measures among all competing models in most scenarios.

Table 5.41: The models' ranks when the standard errors equal 0.5

The true model					
Models	CMFP	MFP	GBM	Scheffé's	Ratio
CMFP	2.5	4	2.5	2.5	4
MFP	5	1	5	2.5	5
GBM	2.5	4	2.5	5	3
Scheffé's	2.5	4	2.5	2.5	2
Ratio	2.5	2	2.5	2.5	1

Table 5.42: The models' ranks when the standard errors have realistic values

The true model					
Models	CMFP	MFP	GBM	Scheffé's	Ratio
CMFP	1	3	4	1	3
MFP	5	1	5	5	5
GBM	4	5	3	3	4
Scheffé's	2	4	2	2	1
Ratio	3	2	1	4	2

Table 5.41 and Table 5.42 are the rank tables that show the performance of each competing model in all true model scenarios. The common ranks are what distinguish Table 5.41.

The scenario of the true Ratio model is the only one that does not contain common ranks when fitting models to datasets that are generated by adding the small standard errors. In Table 5.42,

the CMFP model has the first rank twice, which means it has the best performance among all competing models in the scenarios of the true Scheffé's model and the true CMFP model. At the same time, the MFP model has the highest number of the fifth ranks, which indicates it has the worst performance among all models in all scenarios except for the true MFP model scenario. However, according to ranks Table 5.42, Scheffé's model and the Ratio model often have better performance than the GBM model when fitted to the different scenarios of the true models.

Regarding the results of the MFP model, we should clarify that it has the most variation in producing the values of the mixture proportions. Thus, its estimated maximum is furthest from the true maximum in each scenario. For example, in Table 5.34, Scheffé's model is the true model, and the optimal values of the mixture proportions for this case are 0.799, 0.15, 0.05. However, the values produced from the MFP model could be 0.55, 0.15, and 0.30, although it can sometimes get the correct values of proportions. Three figures of the contour plots of the response surfaces of three different cases of the MFP model: true (fitted the MFP model to data generated from the MFP model without error), good (fitted the MFP model to data generated from the MFP model with accurate values of mixture proportions), and bad (fitted the MFP model to data generated from the MFP model with inaccurate values of mixture proportions) respectively. As shown in Figure 5.3, there are no big differences between the response surfaces for all cases of the MFP model. However, when looking closely at the maximum and minimum positions for each case, we can notice the subtle differences between each response surface.

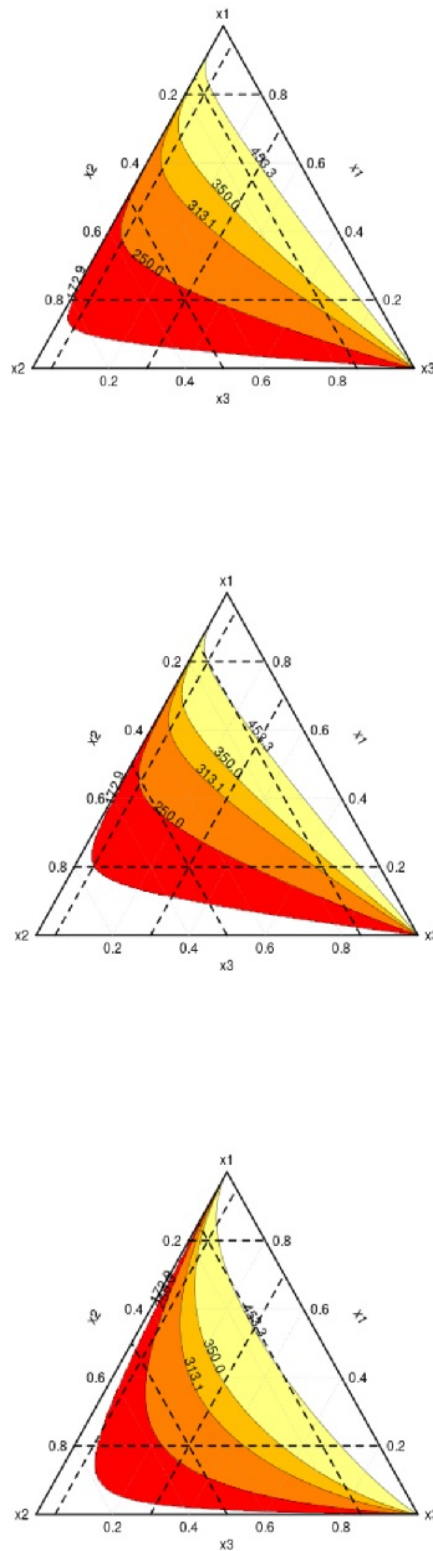


Figure 5.3: The contour plots of the response surfaces of three different cases of the MFP model: true, good, and bad models, respectively

5.7 Overall Summary

- The optimal proportion of mixture components was found through a simulation process that was based on four experimental datasets with 5 'true' scenarios each.
- Outcome measures based on 10,000 simulation runs have been used to measure how close each fitted model's resulting mixture proportions are to the true optimal proportions.
- In most scenarios, the fitted model, whose type is the same as the true model, produces values closest to the true optimal proportions of the mixture. However, there are special cases in which a fitted model with a different type of true model can get optimal values of proportions identical to the true optimal proportions.
- Practically, finding optimal proportions values for datasets with four mixture components is more complicated than for datasets with three mixture components, and we may need to use more reliable optimization algorithms to facilitate the process.
- This optimization approach that was used to find optimal values of mixture proportion was expanded to find the optimal setting of the process variables as well when simulating data of mixture-process variables experiments.
- Mostly in the case of simulating data of mixture-process variables experiments, the fitted model, which has the same type as the true model, can get values closest to the true optimal proportion only in the scenarios when the true model is the CMFP model or the MFP model.

Table 5.43 shows the total number of times each rank was obtained by each model according to the previous tables to summarize the performance of the models when fitted to the datasets generated by adding the realistic standard error.

Table 5.43: Overall distribution of ranks of all models

Models	Rank 1	Rank 2	Rank 3	Rank 4	Rank 5
CMFP	9	6	3	3	2
MFP	7	6	5	3	7
GBM	2	2	4	6	1
Scheffé's	3	5	2	6	4
Ratio	2	4	6	2	6

We can see from Table 5.43 that the CMFP models perform best according to this study. They have rank 1 most often (9 times), and when they are not best, then they are often second best. The performance of the MFP models is more mixed. While they have ranks 1 and 2 quite often, they also have the worst rank 7 times.

Chapter 6

Designing Experiments for CMFP

Models

An optimal design can make data collection and analysis more efficient, which leads to reliable conclusions in an economical way. In the first section of this chapter, we will introduce the area of optimal design of experiments, in particular in the context of mixture experiments. We will then find and visualize optimal continuous designs for CMFP models and study their robustness with respect to misspecifications of the model parameters and terms. Since only exact designs can be applied in practice, we next compare the performance of two strategies for finding (near-) optimal exact designs in Section 6.3. The chapter concludes with several examples of designs where a process variable is present.

6.1 Introduction

Approximate (continuous) designs are an essential tool in constructing optimal designs and, thus, are popular in the literature on optimal design. Although in practice, we can only apply exact designs, solving the optimization problems for finding approximate designs is more flexible than for exact designs in which the number of trials at any design point must be an integer. This flexibility is due to the fact that optimal continuous designs can be found independently of sample size. This

is because the observations' proportions in each design point \mathbf{x}_i in a continuous design can be real numbers varying continuously between 0 and 1. These proportions are called the weights and are denoted by w_i .

Suppose ξ is a design with n trials and n_i replicates, $i = 1, 2, \dots, m$, at distinct support points $\mathbf{x}_1, \mathbf{x}_2, \dots, \mathbf{x}_m$ where $n = \sum_{i=1}^m n_i$. Then this design can be expressed as a continuous design with weights w_i assigned to each support point where w_i satisfies $w_i = \frac{n_i}{n}$, and hence $\sum_{i=1}^m w_i = 1$.

This design can be represented as

$$\xi = \left\{ \begin{array}{cccc} \mathbf{x}_1 & \mathbf{x}_2 & \cdots & \mathbf{x}_m \\ w_1 & w_2 & \cdots & w_m \end{array} \right\}. \quad (6.1)$$

A continuous design ξ can be converted into an exact design directly if nw_i is an integer for all $i \in \{1, 2, \dots, m\}$. Otherwise, rounding has to be applied to nw_i , $i = 1, 2, \dots, m$.

A support point in ξ is \mathbf{x}_i where $\mathbf{x}_i = (x_{i1}, \dots, x_{iq})$ and the information matrix of a continuous design can generally be formulated as follows:

$$M(\xi) = \int_{\chi} f(\mathbf{x})f'(\mathbf{x})\xi(d\mathbf{x}) = \sum_{i=1}^m w_i f(\mathbf{x}_i) f'(\mathbf{x}_i), \quad (6.2)$$

where $f'(\mathbf{x}_i)$ is the row of the design matrix that corresponds to the design point \mathbf{x}_i and χ is the experimental region, which is also called the design space. Although much of the design work in the literature has focused on linear models, optimal designs for nonlinear models are required in many application fields. The main characteristic of nonlinear models is that their information matrix is based on the values of unknown parameters. Hence, the corresponding optimal designs also depend on unknown model parameters and are therefore called locally optimal designs (Chernoff, 1953). Thus, a point prior estimate of the unknown parameters is used to find (locally) optimal designs. According to Fedorov (2013), the most frequent technique to formulate a design problem for a nonlinear model is using a Taylor series expansion up to the first-order term around a given

value of the parameter vector, β_0 , to linearise the regression function $g(\mathbf{x}, \beta)$ in terms of β_c where $c \in \{1, 2, \dots, P\}$. So, the model function becomes

$$g(\mathbf{x}, \beta) \approx g(\mathbf{x}, \beta_0) + \sum_{c=1}^P \left(\left. \frac{\partial g(\mathbf{x}, \beta)}{\partial \beta_c} \right|_{\beta_c = \beta_{c0}} \right) (\beta_c - \beta_{c0}) \quad (6.3)$$

where $\left. \frac{\partial g(\mathbf{x}, \beta)}{\partial \beta_c} \right|_{\beta_c = \beta_{c0}} = f(\mathbf{x}, \beta)$ is the partial derivative of the considered nonlinear regression with respect to parameters in the model, which is the row elements of the design matrix. β and β_0 are $P \times 1$ dimensional vectors where P is the number of parameters in the model. The value of β_0 is often chosen as the prior point estimate of the unknown β . In what follows, we will, however, use the notation $f(\mathbf{x})$ for both linear and nonlinear models. For example, to find $f(\mathbf{x})$ for a first-order CMFP model, such as $g(\mathbf{x}, \beta) = \beta_0 + \beta_1 \left(\frac{x_1}{1-x_1} \right)^{(\alpha)} + \beta_2 \left(\frac{x_2}{1-x_2} \right)^{(\alpha)}$, we find the partial derivative of this model with respect to each parameter (in this model there are four parameters $\alpha, \beta_0, \beta_1, \beta_2$). So, $f(\mathbf{x})$ has four elements and they are: $f(\mathbf{x}) = \left(1, \left(\frac{x_1}{1-x_1} \right)^\alpha, \left(\frac{x_2}{1-x_2} \right)^\alpha, \beta_1 \left(\frac{x_1}{1-x_1} \right)^\alpha \log \left(\frac{x_1}{1-x_1} \right) + \beta_2 \left(\frac{x_2}{1-x_2} \right)^\alpha \log \left(\frac{x_2}{1-x_2} \right) \right)$.

Optimality criteria measures are used to assess the quality of a design, and they help researchers determine which design is the most efficient for the experiment's objectives. An optimality criterion could be related to minimizing experimental error, maximizing statistical power, or reducing parameter estimation variance. So, optimality criteria are different depending on the goals of an experiment conducted. As we are looking for efficient and reliable estimates for all the model parameters simultaneously, we need an optimality criterion that ensures that the information obtained from the experimental data is spread evenly across the parameters, resulting in a robust and accurate estimation process. D-optimality is the most widely used optimization criterion for selecting designs, as it focuses on obtaining a design that provides precise estimates for all the model parameters. The D-optimal design is obtained by maximization of the determinant of the information matrix. A design ξ^* is D-optimal if

$$|M(\xi^*)| = \max_{\xi} |M(\xi)| \quad (6.4)$$

Therefore, a design with a bigger determinant of the information matrix is considered more efficient

and preferable according to the D-optimality criterion. The obtained designs can help maximize the information that is gained from the experiment and improve the efficiency of parameter estimates. Various algorithms and optimization techniques can be used to find approximate designs that satisfy the D-optimal criterion. So, we intend to find the locally D-optimal designs in constrained experimental regions for CMFP models. We will next explain and illustrate, through an example, how we find locally D-optimal designs and how we can check if these designs are indeed D-optimal.

Since we are concerned with the mixture problem, we deal with optimization problems in a restricted area where the components are subject to natural and additional constraints. For constrained optimization, the `constrOptim` function in the R software was applied to find the optimal values of the component proportions x_{ir} and their corresponding optimal weights w_i . It needs a guess of the initial starting values of the components' proportions and their allocated weights. Then, the `constrOptim` process optimizes the function subject to equality and inequality constraints. However, the starting value must be in the feasible region, which is defined by $\mathbf{u}_i \times \boldsymbol{\theta} - \mathbf{c}_i \geq 0$, where \mathbf{u}_i is the $(k \times p)$ constraint matrix, $\boldsymbol{\theta}$ is the vector of the initial guess values and \mathbf{c}_i is the constraint vector of length k . The restrictions $\sum_r^q x_{ir} = 1$, for all \mathbf{x}_i , $i = 1, \dots, m$ and $\sum_i^m w_i = 1$, are placed on both x_{ir} , and w_i so these values must be varying between 0 and 1.

To explain the `constrOptim` process, we provide an example below. Here, we consider the CMFP model with 3 components and one power parameter (same α) to find the constraint matrix \mathbf{u}_i and the constraint vector \mathbf{c}_i . We should have at least four support points for estimating the model parameters since the model has four parameters (Atkinson et al., 2007). We refer to Section 5.3 the example of feeding chicks where restrictions on the proportion of energy supplementation are set as: $0.05 \leq x_{i1} \leq 0.40$, $0.02 \leq x_{i2} \leq 0.89$, $0.06 \leq x_{i3} \leq 0.86$. Assume four support points $\mathbf{x}_1 = (x_{11}, x_{12}, x_{13})$, $\mathbf{x}_2 = (x_{21}, x_{22}, x_{23})$, $\mathbf{x}_3 = (x_{31}, x_{32}, x_{33})$, $\mathbf{x}_4 = (x_{41}, x_{42}, x_{43})$, with weights assigned to each support point w_1 , w_2 , w_3 , and w_4 . Then, constraint matrix \mathbf{u}_i , in this case, can be expressed as in Table 6.1. For simplicity, $0.05 \leq x_{11}, x_{11} \leq 0.40 \rightarrow -x_{11} \geq -0.40$ results in the first and second row. We can use a similar method for all proportions, all support points, and all

weights. Rows 1 - 6 are for the first point, and rows 19 - 24 are for the fourth point. However, the last four rows correspond to the weights.

To get the constraint vector \mathbf{c}_i , all of its elements correspond to the numerical value on the right hand side of each inequality, which we can find to construct the above matrix. So the resulting constraint vector is: $\mathbf{c}_i = (0.05, -0.40, 0.02, -0.89, -0.94, 0.14, 0.05, -0.40, 0.02, -0.89, -0.94, 0.14, 0.05, -0.4, 0.02, -0.89, -0.94, 0.14, 0.05, -0.40, 0.02, -0.89, -0.94, 0.14, 0, 0, 0, -1)$. After the matrix \mathbf{u}_i and the vector \mathbf{c}_i are obtained, we can use the `constrOptim` method, and the statistical D-optimum criterion is our objective function. The optimal weights and proportions of the components resulting from the constrained optimization are represented in Table 6.2.

Table 6.2: D-optimal 4-point design for a first-degree CMFP model

Design points	Weights
$\mathbf{x}_1=(0.05,0.09,0.86)$	$w_1=0.250$
$\mathbf{x}_2=(0.39,0.54,0.07)$	$w_2=0.250$
$\mathbf{x}_3=(0.17,0.15,0.68)$	$w_3=0.250$
$\mathbf{x}_4=(0.39,0.02,0.59)$	$w_4=0.250$

To check if the optimized design using `constrOptim` is an optimal continuous design or not, we can apply the equivalence theorem for D-optimum design by letting

$$d(\mathbf{x}, \boldsymbol{\xi}) = f(\mathbf{x})M^{-1}(\boldsymbol{\xi})f'(\mathbf{x}) \quad (6.5)$$

where $d(\mathbf{x}, \boldsymbol{\xi})$ is a function of the design $\boldsymbol{\xi}$ and the point \mathbf{x} is a point within the design space. This function is called the sensitivity function (Fedorov & Hackl, 1997), and it is the basic tool on which continuous optimization design theory is based to check the optimization mechanism. If $d(\mathbf{x}, \boldsymbol{\xi}) \leq P$ (number of model parameters) for all \mathbf{x} in the experimental region, then the optimized design is a D-optimal continuous design. To illustrate, we check whether the optimal 4-point design in Table 6.2 satisfies the equivalence theorem by first substituting all obtained design points in the sensitivity function (6.5) of the first-degree CMFP model with one power parameter. The numerical expression for $d(\mathbf{x}, \boldsymbol{\xi})$ in this case is:

$$\begin{aligned}
d(\mathbf{x}, \boldsymbol{\xi}) = & 62205.27 - 57315.59 \left(\frac{x_{i1}}{1-x_{i1}}\right)^{0.11} - 4337.07 \left(\frac{x_{i2}}{1-x_{i2}}\right)^{0.11} + 7461.81 \left(\frac{x_{i1}}{1-x_{i1}}\right)^{0.11} \log\left(\frac{x_{i1}}{1-x_{i1}}\right) + \\
& 594.54 \left(\frac{x_{i2}}{1-x_{i2}}\right)^{0.11} \log\left(\frac{x_{i2}}{1-x_{i2}}\right) - 57313.83 \left(\frac{x_{i1}}{1-x_{i1}}\right)^{0.11} + 52851.86 \left(\frac{x_{i1}}{1-x_{i1}}\right)^{0.22} + 3948.26 \left(\frac{x_{i1}}{1-x_{i1}}\right)^{0.11} \\
& \left(\frac{x_{i2}}{1-x_{i2}}\right)^{0.11} - 6871.21 \left(\frac{x_{i1}}{1-x_{i1}}\right)^{0.22} \log\left(\frac{x_{i1}}{1-x_{i1}}\right) - 547.83 \left(\frac{x_{i1}}{1-x_{i1}}\right)^{0.11} \left(\frac{x_{i2}}{1-x_{i2}}\right)^{0.11} \log\left(\frac{x_{i2}}{1-x_{i2}}\right) - 4337.12 \\
& \left(\frac{x_{i2}}{1-x_{i2}}\right)^{0.11} + 3948.26 \left(\frac{x_{i1}}{1-x_{i1}}\right)^{0.11} \left(\frac{x_{i2}}{1-x_{i2}}\right)^{0.11} + 358.25 \left(\frac{x_{i2}}{1-x_{i2}}\right)^{0.22} - 516.36 \left(\frac{x_{i1}}{1-x_{i1}}\right)^{0.11} \left(\frac{x_{i2}}{1-x_{i2}}\right)^{0.11} \\
& \log\left(\frac{x_{i1}}{1-x_{i1}}\right) - 41.17 \left(\frac{x_{i2}}{1-x_{i2}}\right)^{0.22} \log\left(\frac{x_{i2}}{1-x_{i2}}\right) + 14.09(529.14 \left(\frac{x_{i1}}{1-x_{i1}}\right)^{0.11} \log\left(\frac{x_{i1}}{1-x_{i1}}\right) + 42.19 \left(\frac{x_{i2}}{1-x_{i2}}\right)^{0.11} \\
& \log\left(\frac{x_{i2}}{1-x_{i2}}\right)) - 0.12.986 \left(\frac{x_{i1}}{1-x_{i1}}\right)^{0.11} (529.14 \left(\frac{x_{i1}}{1-x_{i1}}\right)^{0.11} \log\left(\frac{x_{i1}}{1-x_{i1}}\right) + 42.19 \left(\frac{x_{i2}}{1-x_{i2}}\right)^{0.11} \log\left(\frac{x_{i2}}{1-x_{i2}}\right)) - \\
& 976 \left(\frac{x_{i2}}{1-x_{i2}}\right)^{0.11} (529.14 \left(\frac{x_{i1}}{1-x_{i1}}\right)^{0.11} \log\left(\frac{x_{i1}}{1-x_{i1}}\right) + 42.19 \left(\frac{x_{i2}}{1-x_{i2}}\right)^{0.11} \log\left(\frac{x_{i2}}{1-x_{i2}}\right)) + 0.0032(529.14 \\
& \left(\frac{x_{i1}}{1-x_{i1}}\right)^{0.11} \log\left(\frac{x_{i1}}{1-x_{i1}}\right) + 42.19 \left(\frac{x_{i2}}{1-x_{i2}}\right)^{0.11} \log\left(\frac{x_{i2}}{1-x_{i2}}\right))^2.
\end{aligned}$$

The sensitivity functions for the points of the optimized design in Table 6.2 is: $d(\mathbf{x}_1, \boldsymbol{\xi}) = 3.99$, $d(\mathbf{x}_2, \boldsymbol{\xi}) = 3.99$, $d(\mathbf{x}_3, \boldsymbol{\xi}) = 4.00$, $d(\mathbf{x}_4, \boldsymbol{\xi}) = 3.99$. As the design points satisfy the condition equal to or less than value 4 (the number of parameters), this design may be D-optimal.

To show the optimality of a design, we next need to show that $d(\mathbf{x}, \boldsymbol{\xi}) \leq P$ for all \mathbf{x} in the experimental region. For the simplest scenario with three mixture components, this could be done graphically by generating a contour plot of $d(\mathbf{x}, \boldsymbol{\xi})$ in the experimental region and checking if P is exceeded. For more complicated cases, this is no longer feasible. Therefore, instead, we evaluated the sensitivity function at a large selection of further points from the experimental region. This way, we can be reasonably confident the design we found is D-optimal or at least close to being D-optimal.

We generated designs with different numbers of support points by optimizing initial designs using the `constrOptim` function and observing the design with the maximum determinant of the information matrix to get the near D-optimal design. We must provide initial design points and their weights in the `constrOptim` function. These initial values of the design points should be in the feasible region of the `constrOptim` function, and they could be arbitrary or used by the XVERT/Fillv approach, which is described below in a different context. So, we tried the design with the number of support points equal to the number of model parameters, then we checked the design when support points increased by one more than the number of model parameters, and so

on until the condition of the equivalence theorem was satisfied or at least close to being satisfied. Applying the equivalence theorem by evaluating the sensitivity function (6.5) is a background process we kept doing for the CMFP models while searching for optimal designs. Optimizing a design within a restricted region with several constraints makes the search for the optimal design more challenging. Therefore, we always tried several different starting designs. We still could not always find a design that strictly satisfied the equivalence theorem, but they were close. (The maximum of $d(\mathbf{x}, \boldsymbol{\xi})$ on our grid of points did not exceed P by more than 5%). Therefore, the continuous designs presented here should be viewed as near-optimal rather than strictly optimal.

Unless all products of the weights with the sample size result in integer values, we cannot use continuous designs directly for an experiment. Therefore, we will next describe a method to find optimal exact designs. The choice of algorithm often depends on the specific needs of the search purpose and the experimental design problem. Several algorithms which offer different approaches to optimizing experimental designs have been developed. Some notable algorithms that have been used in constructing and optimizing designs include the simulated annealing algorithm (Kirkpatrick et al., 1983), known for its simplicity and general applicability but also for its slow convergence that requires a large number of iterations. The tabu search algorithm (Glover, 1986) is another alternative algorithm that uses memory structures to avoid getting stuck in local optima. Still, it needs more memory to store the moves' history and is more complex to implement than the exchange algorithm. Furthermore, the genetic algorithm (Goldberg, 1989) is beneficial for highly complex or non-linear design spaces. Still, it is more computationally intensive than the exchange algorithm and suffers from the complexity of implementation and parameter tuning.


The coordinate exchange algorithm, proposed by Meyer and Nachtsheim (1995), is a significant approach in constructing exact optimal designs. The key idea behind the exchange algorithm is that optimizing subsets of variables individually can potentially find better solutions than traditional optimization methods. The exchange algorithm depends on the choice of initial design, which is a limitation in optimizing some experiments. It is therefore recommended to try different initial designs to reduce the risk of getting stuck in a local optimum. In our research study, we

always found a candidate set of points that covered the design space well, using the XVERT/Fillv approach described below. We then used 100 random starting designs consisting of points from the candidate set. Hence, the exchange algorithm is a powerful optimization tool in this research to find locally optimal designs as, through the choice of the candidate set, takes into account the constraints imposed by the mixture components. Before illustrating the procedure of this algorithm, the XVERT algorithm suggested in Snee and Marquardt (1974) needs to be described first. It is a procedure to generate the coordinates of all extreme vertices of a constrained area, as in the following steps:

- Rank the components in terms of their ranges, where x_1 has the smallest range and x_q has the largest range.
- Form 2^{q-1} combinations of two-level designs from the upper and lower bounds of the components.
- Use $(x_q = 1 - \sum_{r=1}^{q-1} x_r)$ to compute the level of the q^{th} component.
- A given point should be an extreme vertex while satisfying $L_r \leq x_r \leq U_r$. Otherwise, the proportion that is outside the range should be set equal to the upper or the lower limit, whichever is closer to the computed value.
- Generate additional points from points that are out of bounds by adjusting the component level by an amount equal to the difference between computed values for x_q and the substituted upper and lower limits.

To clarify these steps, suppose there are limits on the proportions of the components as follows: $0.05 \leq x_1 \leq 0.40, 0.02 \leq x_2 \leq 0.89, 0.06 \leq x_3 \leq 0.86$. First, calculate the range of each component and rank components in order of increasing ranges. We found that x_1 has the smallest range while x_2 has the largest range. Then, we can form four combinations of two-level design with the components x_1 and x_3 as follows $L_1L_3 \quad L_1U_3 \quad U_1L_3 \quad U_1U_3$. After that, we determine the levels of the omitted components x_2 .

Points	x_1	x_2	x_3
A	0.05	0.89	0.06
B	0.05	0.09	0.86
C	0.40	0.54	0.06
D	0.40	-0.26	0.86



Points	x_1	x_2	x_3
A	0.05	0.89	0.06
B	0.05	0.09	0.86
C	0.40	0.54	0.06
D1	0.40	0.02	0.58
D2	0.12	0.02	0.86

We obtained extreme vertices A, B, and C, which are in the core group, while point D needs to be adjusted because the value -0.26 is outside the limits.

We compute the difference between computed values for x_2 in point D and the lower limit of x_2 , which equals 0.28. Then, the x_2 value is modified to be 0.02, while we subtract the value 0.28 once from x_3 and again from x_1 . This procedure generates two additional points from point D, which are D1 and D2. From these points, we can produce some candidate subgroups for each such point. The centroids and overall centroids points are additional points that can be found by grouping and averaging the vertices that we represented above into groups of two or more vertices, where each vertex has the same value of x_q for one of the components. For instance, A and B vertices have the proportion x_1 in common, that is $x_1 = 0.05$; by grouping these vertices and averaging their compositions, we got a centroid of the two points (A and B) that define a face. All remaining centroid points can be found by following a similar process. In order to further fill the design space with possible design points, we apply a function called Fillv in R, which successively picks points in the middle between the points we already have. We stop the XVERT/Fillv algorithm when the set of points it has produced is sufficiently large and spread out across the design space to become the candidate set for the exchange algorithm.

After describing the methodology of XVERT that finds the boundaries of a region defined by placing limits on the proportions of the mixture components and the Fillv function that fills the space between these points, the procedure of the exchange algorithm will be illustrated as follows: First, generate an initial design of size n (predefined) chosen with replacement from candidate design points found using the XVERT/Fillv algorithm. Then, exchange the first point in the initial

design with each candidate point and evaluate the determinant of the resulting information matrix in each replacement. Then, replace the initial point with the candidate point, which provides the optimum criterion value to improve the design. If none of the candidate points improves the design, keep the point from the initial design. Finally, repeat the same procedure for each point in the initial design. The design search continues until no exchange improves the criterion, and if there is no exchange, the process will stop. The entire procedure of this algorithm can be repeated for many different random initial designs to gain more confidence that the designs are near D-optimal for the area we are interested in.

To further explain the procedure of this algorithm, suppose that our problem is to find a near-optimal design for a constrained region with three restricted mixture components $0.05 \leq x_1 \leq 0.40$, $0.02 \leq x_2 \leq 0.89$, $0.06 \leq x_3 \leq 0.86$ and the first order CMFP model is to be fitted on this restricted region. The restricted experimental region of this example is shown in Figure 6.1.

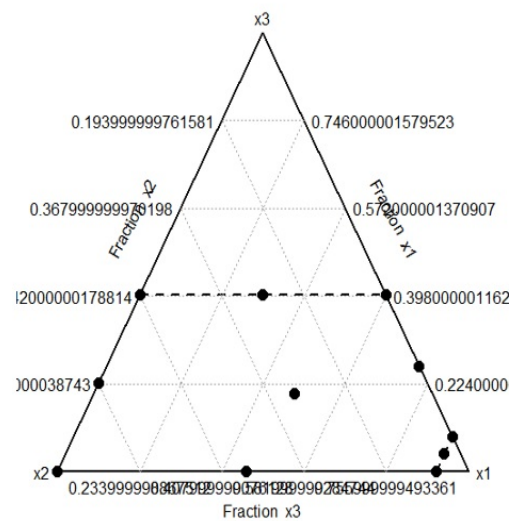


Figure 6.1: A restricted experimental region

Various random starting designs (the number of tries specified here is $N = 100$) are generated with replacements from already found candidate points by applying the XVERT/Fillv algorithm (1001 candidate points found in this case). After this, try every possible exchange for each point in the initial design with each candidate point and calculate the optimum criterion under consideration. If no exchange improves the criteria, then stop. The entire procedure was repeated under the

current example for 100 tries. Table 6.3 provides the initial and resulting designs after performing this process for a first-order CMFP model under the D-optimality criterion. Also, the values of the determinants of these designs are provided at the bottom of this table.

Table 6.3: Initial Design and Optimal Design for the example

Initial Design			Optimal Design		
x_1	x_2	x_3	x_1	x_2	x_3
0.20	0.31	0.49	0.40	0.02	0.58
0.18	0.28	0.54	0.05	0.89	0.06
0.24	0.10	0.66	0.05	0.89	0.06
0.32	0.19	0.49	0.40	0.02	0.58
0.26	0.02	0.72	0.05	0.09	0.86
0.15	0.39	0.46	0.05	0.89	0.06
0.23	0.17	0.60	0.05	0.09	0.86
0.10	0.04	0.86	0.40	0.02	0.58
0.25	0.26	0.49	0.05	0.89	0.06
0.23	0.17	0.60	0.05	0.09	0.86
0.27	0.33	0.40	0.40	0.02	0.58
0.18	0.43	0.39	0.40	0.54	0.06
0.22	0.24	0.54	0.05	0.89	0.06
0.17	0.03	0.80	0.05	0.09	0.86
0.32	0.28	0.40	0.40	0.02	0.58
0.14	0.47	0.39	0.05	0.09	0.86
0.24	0.26	0.50	0.05	0.89	0.06
0.21	0.14	0.65	0.40	0.02	0.58
0.15	0.19	0.66	0.40	0.54	0.06
0.35	0.22	0.43	0.18	0.76	0.06
0.18	0.43	0.39	0.05	0.89	0.06
0.09	0.65	0.26	0.18	0.76	0.06
0.40	0.22	0.38	0.18	0.76	0.06
0.32	0.26	0.42	0.17	0.36	0.47
0.21	0.14	0.65	0.17	0.36	0.47
0.16	0.21	0.63	0.18	0.76	0.06
0.16	0.18	0.66	0.17	0.46	0.37
0.26	0.15	0.59	0.17	0.46	0.37
0.15	0.22	0.63	0.17	0.36	0.47
0.28	0.50	0.22	0.40	0.54	0.06
83909578			21489380578		

Looking more closely at the design generated by the algorithm, we find that all selected points were vertices and repeated. Furthermore, the D-criterion for the initial design and near-optimal design is 83909578 and 21489380578, respectively, and thus the optimal designs significantly improved

the initial design. The computational time required to run this method is about four minutes per scenario for all examples in this chapter, except for the four mixture components example, which takes about thirty-three minutes per scenario because the candidate sets generated by the XVERT/Fillv algorithm for this case are much larger than those that are used in the three mixture components examples. The designs before and after applying the exchange algorithm are shown in Figure 6.2, where it is clear that the initial design, where most of its points are internal points, is then improved by making most of the design points vertices.

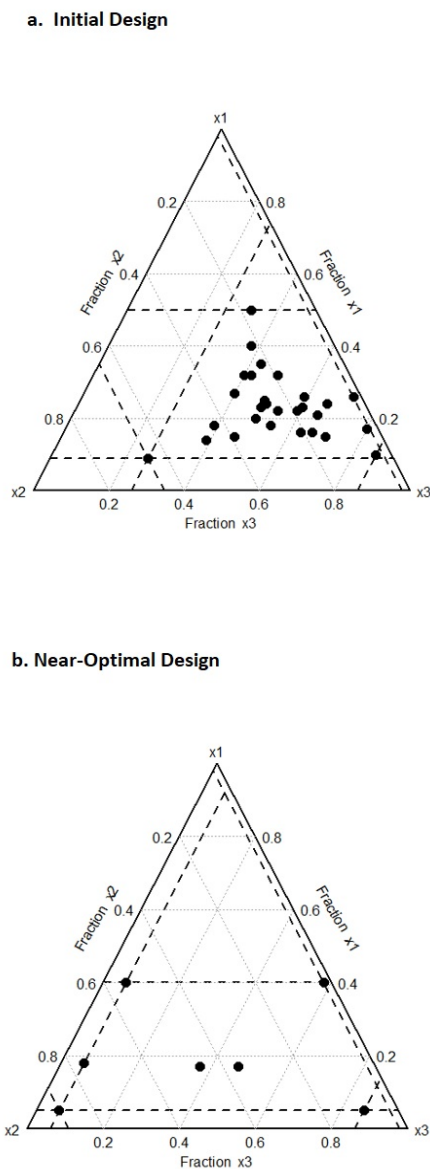


Figure 6.2: a. The initial design, and b. The near-optimal design

To compare the performance of designs, we can use a concept called relative D-efficiency. This efficiency is used to compare the goodness of two designs ξ_1 in the numerator relative to ξ_2 in the denominator by their information matrices $M(\xi_1)$ and $M(\xi_2)$, respectively. The relative D-efficiency is defined as:

$$D_{\text{rel-eff}} = \left\{ \frac{|M(\xi_1)|}{|M(\xi_2)|} \right\}^{\frac{1}{p}}, \quad (6.6)$$

where design ξ_1 is better than design ξ_2 if the relative D-efficiency is greater than one. Also, the value of the relative D-efficiency tells us how many further observations we would need from the worse design to perform as well as the better design. For example, if the relative D-efficiency is 0.5, then ξ_1 provides estimates with reduced precision and accuracy compared to ξ_2 which is approximately half as efficient as ξ_2 in estimating the model parameters. We would need to have twice as many observations when using design ξ_1 to achieve the same precision as ξ_2 .

In this chapter, we will use relative D-efficiency for several purposes. In Section 6.2, we study the robustness of locally D-optimal designs with respect to misspecification of the unknown parameters in β . To do this, we search for the optimum continuous designs for four CMFP models, which are first-order CMFP and second-order CMFP models with one power parameter (same α) and two power parameters (different α 's). In each of these models, we try four different scenarios of the values of the model parameters and compare the resulting designs from these scenarios, and see if changing these parameter values can make a difference in designs or not. For a further study of robustness, we checked the effect of misspecified terms on the designs in Section 6.2.5 and calculated D-efficiencies for designs of misspecified model terms considering the correct model in three different cases. Then, in Section 6.3, we illustrate how to round a continuous design to make it an exact design and make comparisons between rounded continuous optimal designs and exact optimal designs directly found by the exchange algorithm. Also, design plots are used to show the support points and their replication for both designs to illustrate similarities and differences. Moreover, we search for optimal designs in the case of mixture experiments that include a process variable. So, four scenarios of the model parameter values were considered for single power parameter CMFP models and two power parameters CMFP models in Section 6.4.

Table 6.1: Constraint matrix \mathbf{u}_i of four support points design

1	2	3	4	5	6	7	8	9	10	11
1.00	0.00	0.00	0.00	0.00	0.00	0.00	0.00	0.00	0.00	0.00
-1.00	0.00	0.00	0.00	0.00	0.00	0.00	0.00	0.00	0.00	0.00
0.00	1.00	0.00	0.00	0.00	0.00	0.00	0.00	0.00	0.00	0.00
0.00	-1.00	0.00	0.00	0.00	0.00	0.00	0.00	0.00	0.00	0.00
-1.00	-1.00	0.00	0.00	0.00	0.00	0.00	0.00	0.00	0.00	0.00
1.00	1.00	0.00	0.00	0.00	0.00	0.00	0.00	0.00	0.00	0.00
0.00	0.00	1.00	0.00	0.00	0.00	0.00	0.00	0.00	0.00	0.00
0.00	0.00	-1.00	0.00	0.00	0.00	0.00	0.00	0.00	0.00	0.00
0.00	0.00	0.00	1.00	0.00	0.00	0.00	0.00	0.00	0.00	0.00
0.00	0.00	0.00	-1.00	0.00	0.00	0.00	0.00	0.00	0.00	0.00
0.00	0.00	-1.00	-1.00	0.00	0.00	0.00	0.00	0.00	0.00	0.00
0.00	0.00	1.00	1.00	0.00	0.00	0.00	0.00	0.00	0.00	0.00
0.00	0.00	0.00	0.00	1.00	0.00	0.00	0.00	0.00	0.00	0.00
0.00	0.00	0.00	0.00	-1.00	0.00	0.00	0.00	0.00	0.00	0.00
0.00	0.00	0.00	0.00	0.00	1.00	0.00	0.00	0.00	0.00	0.00
0.00	0.00	0.00	0.00	0.00	-1.00	0.00	0.00	0.00	0.00	0.00
0.00	0.00	0.00	0.00	-1.00	-1.00	0.00	0.00	0.00	0.00	0.00
0.00	0.00	0.00	0.00	1.00	1.00	0.00	0.00	0.00	0.00	0.00
0.00	0.00	0.00	0.00	0.00	0.00	1.00	0.00	0.00	0.00	0.00
0.00	0.00	0.00	0.00	0.00	0.00	0.00	-1.00	0.00	0.00	0.00
0.00	0.00	0.00	0.00	0.00	0.00	0.00	0.00	1.00	0.00	0.00
0.00	0.00	0.00	0.00	0.00	0.00	0.00	0.00	-1.00	0.00	0.00
0.00	0.00	0.00	0.00	0.00	0.00	-1.00	-1.00	0.00	0.00	0.00
0.00	0.00	0.00	0.00	0.00	0.00	1.00	1.00	0.00	0.00	0.00
0.00	0.00	0.00	0.00	0.00	0.00	0.00	0.00	1.00	0.00	0.00
0.00	0.00	0.00	0.00	0.00	0.00	0.00	0.00	0.00	1.00	0.00
0.00	0.00	0.00	0.00	0.00	0.00	0.00	0.00	0.00	0.00	1.00
0.00	0.00	0.00	0.00	0.00	0.00	0.00	0.00	-1.00	-1.00	-1.00

6.2 Optimal Continuous Designs for CMFP Models

To find the optimal designs for the first-order CMFP and the second-order CMFP model, which are models (3.9) and (3.10) in Section 3.1, we have tried various designs with different numbers of design points. In order to estimate P model parameters, we need at least P support points. Therefore, we tried P , $P + 1$, $P + 2$, and $P + 3$ support points and so on until the condition from the equivalence theorem was (close to being) satisfied. We found that often $P + 2$ points were a sufficient number for finding the optimum continuous designs for the CMFP models. We considered four CMFP models to study. Each has a different number of model parameters and therefore needs a different number of support points in the design.

6.2.1 Designs for First-Degree CMFP Models with a Single Power Parameter

The first-degree CMFP models for three components with one power parameter have four parameters in total. Then, six design points are used as a starting point to find their near-optimal designs. Our example is based on the chicken feeding data introduced in Section 5.3. The constraint matrix \mathbf{u}_i and constraint vector \mathbf{c}_i of a six support point design is as in Table 8.8 in the appendix. The constraint vector \mathbf{c}_i is: $\mathbf{c}_i = (0.05, -0.40, 0.02, -0.89, -0.94, 0.14, 0.05, -0.40, 0.02, -0.89, -0.94, 0.14, 0.05, -0.40, 0.02, -0.89, -0.94, 0.14, 0.05, -0.40, 0.02, -0.89, -0.94, 0.14, 0, 0, 0, 0, 0, -1)$. To illustrate the influence of the model parameter values on a design, we studied four different scenarios of parameter values for first-order CMFP models with one power parameter. These scenarios are:

- a) All parameters of the model have the estimated values from the real dataset ($\alpha = 0.11$, $\beta_0 = -381.11$, $\beta_1 = 529.14$, $\beta_2 = 42.19$).
- b) All parameters have the estimated values but with opposite signs.

We also wanted to investigate the effect of a large positive and negative value of α and similar values of the linear parameters. Therefore, we also chose the following scenarios:

- c) $\alpha = -1.5$, and β 's set to either one or negative one. In both cases, the designs turn out to be identical.

d) $\alpha = 1.2$, and β 's set to either one or negative one. In both cases, the designs turn out to be identical.

Table 6.4, Table 6.5, Table 6.6, and Table 6.7 show the optimized designs for these scenarios in order.

Table 6.4: The optimized design when all model parameters have the estimated values

Design points	Weights
$\mathbf{x}_1=(0.05,0.09,0.86)$	$w_1=0.21167$
$\mathbf{x}_2=(0.40,0.02,0.58)$	$w_2=0.20722$
$\mathbf{x}_3=(0.17,0.38,0.45)$	$w_3=0.20012$
$\mathbf{x}_4=(0.19,0.75,0.06)$	$w_4=0.04569$
$\mathbf{x}_5=(0.05,0.89,0.06)$	$w_5=0.22969$
$\mathbf{x}_6=(0.40,0.54,0.06)$	$w_6=0.10561$

Table 6.5: The optimized design when all parameters have the estimated values but with opposite signs

Design points	Weights
$\mathbf{x}_1=(0.40,0.54,0.06)$	$w_1=0.15750$
$\mathbf{x}_2=(0.12,0.02,0.86)$	$w_2=0.10170$
$\mathbf{x}_3=(0.40,0.02,0.58)$	$w_3=0.18752$
$\mathbf{x}_4=(0.16,0.40,0.45)$	$w_4=0.21767$
$\mathbf{x}_5=(0.05,0.09,0.86)$	$w_5=0.13937$
$\mathbf{x}_6=(0.05,0.89,0.06)$	$w_6=0.19624$

To look at the optimized designs with large positive and negative parameter values, see the design points in Table 6.6 and Table 6.7. There are only four or five support points in both tables, which seems to be a sufficient number of points in these two cases. This is because some resulting design points are very close to each other. In such a case, we add the weight of the point with a small weight to the weight of the point with a large weight to become one point. For example, in the case of $\alpha = -1.5$ and β 's=1, we found the points $(0.11,0.04,0.85)$ and $(0.10,0.04,0.86)$ with weights 0.00058 and 0.24875 respectively. These two points have identical second component values, and the difference between their first and third component values is only 0.01. So, we added these points together to become the point $(0.10,0.04,0.86)$ with a weight of 0.24933. Likewise, the point $(0.40,0.53,0.07)$, which has a weight of 0.00004, needs to be added to another point $(0.39,0.55,0.06)$, which is close to it and has a bigger weight of 0.25089. We then checked the (near-)optimality of the design by using the equivalence theorem. Of course, the optimal weights in Table 6.6 should each be 0.25, as a D-optimal design with as many support points as there are model parameters that have equal weights. The numerical result is reasonably close, which provides some confidence

in the algorithm, at least in such a simple scenario.

Table 6.6: The optimized design when $\alpha = -1.5$ and β 's=1

Design points	Weights
$\mathbf{x}_1=(0.05,0.89,0.06)$	$w_1=0.25045$
$\mathbf{x}_2=(0.39,0.55,0.06)$	$w_2=0.25093$
$\mathbf{x}_3=(0.40,0.02,0.58)$	$w_3=0.24929$
$\mathbf{x}_4=(0.10,0.04,0.86)$	$w_4=0.24933$

Table 6.7: The optimized design when $\alpha = 1.2$ and β 's=1

Design points	Weights
$\mathbf{x}_1=(0.40,0.03,0.57)$	$w_1=0.17972$
$\mathbf{x}_2=(0.05,0.89,0.06)$	$w_2=0.24901$
$\mathbf{x}_3=(0.05,0.09,0.86)$	$w_3=0.21232$
$\mathbf{x}_4=(0.06,0.78,0.16)$	$w_4=0.19869$
$\mathbf{x}_5=(0.40,0.54,0.06)$	$w_5=0.16025$

To visualize our results, Figure 6.3 shows plots of the support points of the optimized designs for the four different scenarios. In general, the reversal of the model parameter values has only a small effect on the design, as is evident in the second scenario, which is closest to the first. Also, the fourth scenario has the lowest number of design points and one internal point with a different location than the first and second scenarios, while the third scenario has no internal points. Then, we found that the points $(0.40,0.02,0.58)$, $(0.05,0.89,0.06)$, and $(0.40,0.54,0.06)$ are common to all scenarios, while the point $(0.05,0.09,0.86)$ is common to all scenarios except for the one in which $\alpha=-1.5$. The point $(0.17,0.38,0.45)$ or a point close to it is an inner point that exists only when all model parameters have the estimated values or have opposite signs. Moreover, the point $(0.12,0.02,0.86)$ or a point close to it is only present in designs when all parameters have the estimated values but with opposite signs and when $\alpha = -1.5$. Some points are specific to some designs, such as the point $(0.19,0.75,0.06)$ found only in the first scenario when all model parameters are the estimated values. Likewise, the point $(0.06,0.78,0.16)$ exists only when $\alpha = 1.2$. For some scenarios, such as when $\alpha = -1.5$, fewer design points are enough.

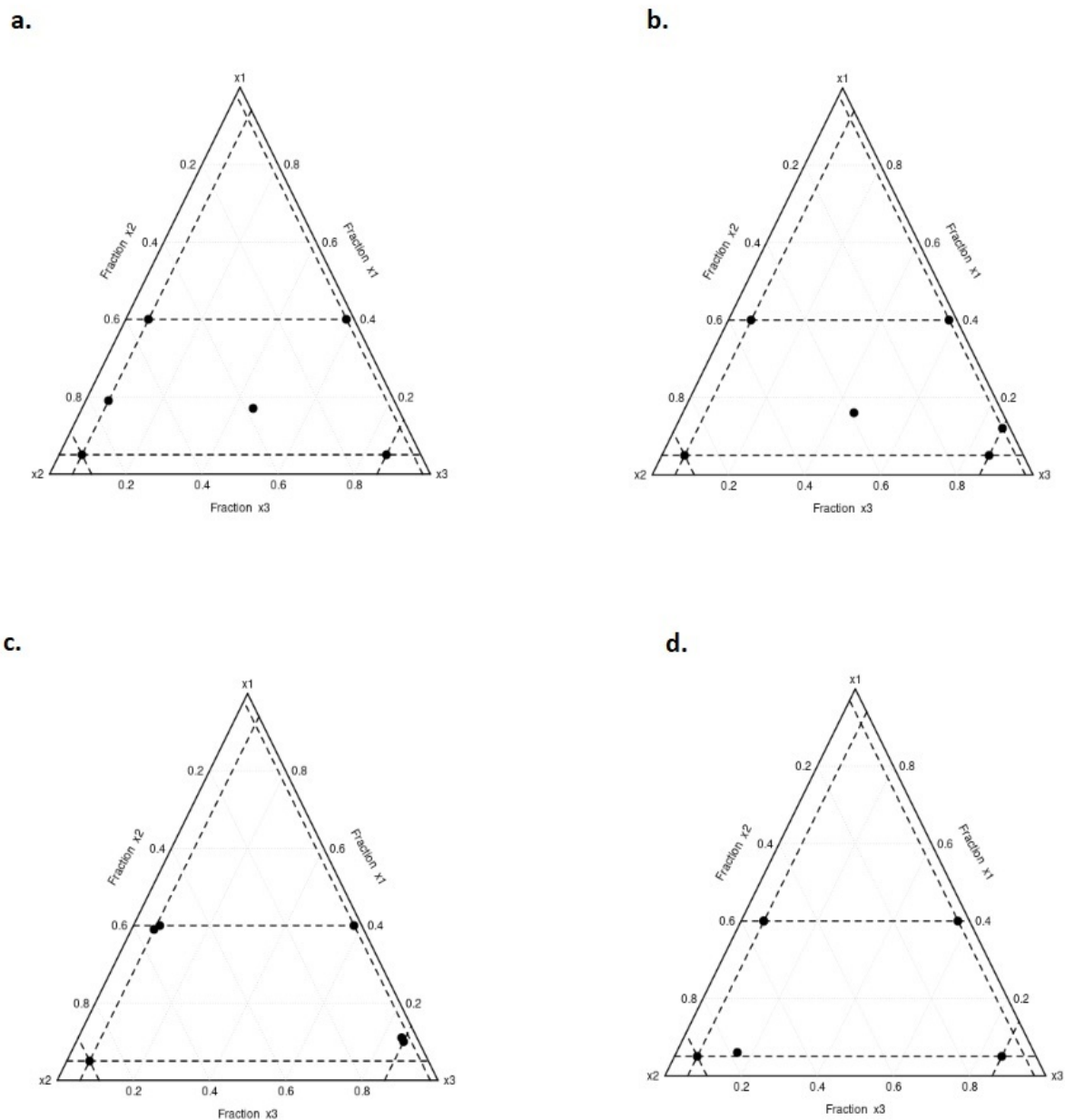


Figure 6.3: Optimized designs for four different scenarios of a first-order CMFP model with a single power parameter

After seeing the similarities and differences of the support points, we would like to know how robust the designs are to the misspecification of the model parameters. For our robustness study, we assume that scenario (a) is the true set of parameter values, and we find the relative D-efficiency (6.6) of the near D-optimal designs with misspecified parameter values relative to the design with the correctly specified parameter values for all scenarios. Thus, we calculated the relative D-efficiency considering that the design (ξ_2) in the denominator is optimal for the parameter values

estimated from the real datasets. The values obtained are expressed as a percentage where a design that produces a relative D-efficiency value close to one is considered an efficient design. For example, in the case of first-degree CMFP models with a single power parameter, the relative D-efficiency is equal to 0.995, 0.841, and 0.661 when all parameters have the estimated values but with opposite signs, $\alpha = -1.5$ and $\alpha = 1.2$, respectively. So, a CMFP model with a single power parameter can produce robust designs even when the estimated values of the model parameters are completely reversed or misspecified. Similarly, next, we will investigate the designs for first-order CMFP models if more power parameters are involved.

6.2.2 Designs for First-Degree CMFP Models with Two Power Parameters

We will again base our examples on the chicken feeding experiment that was introduced in Section 5.3. Seven support point designs were chosen as a starting point for the design search for the first-degree CMFP models with two power parameters. The constraint matrix \mathbf{u}_i is shown in Table 8.9 in the appendix, and the constraint vector \mathbf{c}_i for seven support point designs with two power parameters is as follows: $\mathbf{c}_i = (0.05, -0.40, 0.02, -0.89, -0.94, 0.14, 0.05, -0.40, 0.02, -0.89, -0.94, 0.14, 0.05, -0.4, 0.02, -0.89, -0.94, 0.14, 0.05, -0.40, 0.02, -0.89, -0.94, 0.14, 0.05, -0.4, 0.02, -0.89, -0.94, 0.14, 0, 0, 0, 0, 0, 0, -1)$. To continue illustrating the effect of changing model parameter values on a design, we changed the parameter values of the first-degree CMFP models with two power parameters to several different values. Therefore, four different combinations of power parameters were tried. In particular, we wanted to study the effect of all combinations of signs for the two power parameters. These studied scenarios are:

- a) All parameters of the model have the estimated values from the real dataset ($\alpha_1 = 0.14$, $\alpha_2 = -0.4$, $\beta_0 = -224.25$, $\beta_1 = 422.53$, and $\beta_2 = -6.40$).
- b) All parameters have the estimated values but with opposite signs.
- c) $\alpha_1 = 0.1$, $\alpha_2 = 0.39$, and $\beta_0 = \beta_1 = \beta_2 = 1$ or -1 . In both cases, the designs turn out to be identical.
- d) $\alpha_1 = -0.1$, $\alpha_2 = -0.9$, and $\beta_0 = \beta_1 = \beta_2 = 1$ or -1 . In both cases, the designs turn out to be identical.

Table 6.8: The optimized design when all parameter values have the estimated values

Design points	Weights
$\mathbf{x}_1=(0.40\ 0.21\ 0.39)$	$w_1=0.15965$
$\mathbf{x}_2=(0.40\ 0.02\ 0.58)$	$w_2=0.15167$
$\mathbf{x}_3=(0.14\ 0.02\ 0.84)$	$w_3=0.13725$
$\mathbf{x}_4=(0.05\ 0.89\ 0.06)$	$w_4=0.17074$
$\mathbf{x}_5=(0.17\ 0.12\ 0.72)$	$w_5=0.08431$
$\mathbf{x}_6=(0.05\ 0.09\ 0.86)$	$w_6=0.17445$
$\mathbf{x}_7=(0.18\ 0.76\ 0.06)$	$w_7=0.12193$

Table 6.9: The optimized design when all parameters have the estimated values but with opposite signs

Design points	Weights
$\mathbf{x}_1=(0.05,0.35,0.60)$	$w_1=0.20569$
$\mathbf{x}_2=(0.13,0.02,0.85)$	$w_2=0.17191$
$\mathbf{x}_3=(0.17,0.77,0.06)$	$w_3=0.18297$
$\mathbf{x}_4=(0.40,0.54,0.06)$	$w_4=0.10923$
$\mathbf{x}_5=(0.05,0.89,0.06)$	$w_5=0.19952$
$\mathbf{x}_6=(0.40,0.02,0.58)$	$w_6=0.13068$

Table 6.10: The optimized design when $\alpha_1 = 0.1$, $\alpha_2 = 0.39$ and $\beta^i=1$

Design points	Weights
$\mathbf{x}_1=(0.05,0.09,0.86)$	$w_1=0.05004$
$\mathbf{x}_2=(0.40,0.54,0.06)$	$w_2=0.13014$
$\mathbf{x}_3=(0.05,0.89,0.06)$	$w_3=0.18054$
$\mathbf{x}_4=(0.05,0.45,0.50)$	$w_4=0.18094$
$\mathbf{x}_5=(0.40,0.02,0.58)$	$w_5=0.14998$
$\mathbf{x}_6=(0.16,0.02,0.82)$	$w_6=0.14998$
$\mathbf{x}_7=(0.18,0.76,0.06)$	$w_7=0.15838$

Table 6.11: The optimized design when $\alpha_1 = -0.1$, $\alpha_2 = -0.9$ and $\beta^i=1$

Design points	Weights
$\mathbf{x}_1=(0.40,0.07,0.53)$	$w_1=0.14284$
$\mathbf{x}_2=(0.40,0.02,0.58)$	$w_2=0.15482$
$\mathbf{x}_3=(0.12,0.02,0.86)$	$w_3=0.14586$
$\mathbf{x}_4=(0.05,0.89,0.06)$	$w_4=0.15209$
$\mathbf{x}_5=(0.14,0.05,0.81)$	$w_5=0.11130$
$\mathbf{x}_6=(0.05,0.09,0.86)$	$w_6=0.12817$
$\mathbf{x}_7=(0.20,0.74,0.06)$	$w_7=0.16492$

Some design points become identical after rounding them to just two decimals. Thus, they are written as one point in the table, and we add their weights together. So, we find that there are six points in Table 6.9 instead of seven points. Generally, the fourth scenario (inversion of only one sign of the power parameters) is closest to the first. On the other hand, the designs of the second and third scenarios are close to each other. Then, we found that the points $(0.40,0.02,0.58)$, $(0.05,0.89,0.06)$, and $(0.18,0.76,0.06)$ are common to all scenarios, while the points $(0.05,0.09,0.86)$

are common to all scenarios except for the one in which all parameters have the estimated values but with opposite signs. Furthermore, all scenarios have points close to the point $(0.14, 0.02, 0.84)$. Also, the point $(0.40, 0.54, 0.06)$ is only present in designs when all parameters have the estimated values but with opposite signs and in the third scenario when both power parameters have positive signs. Some points are specific to some designs, such as $(0.40, 0.21, 0.39)$ and $(0.17, 0.12, 0.72)$, found only in the first scenario when all model parameters are the estimated values. Likewise, the point $(0.05, 0.35, 0.60)$ exists only in the scenario when all parameters have the estimated values but with opposite signs. Figure 6.4 makes the description of all design scenarios explicit.

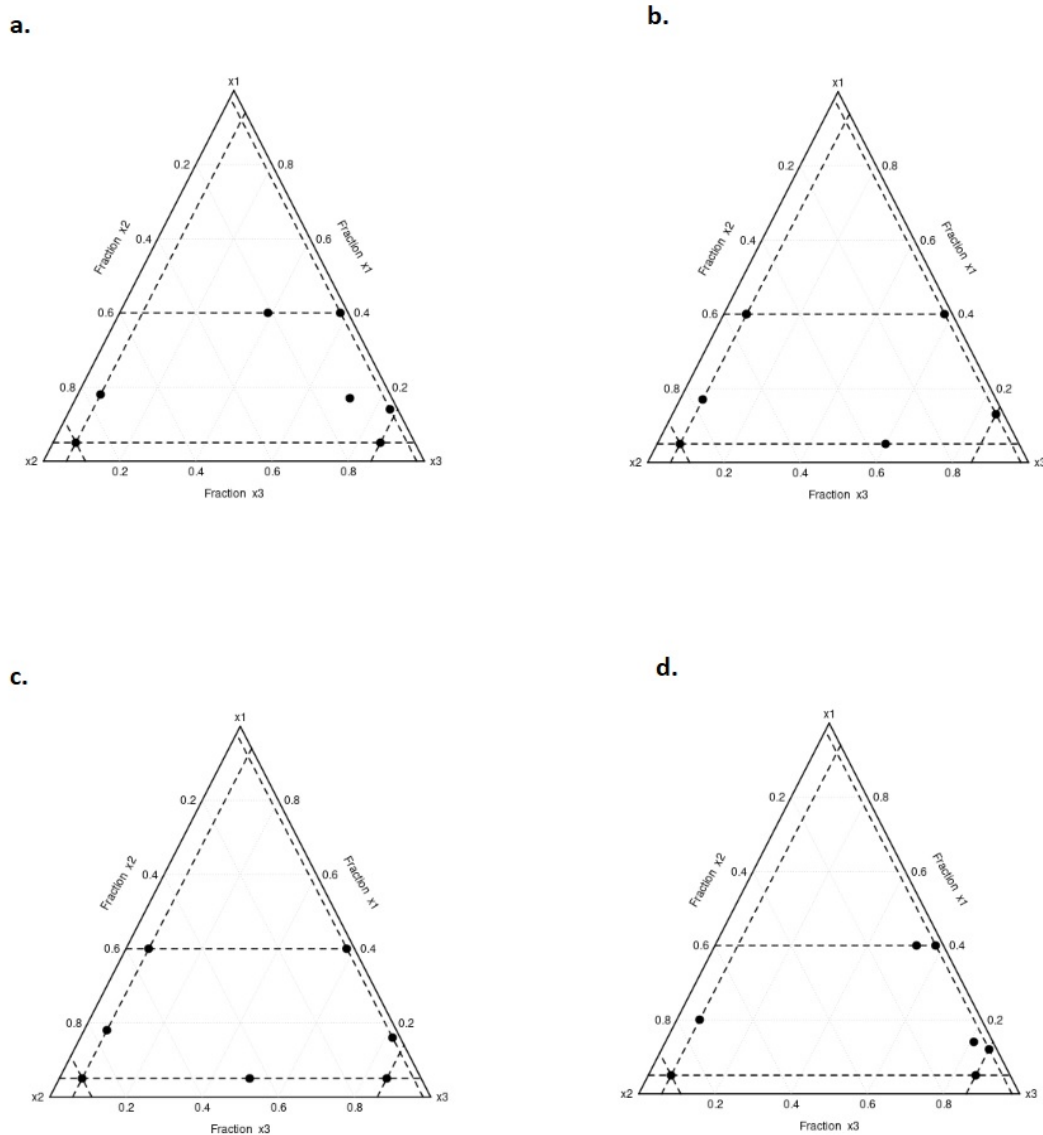


Figure 6.4: Optimized designs for four different scenarios of first-order CMFP models with two power parameters.

As in the previous example, we calculated the relative D-efficiency considering that the design (ξ_2) in the denominator is optimal for the parameter values estimated from the real datasets. In the case of first-order CMFP models with two power parameters, the relative D-efficiency is high for all scenarios and equal to 0.831, 0.875, and 0.981 when all parameters have the estimated values but with opposite signs, $\alpha_1 = 0.1$, $\alpha_2 = 0.39$, and when $\alpha_1 = -0.1$, $\alpha_2 = -0.9$, respectively. Consequently, the fourth scenario, when reversing the sign of only one power parameter, is considered the closest to the first scenario when all model parameter values have the estimated values. Next, we will consider the designs of second-order CMFP models in different parameter value scenarios.

6.2.3 Designs for Second-Order CMFP Models with One Power Parameter

Are models with more parameters giving very different designs? Will there be more interior points for second-order models? This further study illustrates the influence of the second-order CMFP models' parameter values on their optimal designs. Nine design points generated by a model with seven parameters for four different scenarios of parameter values were investigated. These scenarios are:

- a) All parameters of the model have the estimated values from the real dataset ($\alpha = 0.3$, $\beta_0 = -218.27$, $\beta_1 = 553.33$, $\beta_2 = 150.056$, $\beta_3 = -160.53$, $\beta_4 = -36.11$, and $\beta_5 = -109.68$).
- b) All parameters have the estimated values but with opposite signs.
- c) $\alpha = -1.5$, and β 's set to one.
- d) $\alpha = 1.2$, and β 's set to negative one.

Tables 6.12, 6.13, 6.14, and 6.15 show the optimized designs for these scenarios in order.

Table 6.12: The optimized design when all parameter values have the estimated values

Design points	Weights
$\mathbf{x}_1 = (0.05, 0.73, 0.22)$	$w_1 = 0.13857$
$\mathbf{x}_2 = (0.13, 0.23, 0.64)$	$w_2 = 0.07105$
$\mathbf{x}_3 = (0.05, 0.09, 0.86)$	$w_3 = 0.11337$
$\mathbf{x}_4 = (0.40, 0.02, 0.58)$	$w_4 = 0.13342$
$\mathbf{x}_5 = (0.12, 0.02, 0.86)$	$w_5 = 0.10900$
$\mathbf{x}_6 = (0.05, 0.89, 0.06)$	$w_6 = 0.14205$
$\mathbf{x}_7 = (0.14, 0.24, 0.62)$	$w_7 = 0.07000$
$\mathbf{x}_8 = (0.22, 0.72, 0.06)$	$w_8 = 0.10000$
$\mathbf{x}_9 = (0.40, 0.54, 0.06)$	$w_9 = 0.12254$

Table 6.13: The optimized design when all parameters values have the estimated values but with opposite signs

Design points	Weights
$\mathbf{x}_1=(0.11,0.83,0.06)$	$w_1=0.11438$
$\mathbf{x}_2=(0.09,0.09,0.82)$	$w_2=0.05775$
$\mathbf{x}_3=(0.05,0.09,0.86)$	$w_3=0.09947$
$\mathbf{x}_4=(0.40,0.02,0.58)$	$w_4=0.12562$
$\mathbf{x}_5=(0.12,0.02,0.86)$	$w_5=0.12525$
$\mathbf{x}_6=(0.05,0.89,0.06)$	$w_6=0.13589$
$\mathbf{x}_7=(0.09,0.10,0.80)$	$w_7=0.06379$
$\mathbf{x}_8=(0.28,0.18,0.54)$	$w_8=0.15690$
$\mathbf{x}_9=(0.40,0.54,0.06)$	$w_9=0.12095$

Table 6.14: The optimized design when $\alpha = -1.5$ and β 's=1

Design points	Weights
$\mathbf{x}_1=(0.05,0.53,0.42)$	$w_1=0.14137$
$\mathbf{x}_2=(0.14,0.03,0.83)$	$w_2=0.12386$
$\mathbf{x}_3=(0.40,0.05,0.55)$	$w_3=0.12491$
$\mathbf{x}_4=(0.40,0.02,0.58)$	$w_4=0.18860$
$\mathbf{x}_5=(0.12,0.02,0.86)$	$w_5=0.10901$
$\mathbf{x}_6=(0.08,0.86,0.06)$	$w_6=0.13700$
$\mathbf{x}_7=(0.40,0.54,0.06)$	$w_7=0.02918$
$\mathbf{x}_8=(0.25,0.69,0.06)$	$w_8=0.14607$

Table 6.15: The optimized design when $\alpha = 1.2$ and β 's=-1

Design points	Weights
$\mathbf{x}_1=(0.08, 0.86,0.06)$	$w_1=0.14870$
$\mathbf{x}_2=(0.40,0.02,0.58)$	$w_2=0.06156$
$\mathbf{x}_3=(0.05,0.10,0.85)$	$w_3=0.16325$
$\mathbf{x}_4=(0.40,0.54,0.06)$	$w_4=0.10778$
$\mathbf{x}_5=(0.32,0.02,0.66)$	$w_5=0.16151$
$\mathbf{x}_6=(0.05,0.89,0.06)$	$w_6=0.12558$
$\mathbf{x}_7=(0.05,0.74,0.21)$	$w_7=0.11261$
$\mathbf{x}_8=(0.27,0.67,0.06)$	$w_8=0.11901$

Only the designs in the first and second scenarios have interior points, and they have five points in common. Thus, they are the scenarios most similar to each other in designs. However, the points $(0.40,0.02,0.58)$, $(0.40,0.54,0.06)$, and $(0.05,0.89,0.06)$ are common among all four optimized designs. Also, the point $(0.12,0.02,0.86)$ is common in all optimized designs except the fourth design, while the point $(0.05,0.09,0.86)$ (or a point very close to it) is common in all optimized designs except the third optimized design. Some design points are common only in two scenarios, such as $(0.08,0.86,0.06)$ and $(0.40,0.05,0.55)$ in the third and fourth scenarios. However, each design has at least two distinguishing points, such as $(0.22,0.72,0.06)$, $(0.13,0.23,0.64)$, and $(0.14,0.24,0.62)$ in the first scenario design. Figure 6.5 shows the distinguishing points and common points between

the optimized designs in the four studied scenarios of the second-order CMFP models with a single power parameter.

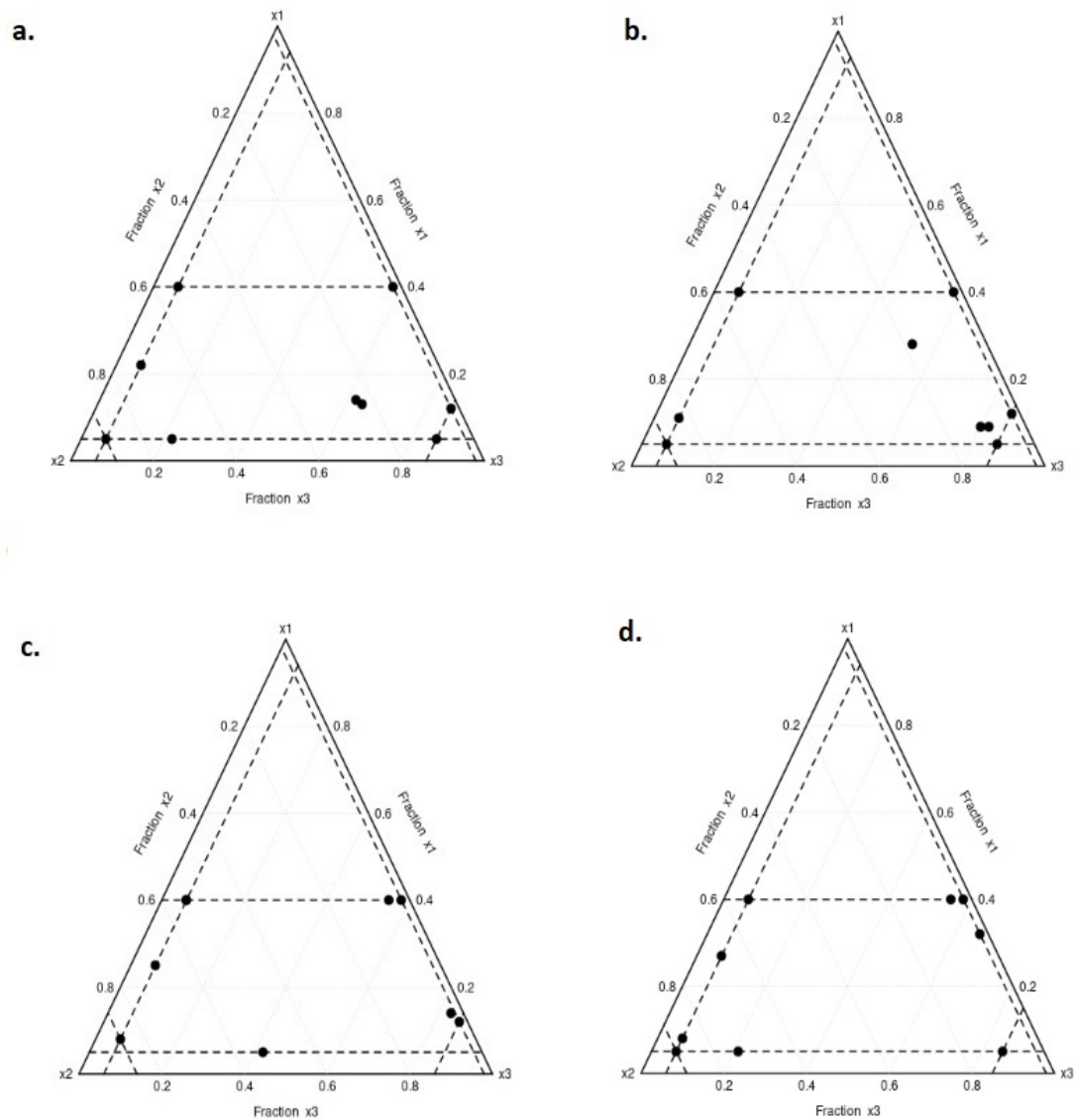


Figure 6.5: Optimized designs for four different scenarios of quadratic CMFP models with one power parameter.

The relative D-efficiency of all studied scenarios for quadratic CMFP models with a single power parameter is computed when the design (ξ_2) corresponds to the estimated values of model parameters to measure the goodness of these optimized designs under parameter misspecification. As a result, the relative D-efficiency is equal to 0.632, 0.516, and 0.365 when all parameters have the estimated values but with opposite signs, $\alpha = -1.5$ and $\alpha = 1.2$, respectively. These are now quite low, but then the misspecifications we have chosen are quite severe. The relative D-efficiency of

the second-order CMFP models with one power parameter indicates that the designs of the first-order CMFP model with a single power parameter are more robust with respect to misspecified values of the model parameters. It is likely that this is because there are more parameters in the second-order models, and hence a misspecified model will be 'more different' in some sense than in the first-degree case. To see if this trend continues, we optimize the designs for the second-degree CMFP model with two power parameters and look at how different and similar the design points are in each scenario compared to the others.

6.2.4 Designs for Second-Order CMFP Models with Two Power Parameters

Four different scenarios of parameter values for the second-order CMFP models with two power parameters were studied to further investigate the influence of changing the parameter values on a design. These scenarios are:

- a) All parameters of the model have the estimated values from the real dataset ($\alpha_1 = -0.545$, $\alpha_2 = 0.297$, $\beta_0 = 232.81$, $\beta_1 = -87.32$, $\beta_2 = 51.32$, $\beta_3 = 7.09$, $\beta_4 = -40.04$ and $\beta_5 = 13.55$).
- b) All parameters have the same estimated values but with opposite signs.
- c) $\alpha_1 = 0.1$, $\alpha_2 = 0.6$, $\beta_0 = 300$, $\beta_1=\beta_2=\beta_3=\beta_4=-1$, and $\beta_5=10$.
- d) $\alpha_1 = -0.1$, $\alpha_2 = -0.9$, and β 's set to one.

Table 6.16, 6.17, 6.18, and 6.19 show the optimized designs for these scenarios in order. The points (0.40,0.02,0.58), (0.05,0.89,0.06), and (0.40,0.54,0.06) are common in all optimized designs of second-order CMFP models with two power parameters. Also, all designs have the point (0.05,0.09,0.86), except for the second scenario design, which has a very close but not completely identical point. Moreover, all four designs have points close to (0.12,0.02,0.86). However, there are at least three distinct points for each design. The plots in Figure 6.6 show the design points in the four studied scenarios of the second-order CMFP models with two power parameters.

Table 6.16: The optimized design when all parameter values have the estimated values

Design points	Weights
$\mathbf{x}_1=(0.05,0.89,0.06)$	$w_1=0.12616$
$\mathbf{x}_2=(0.23,0.71,0.06)$	$w_2=0.09083$
$\mathbf{x}_3=(0.40,0.02,0.58)$	$w_3=0.10987$
$\mathbf{x}_4=(0.08,0.40,0.52)$	$w_4=0.06374$
$\mathbf{x}_5=(0.40,0.54,0.06)$	$w_5=0.08515$
$\mathbf{x}_6=(0.05,0.09,0.86)$	$w_6=0.12010$
$\mathbf{x}_7=(0.08,0.86,0.06)$	$w_7=0.09378$
$\mathbf{x}_8=(0.12,0.02,0.86)$	$w_8=0.10992$
$\mathbf{x}_9=(0.22,0.16,0.62)$	$w_9=0.11094$
$\mathbf{x}_{10}=(0.05,0.75,0.20)$	$w_{10}=0.08951$

Table 6.17: The optimized design when all parameters values have the estimated values but with opposite signs

Design points	Weights
$\mathbf{x}_1=(0.14,0.02,0.84)$	$w_1=0.14528$
$\mathbf{x}_2=(0.40,0.02,0.58)$	$w_2=0.12846$
$\mathbf{x}_3=(0.20,0.55,0.25)$	$w_3=0.03420$
$\mathbf{x}_4=(0.17,0.77,0.06)$	$w_4=0.09574$
$\mathbf{x}_5=(0.30,0.05,0.65)$	$w_5=0.09516$
$\mathbf{x}_6=(0.40,0.54,0.06)$	$w_6=0.10962$
$\mathbf{x}_7=(0.05,0.36,0.59)$	$w_7=0.10096$
$\mathbf{x}_8=(0.05,0.89,0.06)$	$w_8=0.11206$
$\mathbf{x}_9=(0.08,0.06,0.86)$	$w_9=0.15882$
$\mathbf{x}_{10}=(0.27,0.02,0.71)$	$w_{10}=0.01970$

Table 6.18: The optimized design when $\alpha_1 = 0.1$, $\alpha_2 = 0.6$, $\beta_0 = 300$, $\beta_1=\beta_2=\beta_3=\beta_4=-1$, and $\beta_5=10$.

Design points	Weights
$\mathbf{x}_1=(0.16,0.40,0.44)$	$w_1=0.12666$
$\mathbf{x}_2=(0.05,0.79,0.16)$	$w_2=0.11206$
$\mathbf{x}_3=(0.15,0.02,0.83)$	$w_3=0.11192$
$\mathbf{x}_4=(0.40,0.54,0.06)$	$w_4=0.12524$
$\mathbf{x}_5=(0.05,0.89,0.06)$	$w_5=0.14935$
$\mathbf{x}_6=(0.05,0.22,0.73)$	$w_6=0.03191$
$\mathbf{x}_7=(0.40,0.02,0.58)$	$w_7=0.12804$
$\mathbf{x}_8=(0.05,0.09,0.86)$	$w_8=0.10099$
$\mathbf{x}_9=(0.13,0.81,0.06)$	$w_9=0.11383$

Table 6.19: The optimized design when $\alpha_1 = -0.1$, $\alpha_2 = -0.9$ and β 's=1

Design points	Weights
$\mathbf{x}_1=(0.40,0.54,0.06)$	$w_1=0.10387$
$\mathbf{x}_2=(0.40,0.02,0.58)$	$w_2=0.13492$
$\mathbf{x}_3=(0.12,0.02,0.86)$	$w_3=0.12772$
$\mathbf{x}_4=(0.20,0.07,0.73)$	$w_4=0.11218$
$\mathbf{x}_5=(0.40,0.03,0.57)$	$w_5=0.12377$
$\mathbf{x}_6=(0.40,0.12,0.48)$	$w_6=0.03716$
$\mathbf{x}_7=(0.05,0.89,0.06)$	$w_7=0.11903$
$\mathbf{x}_8=(0.16,0.78,0.06)$	$w_8=0.12227$
$\mathbf{x}_9=(0.05,0.09,0.86)$	$w_9=0.11908$

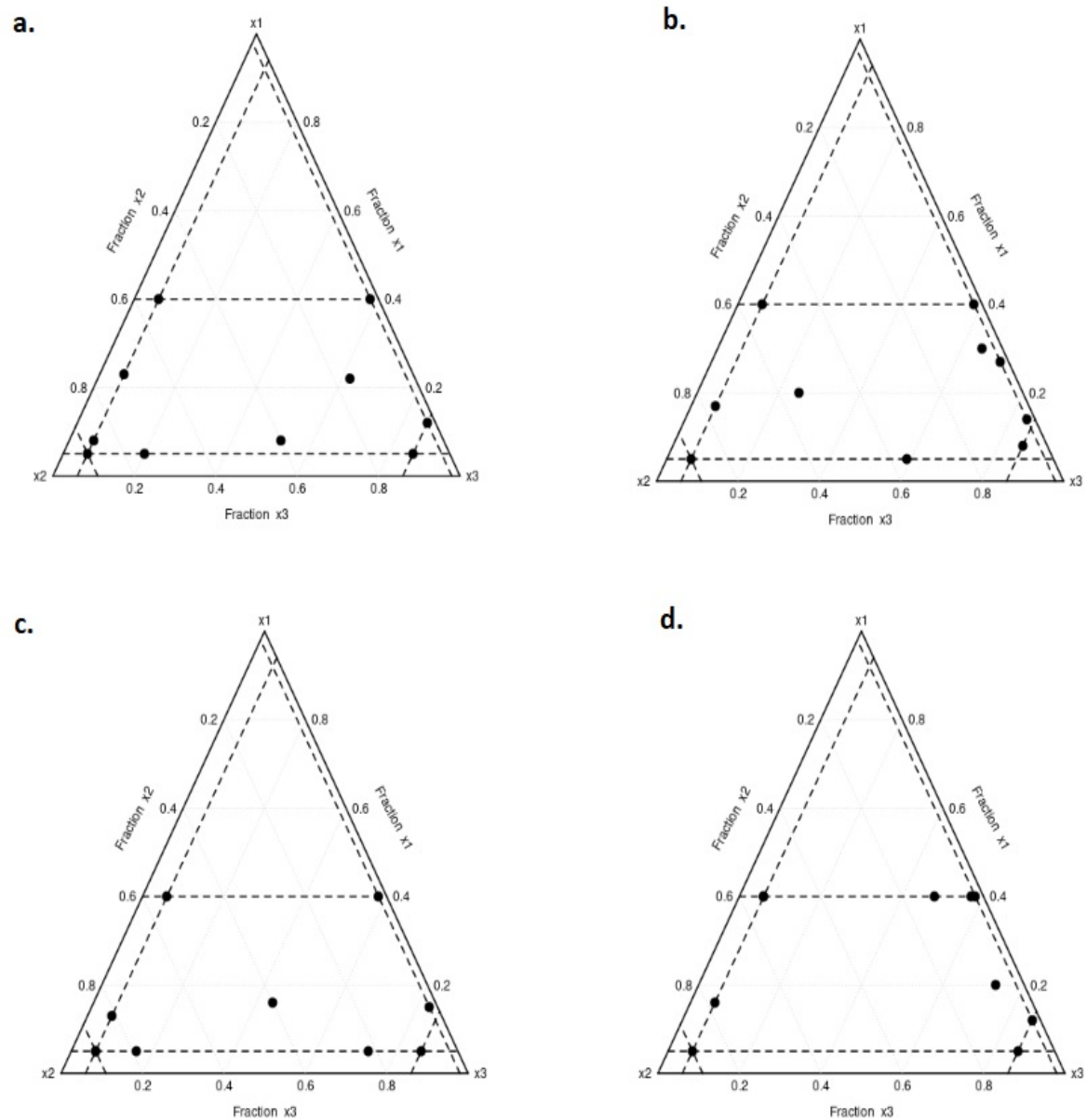


Figure 6.6: Optimized designs for four different scenarios of second-order CMFP models with two power parameters

For all the scenarios considered, The D-efficiency relative to the design that is optimal for the estimated parameter values is equal to 0.508, 0.775, and 0.399 when all parameters have the estimated values but with opposite signs, $\alpha_1 = 0.1$, $\alpha_2 = 0.6$, and $\alpha_1 = -0.1$, $\alpha_2 = -0.9$, respectively. The designs of the first and third scenarios have almost seven points in common that are either identical or close to each other. Therefore, the relative D-efficiency of the second-order CMFP models with two power parameters indicates that the design of the third scenario has the highest relative D-efficiency among other scenarios. According to the relative D-efficiency numbers,

designs of first-order CMFP models in both cases for power parameters (same or different) appear more robust to parameter misspecification than designs of second-order CMFP models in both cases. Therefore, if a second-order model is to be fitted to the data, the experimenter should try to obtain a reasonable guess of the model parameters, e.g. through data from similar experiments. If this is not possible, more robust design strategies such as sequential design, Bayesian design, or maximin-efficient design should be adopted to avoid potentially big losses in efficiency.

6.2.5 The CMFP Models with Misspecified Terms.

We have studied designs where the parameters were misspecified and found D-efficiencies for these cases earlier. These previous studies considered first and second-order CMFP model designs with one and two power parameters. It would be interesting to see the effect of misspecified terms on the designs. We therefore calculate D-efficiencies for designs where the model has misspecified terms. For this robustness study, again the chick feeding experimental data provided in Table 8.5 was used. The nature of CMFP models is that one component of the mixture is implicit and not explicit. For example, if there are five mixture components, only four will appear in the CMFP model. Therefore, since the chick feeding experiment data contains three mixture components x_1 , x_2 , and x_3 , we assume three possible scenarios for the correct models, which have the following forms:

$$\begin{aligned}
 & -381.11 + 529.14 \left(\frac{x_1}{1-x_1} \right)^{0.11} + 42.19 \left(\frac{x_2}{1-x_2} \right)^{0.11} \\
 & -381.11 + 529.14 \left(\frac{x_1}{1-x_1} \right)^{0.11} + 42.19 \left(\frac{x_3}{1-x_3} \right)^{0.11} \\
 & -381.11 + 529.14 \left(\frac{x_2}{1-x_2} \right)^{0.11} + 42.19 \left(\frac{x_3}{1-x_3} \right)^{0.11}
 \end{aligned}$$

If the first scenario, that is where the CMFP model with combination x_1x_2 is correct, we generate the optimal designs of the other CMFP models with combinations x_1x_3 and x_2x_3 . Thereafter, we find the respective determinants of the optimal designs for the misspecified models using the information matrix of the correct model and calculate the D-efficiencies considering the determinant of the optimal design for the correct model in the denominator. The D-efficiencies of all misspecified terms models in each scenario are shown in Table 6.20.

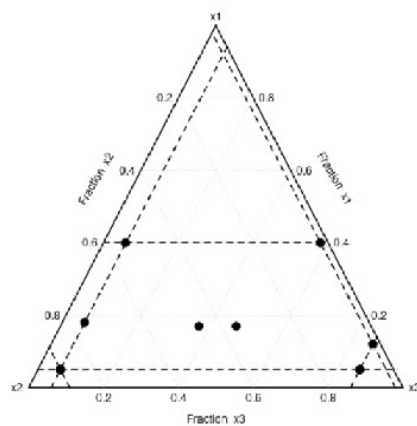
Table 6.20: D-efficiencies for optimal designs for the misspecified models relative to the optimal designs for the correct model

Misspecified models	D-eff relative to x_1x_2	D-eff relative to x_1x_3	D-eff relative to x_2x_3
x_1x_2	—	0.973	0.924
x_1x_3	0.962	—	0.948
x_2x_3	0.730	0.674	—

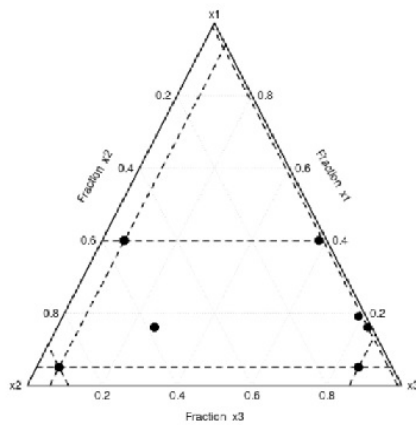
The D-efficiencies of the optimal designs for misspecified terms models x_1x_2 and x_1x_3 are very high and close to one in all scenarios, which means that these designs can efficiently estimate the other models. However, the D-efficiencies of the optimal design for misspecified terms model x_2x_3 is only approximately 0.7, which means the optimal design for this model is not as efficient at estimating the other two models. As we set all parameters to be the same in the 3 models under consideration, these differences in efficiency must be related to the different ranges we have for the proportions x_1, x_2 , and x_3 . The proportions x_2 and x_3 only slightly differ in their ranges, which are 0.87 and 0.8, respectively. So, replacing x_2 by x_3 or vice versa does not seem to change the optimal design by much. However, the optimal design for x_2x_3 seems less efficient for estimating a model containing x_1 , presumably because the x_1 proportion has a narrow range (0.35) compared with the ranges of the other proportions.

The plots in Figure 6.7 show how the designs for all the studied scenarios are similar and have almost five common points. The first design of the x_1x_2 model has the largest number of points, which is 8, two of which are internal points. The second design of the x_1x_3 model has 7 points, one of which is an interior point. The third design of the x_2x_3 model showed the lowest robustness, with only 6 points without any internal points.

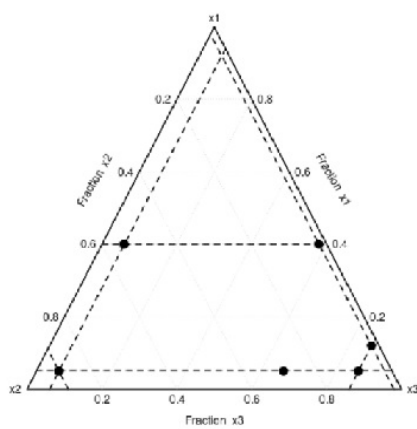
a.



b.



c.

Figure 6.7: Optimal designs for a. x_1x_2 , b. x_1x_3 , and c. x_2x_3

6.2.6 Designs for CMFP models with 4-Mixture Components

We also considered optimal designs for four components. This is numerically more tricky, and the `constrOptim` function could not cope with this situation. We will discuss two further optimization functions in R that can be used in such a case. To find the optimal designs for four mixture components, where each has an upper and lower bound, we used the experimental dataset of the illumination candle experiment presented by Box and Draper (2007), which have been introduced in Section 5.4 and are shown in Table 8.6. Here, we tried other optimization functions, such as the `solnp` and `nloptr` functions. The `solnp` function was previously mentioned and has been used in the simulation study in Chapter 5. The `nloptr` function is an R interface to NLOpt, which is an open-source library for nonlinear optimization that provides some interface optimization routines online for free. Bhadani (2021) presented several examples that have been solved using `nloptr`. Therefore, it is an opportunity to apply the `nloptr` function to find the optimal continuous design points and their corresponding optimal weights in the experimental dataset containing more than three mixture components with equality and inequality constraints. To do this, we used the CMFP model with the following form:

$$\beta_0 + \beta_1 \left(\frac{x_1}{1-x_1} \right)^{(\alpha)} + \beta_2 \left(\frac{x_2}{1-x_2} \right)^{(\alpha)} + \beta_3 \left(\frac{x_3}{1-x_3} \right)^{(\alpha)}$$

This form of the CMFP model has five parameters, which are β_0 , β_1 , β_2 , and β_3 , in addition to the power parameter α . Since we need design points greater than or equal to the number of model parameters, we optimize a continuous design with six support points using the `nloptr` function. The `nloptr` function implements many algorithms for nonlinear optimization and supports both local and global optimization methods. The choice of algorithm and specific options can be controlled using the `opts` arguments. For example, the Nelder Mead algorithm, which is known as the downhill simplex method, is a popular local optimization algorithm that uses a simplex to search for the minimum of a function. Moreover, the *NLOPT – GN – ISRES* algorithm is a global optimization method based on improved stochastic ranking evolution strategies implemented in the NLOpt library. To use the `nloptr` function, we define the set of inequality constraints. By exploiting the natural condition of the mixture components, we write inequality constraints in term of the

fourth proportion of the mixture $x_4 = 1 - x_1 - x_2 - x_3$. The restrictions on the fourth proportion are $0.03 \leq x_4 \leq 0.08$, and each of them needs to be written in the form $g(x) \leq 0$. Consequently, the lower bound is written as $0.03 - (1 - x_1 - x_2 - x_3) \leq 0$, and the upper bound is written as $(1 - x_1 - x_2 - x_3) - 0.08 \leq 0$. Therefore, we have to set twelve inequality constraints for the six design points. Then, we provide initial starting values of the proportions and allocated weights while considering each mixture proportion's upper and lower limits, which must be explicitly placed as one of the `nloptr` arguments.

In fact, we got a good optimization for the continuous design from running this function compared to that resulting from the `constrOptim` function. This was a motive to search for more optimization algorithms that can find optimal designs for first-order CMFP models with four components. That is why we decided to also consider the performance of the `solnp` function (see Section 5.2.2) in this part. So, we optimized designs by using the `solnp` function and that method also gave us better optimization for the designs in the case of 4 mixture components.

The optimized continuous designs in the scenario when the model parameter values are the estimated values and in the scenario when the model parameter values are estimated values with opposite signs are shown in Table 6.21 and Table 6.22, respectively.

Table 6.21: The optimized design when the parameter values have the estimated values

Design points	Weights
$\mathbf{x}_1 = (0.4115, 0.2684, 0.2402, 0.08)$	$w_1 = 0.15605$
$\mathbf{x}_2 = (0.4000, 0.4700, 0.1000, 0.03)$	$w_2 = 0.19873$
$\mathbf{x}_3 = (0.4000, 0.1000, 0.4700, 0.03)$	$w_3 = 0.19881$
$\mathbf{x}_4 = (0.6000, 0.2200, 0.1000, 0.08)$	$w_4 = 0.16637$
$\mathbf{x}_5 = (0.4000, 0.2886, 0.2814, 0.03)$	$w_5 = 0.10992$
$\mathbf{x}_6 = (0.6000, 0.1752, 0.1948, 0.03)$	$w_6 = 0.17012$

Table 6.22: The optimized design when the parameter values have the estimated values but with opposite signs

Design points	Weights
$\mathbf{x}_1 = (0.4004, 0.3268, 0.2429, 0.03)$	$w_1 = 0.19899$
$\mathbf{x}_2 = (0.4000, 0.1000, 0.4700, 0.03)$	$w_2 = 0.17360$
$\mathbf{x}_3 = (0.6000, 0.1000, 0.2700, 0.03)$	$w_3 = 0.08191$
$\mathbf{x}_4 = (0.5716, 0.2984, 0.1000, 0.03)$	$w_4 = 0.17354$
$\mathbf{x}_5 = (0.4000, 0.4200, 0.1000, 0.08)$	$w_5 = 0.17941$
$\mathbf{x}_6 = (0.6000, 0.1522, 0.1678, 0.08)$	$w_6 = 0.19255$

As shown in both designs for the two studied scenarios, the optimal proportions of the first and the fourth mixture components reach their respective bounds. So, we find two similar points in both designs that have a proportion of 0.08 for the fourth component, one companion to the upper bound of the first component and another with the lower bound of the first component. The second proportion never reaches its upper limit, whereas the third proportion reaches it at the common point (0.4000,0.1000,0.4700,0.03). However, all mixture components reach the minimum proportion more than once in both designs. As in all previous cases, the relative D-efficiency needed to be calculated to continue the robustness study of CMFP model designs. The relative D-efficiency is equal to 0.721 when calculating the relative D-efficiency of the near-optimal designs with misspecified parameter values relative to the design with the correctly specified parameter values. This indicates that the designs of CMFP models are reasonably robust in the case of misspecified parameter values, even in such more complicated cases.

After studying the robustness of the designs when the model parameters or the model terms have been misspecified, we would like to compare two strategies for finding exact designs in the next section.

6.3 Strategies for Finding Optimal Exact Designs

In practice, only exact designs can be run, and therefore any continuous design must be rounded to become an exact design to be viable. There is no single standard algorithm to find the optimal exact designs or any unifying theory for determining and studying their properties, making the search for optimal exact designs complex. Furthermore, each optimal exact design search has distinctive technical characteristics that depend on the proposed model, an optimality criterion, and, in particular, a fixed total number of observations, which leads to discrete optimization. For this situation, there is no equivalence theorem available, and we therefore cannot check the optimality of a design. A commonly used algorithm to find exact designs is the exchange algorithm introduced in Section 6.1, which relies on a candidate set of points. However, as the dimension of the design space (i.e. the number of proportions in our situation) increases, these points will either be quite sparse in the experimental region, or the candidate set of possible design points

will need to become very large. In the first case, we may not be able to find a good design as the candidate points may be too far away from the actual 'optimal' points. In the second case, the algorithm may not be able to find an optimal or near-optimal design in a reasonable amount of time.

We want to investigate if, for CMFP models, it is more advantageous to use the exchange algorithm to find exact optimal designs directly (using a moderate sized candidate set) or if rounded versions of continuous optimal designs will perform better. But first, let's illustrate the difference between exact and continuous designs. For example, consider a design with $n = 12$ trials and three design points $\mathbf{x}_1, \mathbf{x}_2$ and \mathbf{x}_3 , where $n = n_1 + n_2 + n_3$ and n_i is the replication of point \mathbf{x}_i . Suppose that the first design point has $n_1 = 4$, the second design point has $n_2 = 4$, and the third design point also has $n_3 = 4$. The weights of the design can then be represented by $w_i = n_i/n = 4/12 = 1/3$, $i = 1, 2, 3$. Thus, the optimal design can be represented as

$$\boldsymbol{\xi}^* = \begin{pmatrix} \mathbf{x}_1 & \mathbf{x}_2 & \mathbf{x}_3 \\ 1/3 & 1/3 & 1/3 \end{pmatrix}. \quad (6.7)$$

A design is considered an exact design if nw_i are integers for all $i = (1, 2, \dots, m)$. So, the resulting design is an exact design and can be implemented in practice since $n_1 = n_2 = n_3 = 1/3 \cdot 12 = 4$.

On the other hand, suppose that $n = 11$, then $n_1 = n_2 = n_3 = 1/3 \cdot 11 = 3.67$ which is a fractional number. We need to round the weights of such a design to be an exact design to be practically applicable. So, the exact design with $n = 11$ trials could be defined as \mathbf{x}_1 has $n_1 = 4$, \mathbf{x}_2 has $n_2 = 4$, and \mathbf{x}_3 has $n_3 = 3$, which can be written as

$$\boldsymbol{\xi}^{**} = \begin{pmatrix} \mathbf{x}_1 & \mathbf{x}_2 & \mathbf{x}_3 \\ 4/11 & 4/11 & 3/11 \end{pmatrix} \quad (6.8)$$

As we have seen, not every continuous design can be expressed directly as an exact design, while

any exact design can be defined as an equivalent continuous design. As a rule, the continuous design ξ^{***} for the exact design ξ can be represented as

$$\xi^{***} = \left\{ \begin{array}{cccc} \mathbf{x}_1 & \mathbf{x}_2 & \cdots & \mathbf{x}_m \\ \frac{n_1}{n} & \frac{n_2}{n} & \cdots & \frac{n_m}{n} \end{array} \right\}. \quad (6.9)$$

To study the efficiency of the exact design and the rounded continuous design of each scenario for parameter values in the CMFP model, two procedures are investigated. First, search for the optimal exact designs using the exchange algorithm. Second, round the respective continuous optimal designs from each scenario.

6.3.1 Comparison Between Exact Designs and Rounded Continuous Designs

We round the continuous optimal design from each scenario for the CMFP models and compare it to the optimized exact design for the same scenario. To do this, multiply the allocated weights w_i for each point \mathbf{x}_i by n (number of trials), and round each of the multiplication results to the nearest integer n_i which is then representing the number of replications for each design point \mathbf{x}_i . It is important to make sure during the rounding procedure that $n = n_1 + n_2 + \dots + n_m$. For example, suppose there are six points for the near-optimal continuous design with weights 0.1657, 0.1970, 0.2053, 0.0839, 0.2377, and 0.1104, respectively. Then, multiply each weight by the number of trials. If the number of trials in this example is 30, then the result of the multiplication is 4.971, 5.913, 6.158, 2.518, 7.130, and 3.311, respectively. Next, round each number in the result of this multiplication to be an integer while their sum is 30. So, the replication will be 5, 6, 6, 3, 7, and 3 for the six design points, respectively. Now, there is a rounded continuous design with 30 points, ready to be compared with the exact design generated from the exchange algorithm for the same scenario of parameter values. This rounding procedure is recommended in Pukelsheim and Rieder (1992).

To consider the performance of the exact designs and the rounded continuous designs under D-

efficiency, the relative D-efficiency is computed considering the exact design in the denominator for each scenario of parameter values in the CMFP models, whether the power parameters are the same or different. We will again consider the scenarios introduced in Section 6.2.1. In the case of the first-order CMFP models with one power parameter, when all parameters of the model have the same values estimated from the real dataset ($\alpha = 0.11$, $\beta_0 = -381.11$, $\beta_1 = 529.14$, $\beta_2 = 42.19$), the relative D-efficiency is 0.995. Similar relative D-efficiency to the first scenario is obtained when all parameters have the same estimated values but with opposite signs and when $\alpha = 1.2$. Higher relative D-efficiency is obtained in the third scenario when the power parameter value is -1.5, where the relative D-efficiency is 0.997.

The relative D-efficiency for all scenarios in the case of a single power parameter of a first-order CMFP model is approximately one, which means that there are no significant differences between the exact design, which results from the numeric algorithm and the rounded continuous design. Figure 6.8 visualizes the support points and their replication for both rounded continuous designs and exact designs to make the similarities and differences more noticeable.

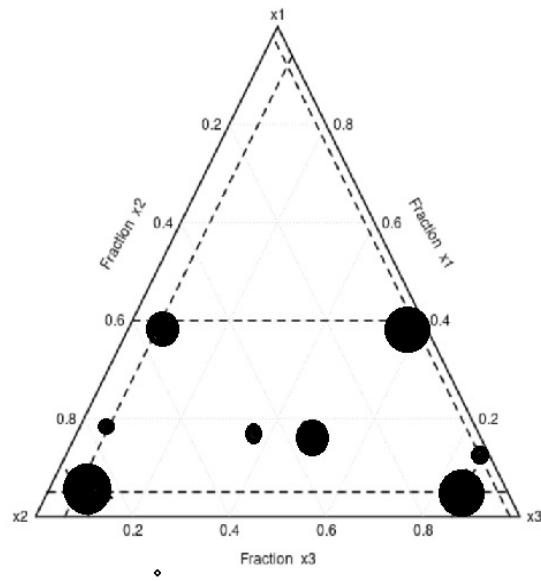
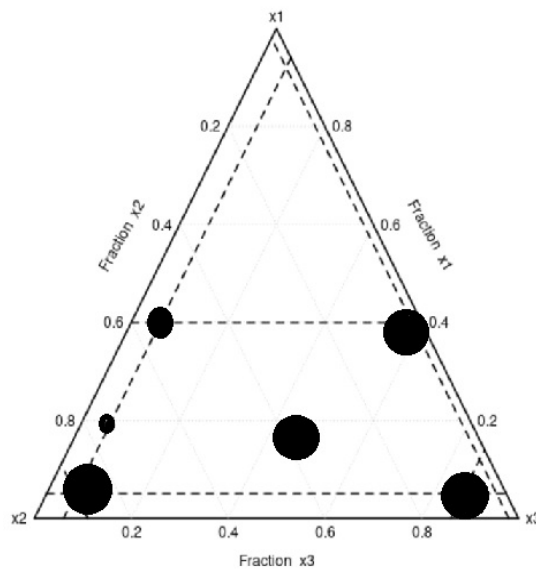
a. Exact design**b. Rounded continuous design**

Figure 6.8: The optimal support points and their replication for a first-order CMFP model with one power parameter when all parameters have the estimated values (Scenario a in Section 6.2.1)

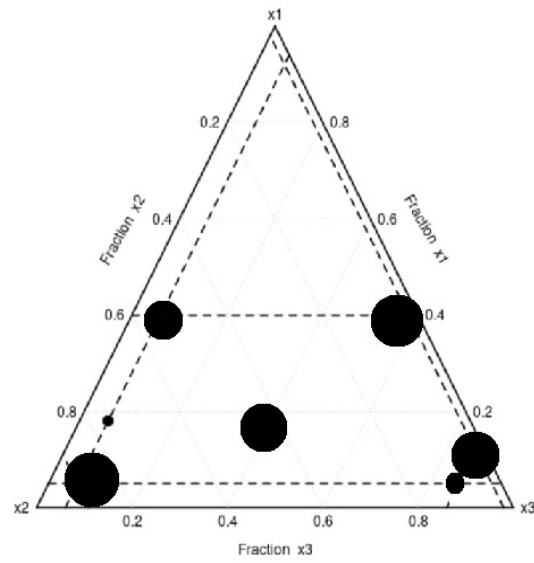
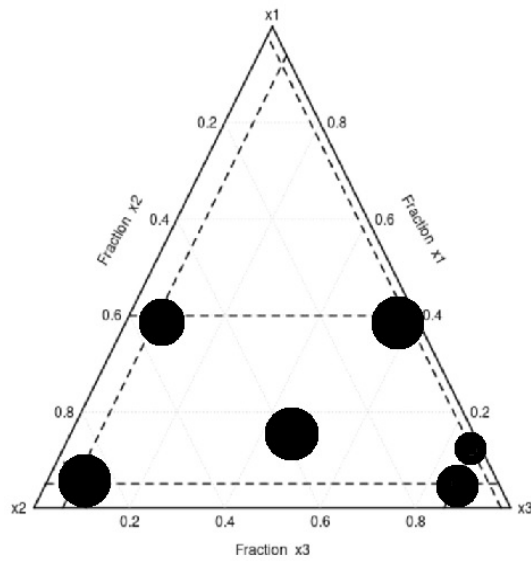
a. Exact design**b. Rounded continuous design**

Figure 6.9: The optimal support points and their replication for a first-order CMFP model with one power parameter when all parameters have the estimated values but with opposite signs (Scenario b in Section 6.2.1)

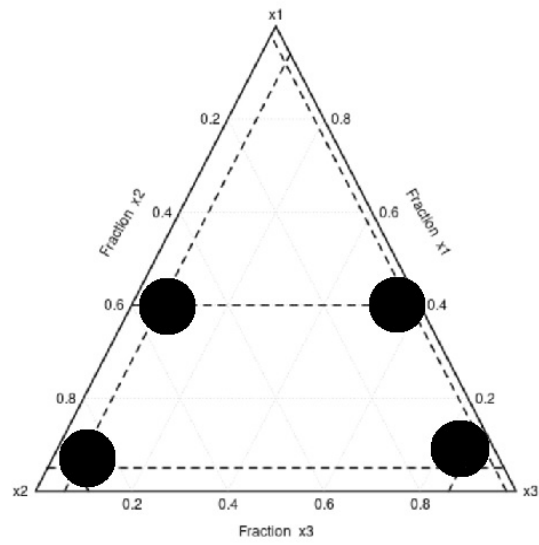
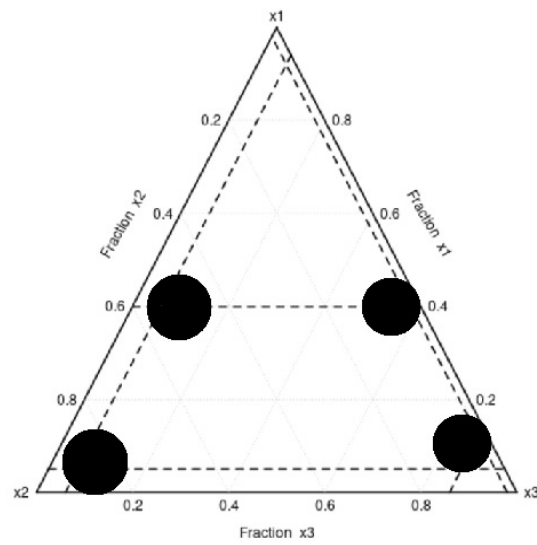
a. Exact design**b. Rounded continuous design**

Figure 6.10: The optimal support points and their replication for a first-order CMFP model with one power parameter when $\alpha = -1.5$ (Scenario c in Section 6.2.1)

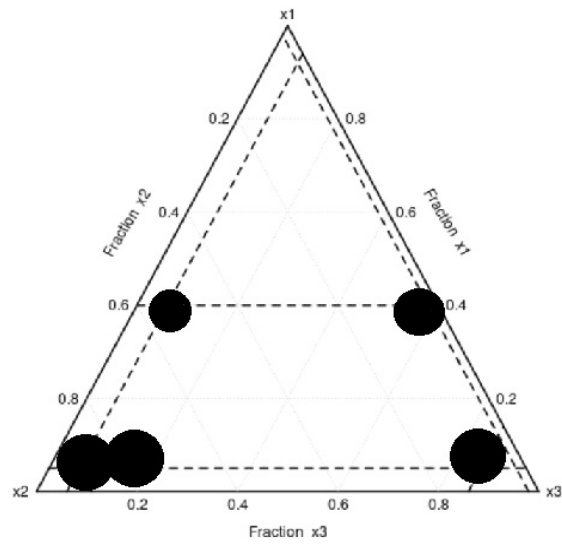
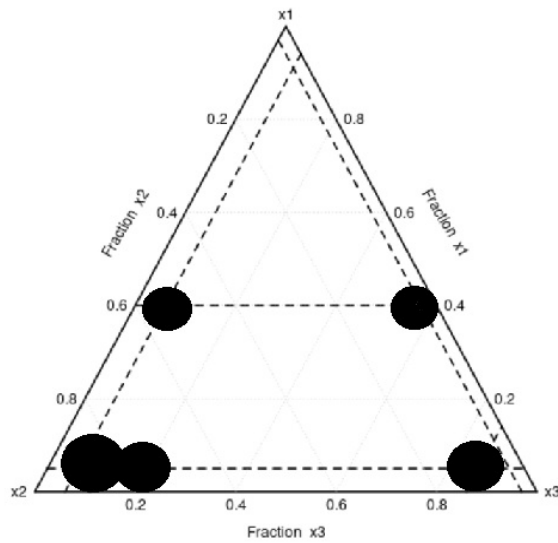
a. Exact design**b. Rounded continuous design**

Figure 6.11: The optimal support points and their replication for a first-order CMFP model with one power parameter when $\alpha = 1.2$ (Scenario d in Section 6.2.1)

The exact designs and rounded designs are generally similar. In the first scenario, when all model parameters are set to the original estimated values, the 6 points in the rounded continuous design are a subset of the 8 points of the exact design, which are clearly shown in the plots. Often, all design points in the rounded continuous design are present in the exact design but with different replications. The same status was observed in the second scenario when all parameters had the same estimated values but with opposite signs. However, the similarity becomes stronger when the power parameter value is -1.5 or 1.2. In both cases, the exact design and rounded continuous design almost have the same design points and replications.

In the case of a first-order CMFP model with two power parameters, the relative D-efficiency is 0.996 when all parameters of the model have the values estimated from the real dataset ($\alpha_1 = 0.14$, $\alpha_2 = -0.4$, $\beta_0 = -224.25$, $\beta_1 = 422.53$, and $\beta_2 = -6.40$). Also, the relative D-efficiency is 0.995 when all parameters have the estimated values but with opposite signs. As well, the relative D-efficiency is 0.994 when $\alpha_1 = 0.1$, $\alpha_2 = 0.39$ and equal to 0.987 when $\alpha_1 = -0.1$, $\alpha_2 = -0.9$. Similar to the case of one power parameter, the exact and rounded designs are generally similar. The relative D-efficiency for all scenarios in the case of two power parameters of a first-order CMFP model is almost one. So, there are no significant differences between the exact designs and the rounded continuous designs. The plots in the figures [6.12](#), [6.13](#), [6.14](#), and [6.15](#) visualize these designs' points and their replications for both rounded continuous designs and exact designs to make similarities and differences more obvious.

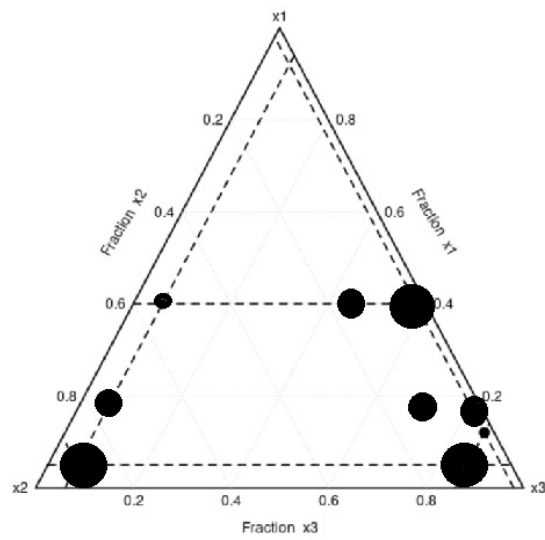
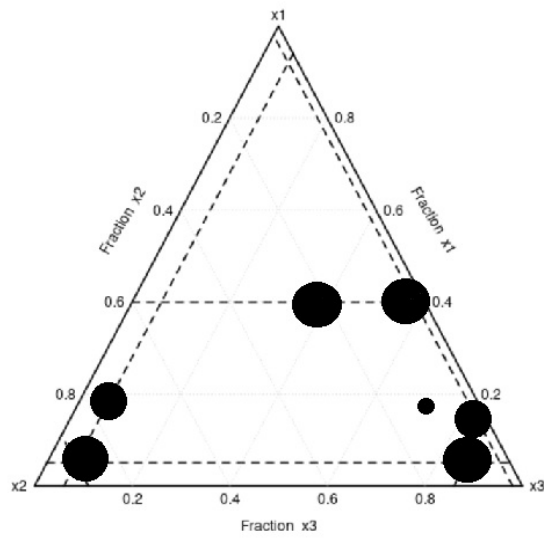
a. Exact design**b. Rounded continuous design**

Figure 6.12: The optimal support points and their replication for a first-order CMFP model with two power parameters when parameters have the estimated values (Scenario a in Section 6.2.2)

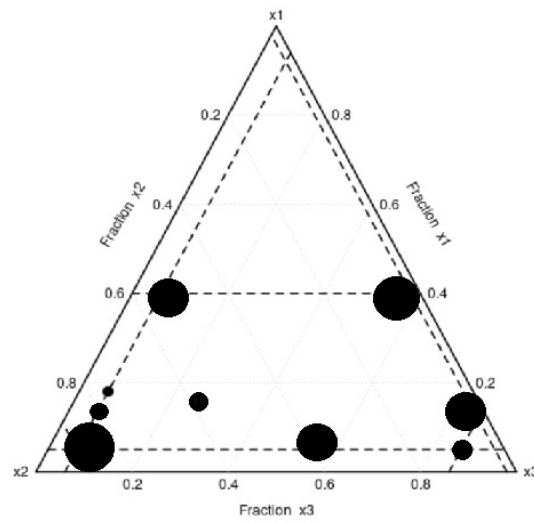
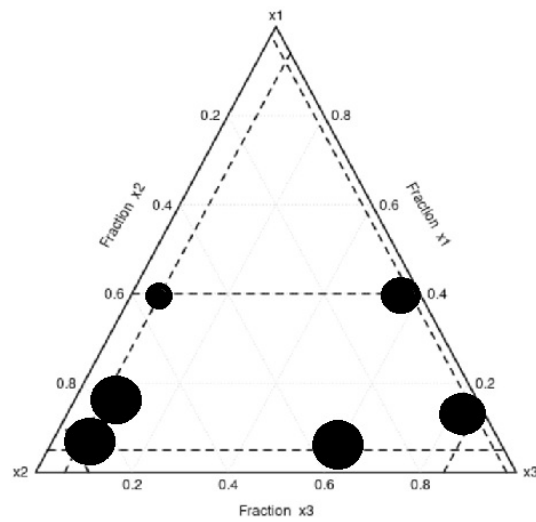
a. Exact design**b. Rounded continuous design**

Figure 6.13: The optimal support points and their replication for a first-order CMFP model with two power parameters when parameters have the estimated values but with opposite signs (Scenario b in Section 6.2.2)

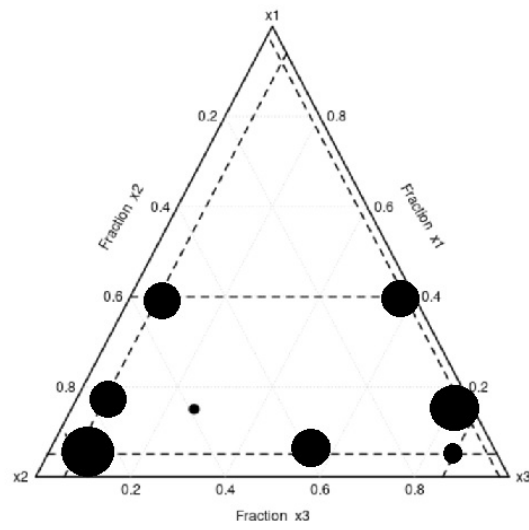
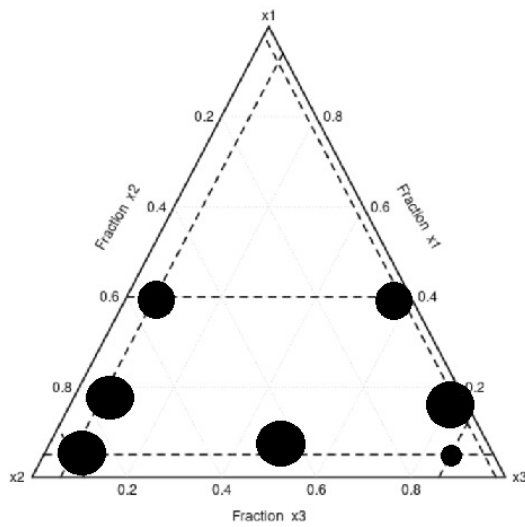
a. Exact design**b. Rounded continuous design**

Figure 6.14: The optimal support points and their replication for a first-order CMFP model with two power parameters when $\alpha_1 = 0.1$, $\alpha_2 = 0.39$ (Scenario c in Section 6.2.2)

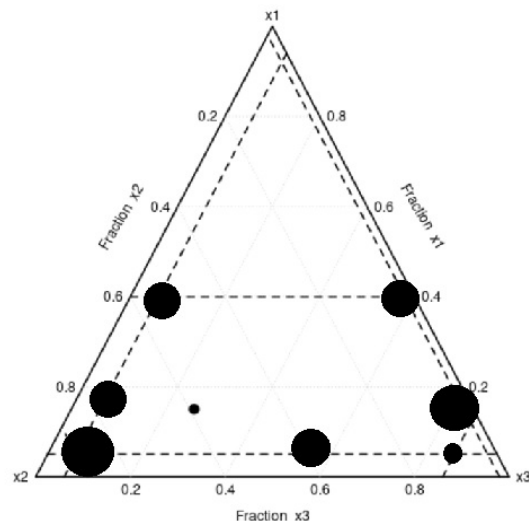
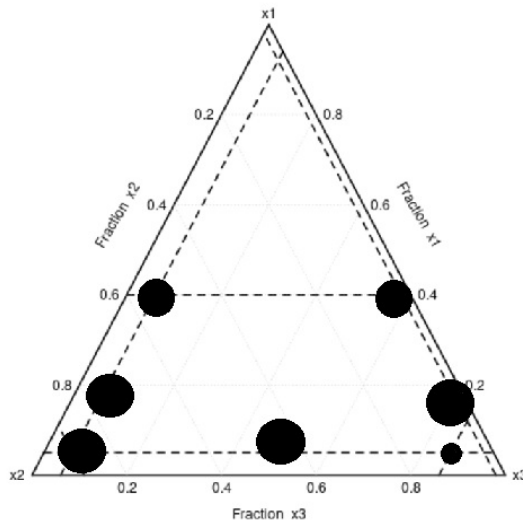
a. Exact design**b. Rounded continuous design**

Figure 6.15: The optimal support points and their replication for a first-order CMFP model with two power parameters when $\alpha_1 = -0.1$, $\alpha_2 = -0.9$ (Scenario d in Section 6.2.2)

From the plots of the optimal designs for first-order CMFP models with two power parameters, we can see that the points of the rounded continuous design are subsets of the exact design points in all considered scenarios. To extend this study, we examined several scenarios for the second-order CMFP model with one power parameter and the second-order CMFP model with two power parameters. As before, in each case, we set the model parameters to different combinations of values.

In the case of a single power parameter, the relative D-efficiency is 0.992 when the power parameter and all other model parameters are set to the estimated values from the real dataset. We also considered the case when the power parameter and other model parameters have the estimated values but with opposite signs, and the relative D-efficiency is 0.984. We also find that the relative D-efficiency is 0.927 when the power parameter is -1.5, and the other model parameters are set to 1. Moreover, when the power parameter is 1.2, and the other model parameters are set to -1, the relative D-efficiency is 0.983. Consequently, in the case of the same power parameters, the rounded continuous optimal designs for first-order CMFP models have higher relative D-efficiency than those for second-order CMFP models. In other words, the differences in efficiency between rounded continuous designs and exact designs were very small for first-order models but were more noticeable for second-order models with a single power parameter. In all cases, the exact designs found by the exchange algorithm are performing better. The plots in figures 6.16, 6.17, 6.18, and 6.19 visualize the design points and their replication for both rounded continuous designs and exact designs to visualize the similarities and differences in these designs.

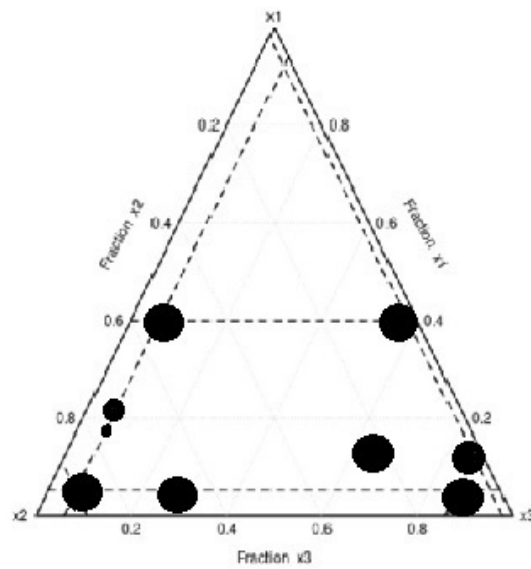
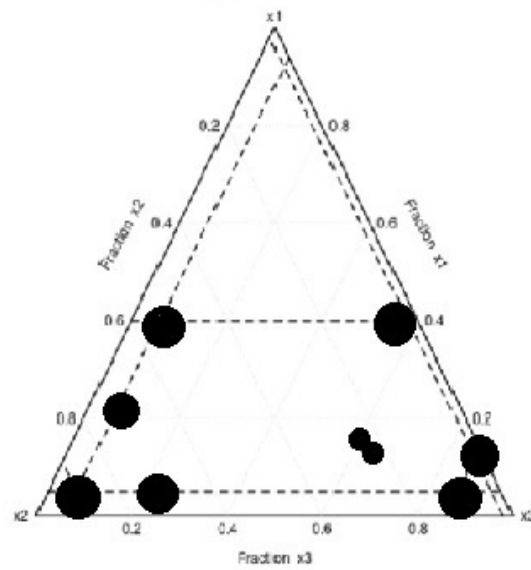
a- Exact design**b- Rounded design**

Figure 6.16: The design points and their replication in the exact design and the rounded continuous design when all parameter values have the estimated values (Scenario a in Section 6.2.3)

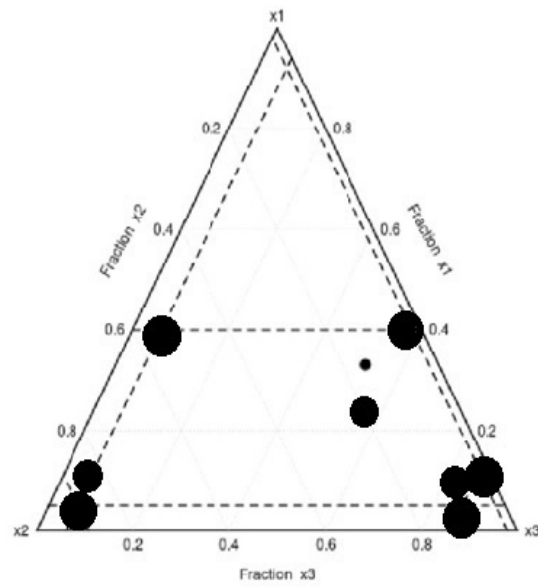
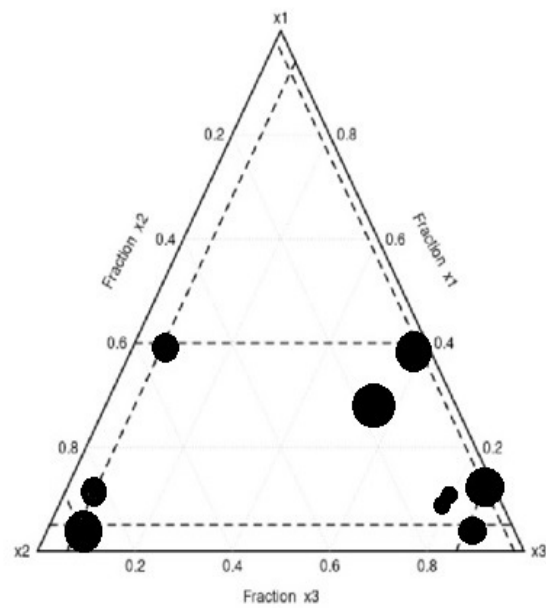
a- Exact design**b- Rounded design**

Figure 6.17: The design points and their replication in the exact design and the rounded continuous design when all parameter values have the estimated values but with opposite signs (Scenario b in Section 6.2.3)

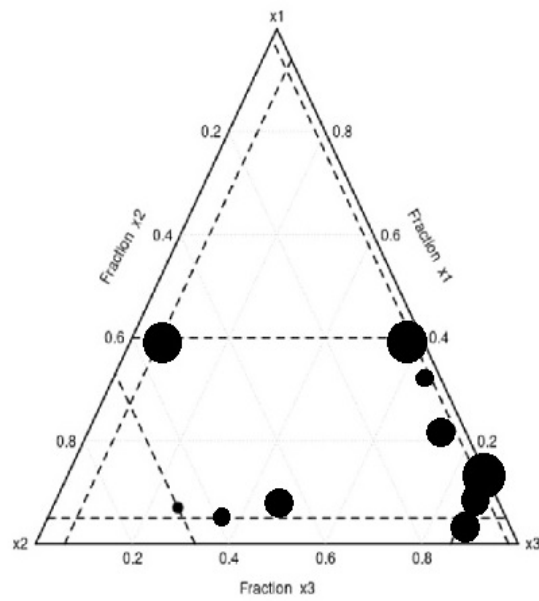
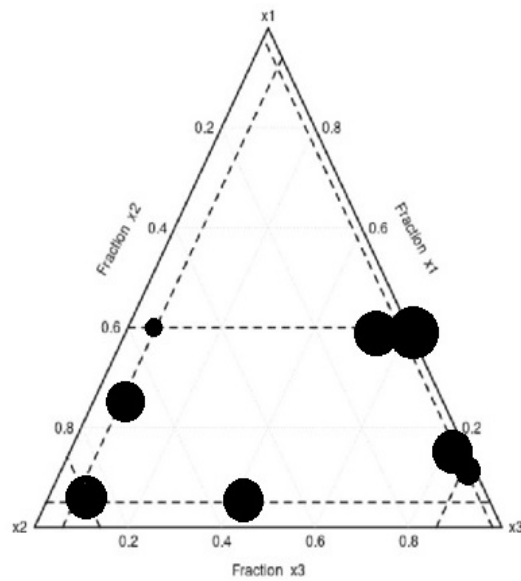
a- Exact design**b- Rounded design**

Figure 6.18: The design points and their replication in the exact design and the rounded continuous design when $\alpha = -1.5$ (Scenario c in Section 6.2.3)

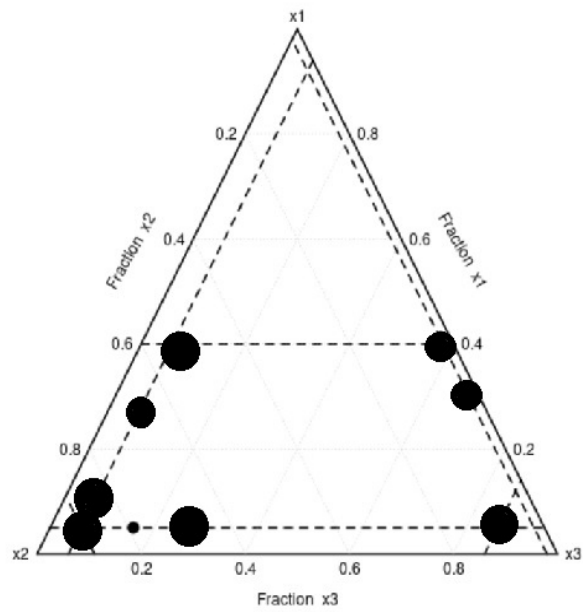
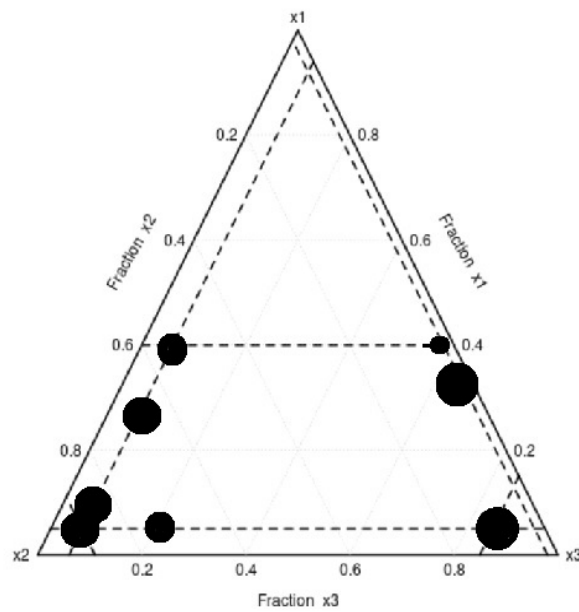
a. Exact design**b. Rounded continuous design**

Figure 6.19: The design points and their replication in the exact design and the rounded continuous design when $\alpha = 1.2$ (Scenario d in Section 6.2.3)

The plots show that in most cases of second-order CMFP models with a single power parameter, the design points are common in the rounded continuous design and the exact design. Therefore, the rounded continuous designs are similar to the exact designs or a subset of them except for the scenario when the power parameter is -1.5, in which the rounded continuous design differs from the exact design.

In the case of two power parameters, the relative D-efficiency is 0.998 when the power parameters and all other model parameters have the estimated values from the real dataset. We also considered the case when the power parameters and the other model parameters have the estimated values but with opposite signs. The relative D-efficiency is 0.958 in this case. We also find that the relative D-efficiency is 0.983 when the values of the first and second power parameters are positive and equal to 0.1 and 0.6. Moreover, when the values of the first and second power parameters are both negative and equal to -0.1 and -0.9, respectively, and the other model parameters are set to 1, the relative D-efficiency is 0.965. According to these results in the case of two power parameters, the first-order CMFP models mostly have higher relative D-efficiency than the second-order CMFP models. The following plots in figures 6.20, 6.21, 6.22, and 6.23 visualize the design points and their replication for both rounded continuous designs and exact designs for different scenarios of the second-order CMFP model with two power parameters to see the similarities and differences in these designs.

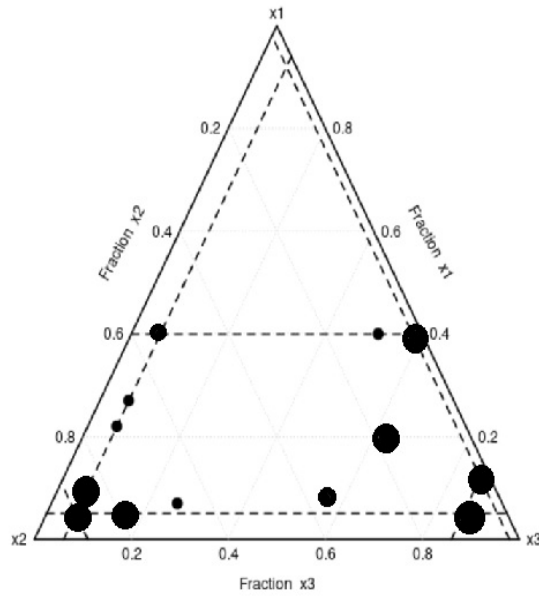
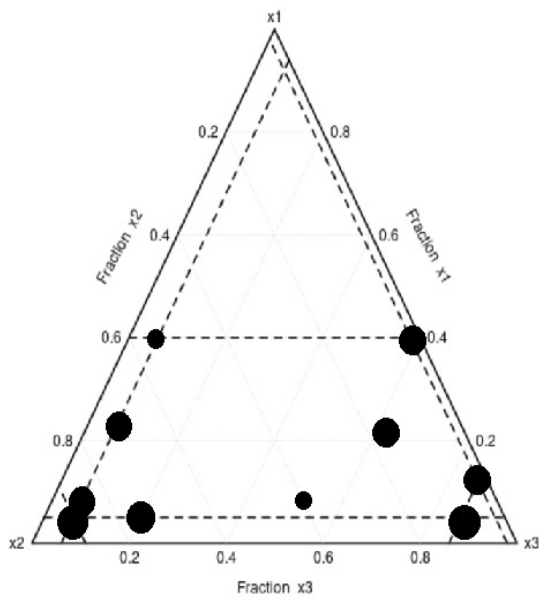
a- Exact design**b- Rounded design**

Figure 6.20: The design points and their replication in the exact design and the rounded continuous design when all parameter values have the estimated values (Scenario a in Section 6.2.4)

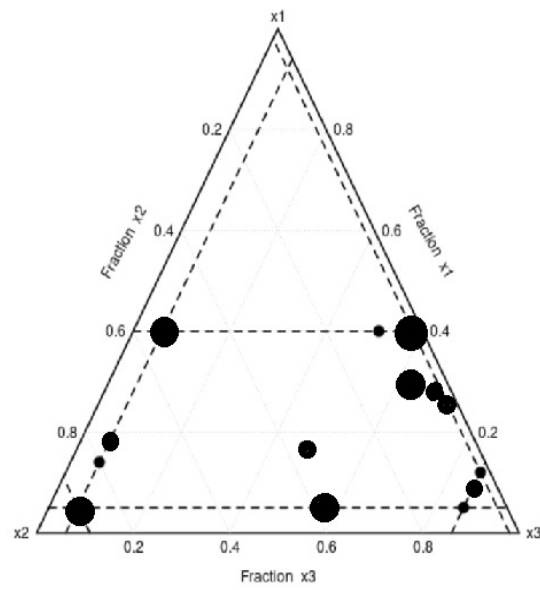
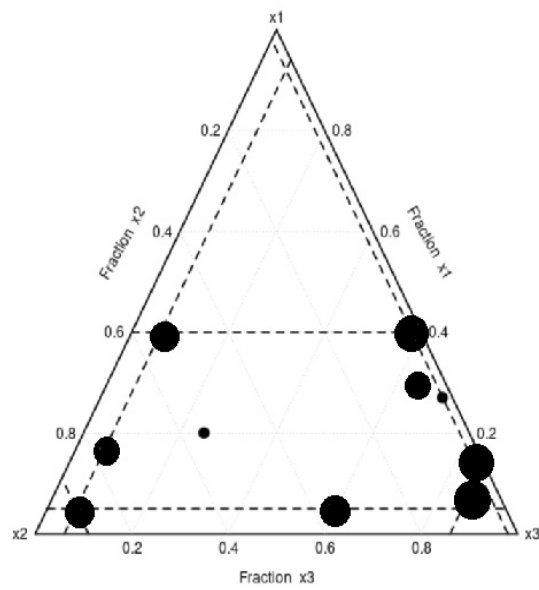
a- Exact design**b- Rounded design**

Figure 6.21: The design points and their replication in the exact design and the rounded continuous design when all parameter values have the estimated values but with opposite signs (Scenario b in Section 6.2.4)

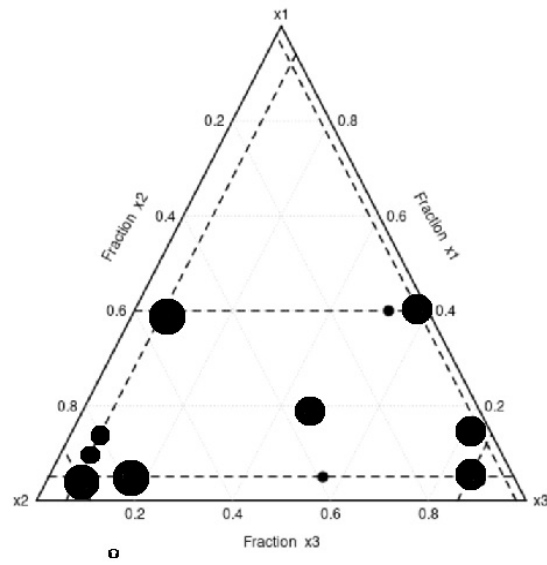
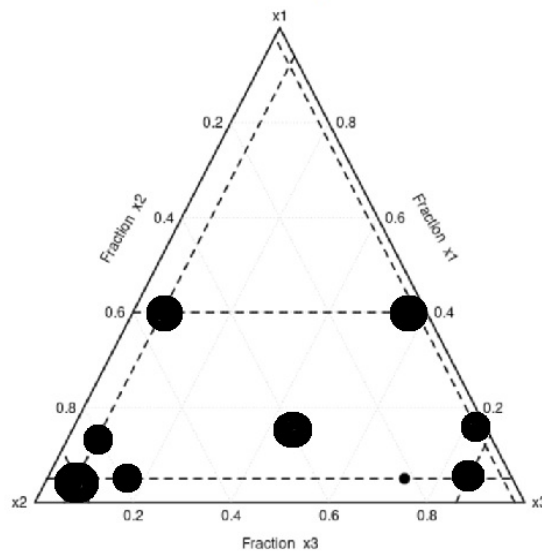
a. Exact design**b. Rounded continuous design**

Figure 6.22: The design points and their replication in the exact design and the rounded continuous design when $\alpha_1 = 0.1$, $\alpha_2 = 0.6$ (Scenario c in Section 6.2.4)

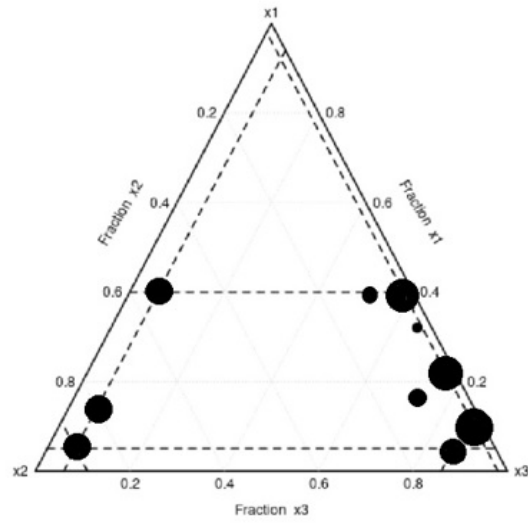
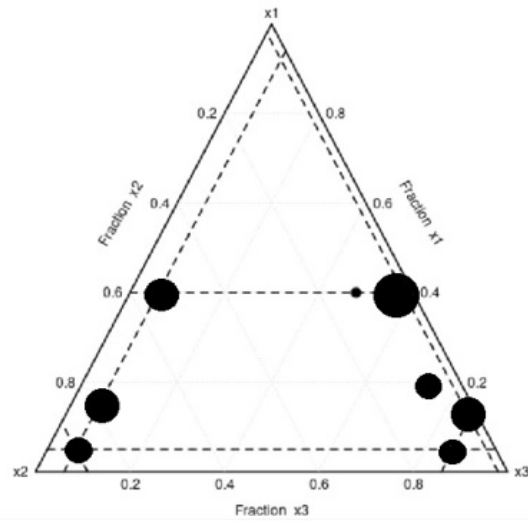
a- Exact design**b- Rounded design**

Figure 6.23: The design points and their replication in the exact design and the rounded continuous design when $\alpha_1 = -0.1$, $\alpha_2 = -0.9$ (Scenario d in Section 6.2.4)

From the plots of all cases of second-order CMFP models with two power parameters, any point present in the rounded continuous design also exists in the exact design or is close to a point in the exact design. The slight difference between the rounded continuous designs and the exact designs is in the frequencies of the points in each design.

In the case of four mixture components, to compare the rounded continuous design relative to the exact design of the same scenario, we use designs that we got in table 6.21 and 6.22. As in the previous examples of three mixture component designs, the exact designs need to be generated by the exchange algorithm to perform a comparison with rounded continuous designs for the same model parameter values. We are particularly interested in whether the candidate set that we use to generate the exact design can sufficiently fill a four-dimensional space to find an efficient design. Since constrained optimization algorithms struggle with continuous design in the case of the four components of the mixture, it will be helpful to look at the performance of the exact design. For that, the exchange algorithm is used to generate the optimized exact designs. This algorithm can generate exact designs smoothly in the case of four mixture component designs, similar to the case of three mixture component designs. The D-efficiency is 0.97 and 0.98 for the scenarios when the parameter values are the estimated values and the estimated values with opposite signs, respectively. The high value of D-efficiency, approximately one in both scenarios, means that the rounded continuous design of each scenario is equivalent to the exact design of the same scenario. Overall, we note that the exact designs and the rounded continuous designs have very similar performance, with the exact designs always being very slightly better.

If there are cases where the exact designs underperform compared to the rounded continuous designs, we propose to augment candidate sets for the exchange algorithm with optimal points found by continuous optimization to improve the candidate set. This has not been necessary for the scenarios we considered, as the candidate sets already contained the 'good' points.

6.4 Designs when Considering a Process Variable

In this section, we want to investigate the structure of D-optimal designs for CMFP models with a process variable. We are interested in assessing how the presence of a process variable in the model will affect the design features, such as the number and location of the design points. First-order CMFP model designs are more robust in parameter misspecification cases compared to designs of second-order CMFP models, as shown in Section 6.2. So, we want to compare the features of designs for first-order CMFP models when process variable terms are included with designs for

first-order CMFP models without process variables. Here, we use a special form of model (3.18), which contains the terms of the interaction effect of the mixture proportions with the process variables but without the pure quadratic terms of process variables. The model that is used in this section has the following form:

$$\begin{aligned} \beta_0 + \beta_1 \left(\frac{x_1}{1-x_1} \right)^{(\alpha_1)} + \beta_2 \left(\frac{x_2}{1-x_2} \right)^{(\alpha_2)} + \beta_3 \left(\frac{x_1}{1-x_1} \right)^{(\alpha_1)} \left(\frac{x_2}{1-x_2} \right)^{(\alpha_2)} + \beta_4 \left(\frac{x_1}{1-x_1} \right)^{(\alpha_1)} z \\ + \beta_5 \left(\frac{x_2}{1-x_2} \right)^{(\alpha_2)} z \end{aligned}$$

In Section 6.3, we have seen (albeit in scenarios without process variables) that the exact designs found by the exchange algorithm seem to be slightly more efficient than rounded continuous designs. We therefore use this approach to find exact designs in this study. The exact designs were generated by optimizing an initial 60-point design using the exchange algorithm that was illustrated in Section 6.1. We considered three datasets of mixture experiments with a process variable, each of which has either two or three levels. The four scenarios of parameter values that were studied in the case of one power parameter are as follows:

- a) All model parameters have the values estimated from the experimental dataset.
- b) All model parameters have the estimated values with opposite signs.
- c) $\alpha = 0.88$, and all linear parameters have been set to negative one.
- d) $\alpha = -0.93$, and all linear parameters have been set to positive one.

Likewise, the four scenarios of parameter values studied for CMFP models with two power parameters are as follows:

- a) All model parameters have the values estimated from the experimental dataset.
- b) All model parameters have the estimated values but with opposite signs.
- c) $\alpha_1 = -0.50$, $\alpha_2 = 0.77$, and all linear parameters have been set to negative one.
- d) $\alpha_1 = 0.85$, $\alpha_2 = -0.60$, and all linear parameters have been set to positive one.

The following sections 6.4.1, 6.4.2, and 6.4.3 show optimized designs through tables and plots for three mixture experiments with a process variable for the above scenarios in order.

6.4.1 Example 1: MPV Designs for the Opacity of Printable Coating Material Experiment with a 2-level Process Variable

An experimental dataset by Chau and Kelley (1993), which has been introduced in Section 4.2, represents the opacity of a printable coating material used for identification labels and tags (see Table 8.1 in the appendix). The coating material is a mixture of two pigments, x_1 and x_2 , and a polymeric binder, x_3 . Coating opacity was affected by the mixture of the three proportions and coating thickness (z) as a two-level process variable (pro.var). The proportions of the components were subject to limitations and were:

$0.13 \leq x_1 \leq 0.45, 0.21 \leq x_2 \leq 0.67, 0.20 \leq x_3 \leq 0.34$. In the case when the power parameters are the same, the first and fourth scenarios resulted in only nine design points, while the second scenario resulted in ten design points. More design points resulted in the third scenario. In the case when the power parameters are different, the first scenario resulted in only nine design points, the third scenario resulted in ten design points while the second and fourth scenarios resulted in eleven design points. All optimized MPV designs in the case of a single power parameter with the levels of the process variable are shown in tables 6.23, 6.24, 6.25, and 6.26 and are visualized in Figure 6.24.

Table 6.23: The MPV design when all parameter values have the estimated values

Design points	Replications	The pro.var level
$\mathbf{x}_1=(0.45,0.21,0.34)$	8	$z=1$
$\mathbf{x}_2=(0.45,0.21,0.34)$	8	$z=-1$
$\mathbf{x}_3=(0.13,0.67,0.20)$	6	$z=-1$
$\mathbf{x}_4=(0.13,0.67,0.20)$	7	$z=1$
$\mathbf{x}_5=(0.13,0.53,0.34)$	6	$z=1$
$\mathbf{x}_6=(0.13,0.53,0.34)$	7	$z=-1$
$\mathbf{x}_7=(0.37,0.43,0.20)$	9	$z=1$
$\mathbf{x}_8=(0.33,0.47,0.20)$	4	$z=-1$
$\mathbf{x}_9=(0.29,0.51,0.20)$	5	$z=-1$

Table 6.24: The MPV design when all parameter values have the estimated values but with opposite signs

Design points	Replications	The pro.var level
$\mathbf{x}_1=(0.13,0.67,0.20)$	8	$z=-1$
$\mathbf{x}_2=(0.13,0.67,0.20)$	8	$z=1$
$\mathbf{x}_3=(0.45,0.21,0.34)$	6	$z=-1$
$\mathbf{x}_4=(0.45,0.21,0.34)$	8	$z=1$
$\mathbf{x}_5=(0.45,0.35,0.20)$	6	$z=-1$
$\mathbf{x}_6=(0.13,0.53,0.34)$	9	$z=1$
$\mathbf{x}_7=(0.37,0.43,0.20)$	1	$z=1$
$\mathbf{x}_8=(0.21,0.45,0.34)$	8	$z=-1$
$\mathbf{x}_9=(0.45,0.35,0.20)$	2	$z=1$
$\mathbf{x}_{10}=(0.33,0.47,0.20)$	4	$z=1$

Table 6.25: The MPV design when $\alpha = 0.88$ and $\beta's=-1$

Design points	Replications	The pro.var level
$\mathbf{x}_1=(0.13,0.67,0.20)$	8	$z = -1$
$\mathbf{x}_2=(0.45,0.21,0.34)$	7	$z = 1$
$\mathbf{x}_3=(0.45,0.21,0.34)$	7	$z = -1$
$\mathbf{x}_4=(0.13,0.67,0.20)$	8	$z = 1$
$\mathbf{x}_5=(0.45,0.35,0.20)$	4	$z = -1$
$\mathbf{x}_6=(0.45,0.35,0.20)$	4	$z = 1$
$\mathbf{x}_7=(0.21,0.45,0.34)$	3	$z = -1$
$\mathbf{x}_8=(0.21,0.45,0.34)$	2	$z = 1$
$\mathbf{x}_9=(0.17,0.49,0.34)$	5	$z = -1$
$\mathbf{x}_{10}=(0.17,0.49,0.34)$	6	$z = 1$
$\mathbf{x}_{11}=(0.33,0.47,0.20)$	3	$z = 1$
$\mathbf{x}_{12}=(0.33,0.47,0.20)$	3	$z = -1$

Table 6.26: The MPV design when $\alpha = -0.93$ and $\beta's=1$

Design points	Replications	The pro.var level
$\mathbf{x}_1=(0.45,0.21,0.34)$	9	$z = 1$
$\mathbf{x}_2=(0.13,0.67,0.20)$	6	$z = -1$
$\mathbf{x}_3=(0.45,0.21,0.34)$	9	$z = -1$
$\mathbf{x}_4=(0.13,0.67,0.20)$	6	$z = 1$
$\mathbf{x}_5=(0.13,0.53,0.34)$	6	$z = -1$
$\mathbf{x}_6=(0.13,0.53,0.34)$	6	$z = 1$
$\mathbf{x}_7=(0.33,0.47,0.20)$	8	$z = -1$
$\mathbf{x}_8=(0.25,0.41,0.34)$	4	$z = 1$
$\mathbf{x}_9=(0.29,0.51,0.20)$	6	$z = 1$

In the first and fourth scenarios, the designs have nine design points. Three of these points ((0.45, 0.21, 0.34), (0.13, 0.67, 0.20), and (0.13, 0.53, 0.34)) are identical and common in both levels of the process variable. However, MPV designs have more design points for the second and third scenarios. The points that are common in the second and third scenarios are (0.45, 0.35, 0.20), (0.45, 0.21, 0.34), and (0.13, 0.67, 0.20). Thus, each MPV design has at least nine design points. Three of them are common in both levels of the process variable, while the rest of the points are produced at only one level of the process variable (low level or high level) except in the third scenario, in which all design points are common in both levels of the process variable. Two points appear in all MPV designs for the four studied scenarios: (0.13,0.67,0.20) and (0.45,0.21,0.34). These points are two of the vertices of the experimental region. The other two vertices also feature in some designs. Generally, all points lie on the boundary of the experimental region. This is similar to what we have seen before when investigating first-order CMFP models without process variables.

Next, the tables 6.27, 6.28, 6.29, and 6.30, as well as the plots in Figure 6.25, show the MPV designs for the four different scenarios in the case of two power parameters.

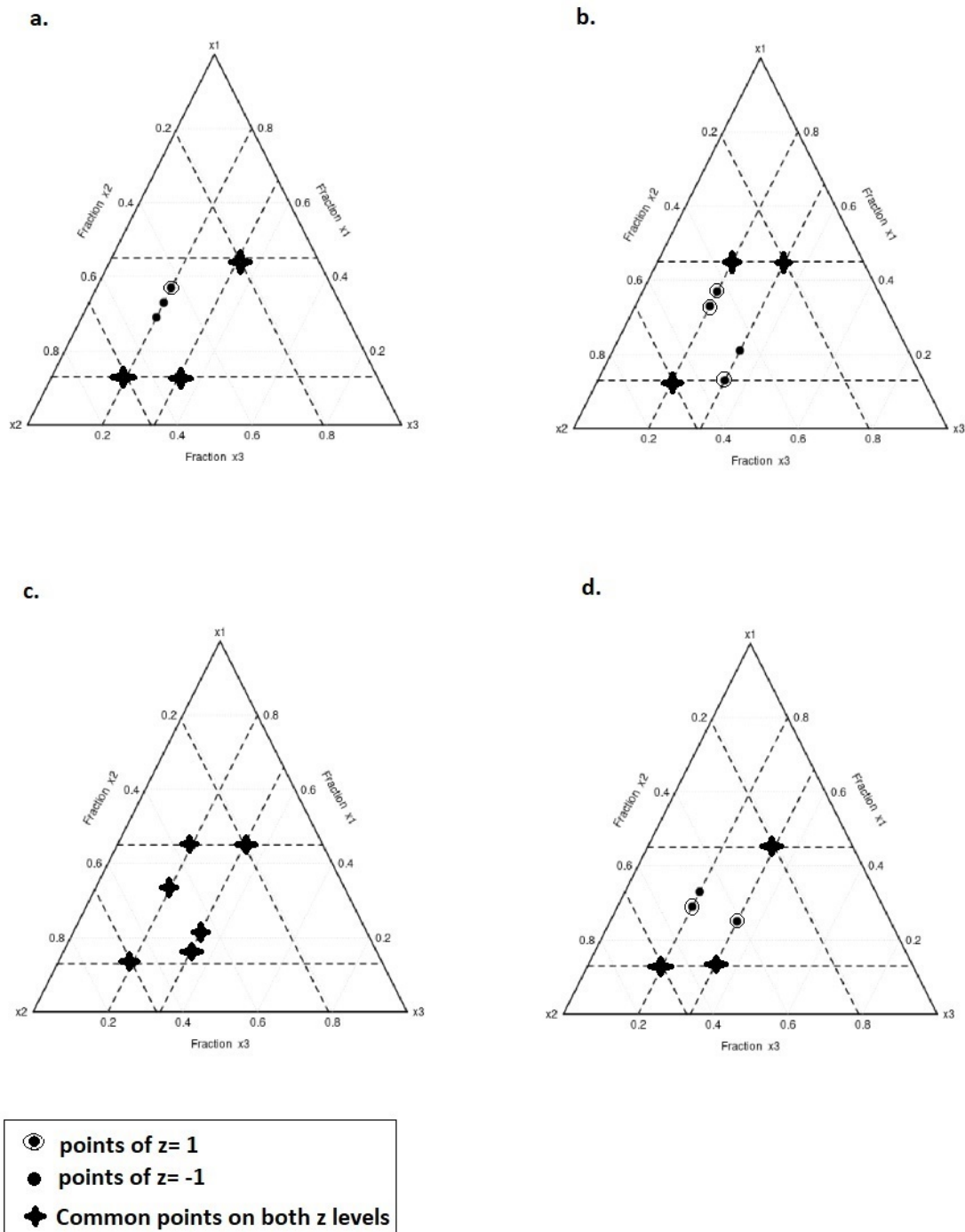


Figure 6.24: MVP designs for CMFP models with a single power parameter for the four studied scenarios

Table 6.27: The MPV design when all parameter values have the estimated values

Design points	Replications	The pro.var level
$\mathbf{x}_1=(0.45,0.21,0.34)$	8	$z=1$
$\mathbf{x}_2=(0.45,0.21,0.34)$	7	$z=-1$
$\mathbf{x}_3=(0.13,0.67,0.20)$	6	$z=-1$
$\mathbf{x}_4=(0.13,0.67,0.20)$	6	$z=1$
$\mathbf{x}_5=(0.13,0.53,0.34)$	7	$z=-1$
$\mathbf{x}_6=(0.13,0.53,0.34)$	7	$z=1$
$\mathbf{x}_7=(0.45,0.35,0.20)$	7	$z=1$
$\mathbf{x}_8=(0.33,0.47,0.20)$	7	$z=-1$
$\mathbf{x}_9=(0.25,0.55,0.20)$	5	$z=1$

Table 6.28: The MPV design when all parameters values have the estimated values but with opposite signs

Design points	Replications	The pro.var level
$\mathbf{x}_1=(0.13,0.67,0.20)$	7	$z=-1$
$\mathbf{x}_2=(0.13,0.67,0.20)$	8	$z=1$
$\mathbf{x}_3=(0.45,0.21,0.34)$	7	$z=1$
$\mathbf{x}_4=(0.45,0.35,0.20)$	6	$z=-1$
$\mathbf{x}_5=(0.13,0.53,0.34)$	7	$z=1$
$\mathbf{x}_6=(0.45,0.21,0.34)$	7	$z=-1$
$\mathbf{x}_7=(0.41,0.39,0.20)$	7	$z=1$
$\mathbf{x}_8=(0.13,0.53,0.34)$	3	$z=-1$
$\mathbf{x}_9=(0.17,0.49,0.34)$	2	$z=-1$
$\mathbf{x}_{10}=(0.25,0.41,0.34)$	3	$z=-1$
$\mathbf{x}_{11}=(0.25,0.55,0.20)$	3	$z=-1$

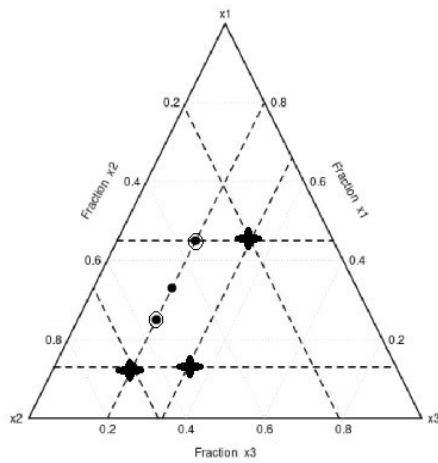
Table 6.29: The MPV design when $\alpha_1 = -0.50$, $\alpha_2 = 0.77$ and β 's=-1

Design points	Replications	The pro.var level
$\mathbf{x}_1=(0.13,0.67,0.20)$	7	$z=1$
$\mathbf{x}_2=(0.45,0.21,0.34)$	8	$z=1$
$\mathbf{x}_3=(0.13,0.53,0.34)$	7	$z=-1$
$\mathbf{x}_4=(0.13,0.67,0.20)$	7	$z=-1$
$\mathbf{x}_5=(0.13,0.53,0.34)$	7	$z=1$
$\mathbf{x}_6=(0.45,0.21,0.34)$	6	$z=-1$
$\mathbf{x}_7=(0.45,0.35,0.20)$	6	$z=1$
$\mathbf{x}_8=(0.25,0.55,0.20)$	7	$z=-1$
$\mathbf{x}_9=(0.25,0.55,0.20)$	4	$z=1$
$\mathbf{x}_{10}=(0.45,0.35,0.20)$	1	$z=-1$

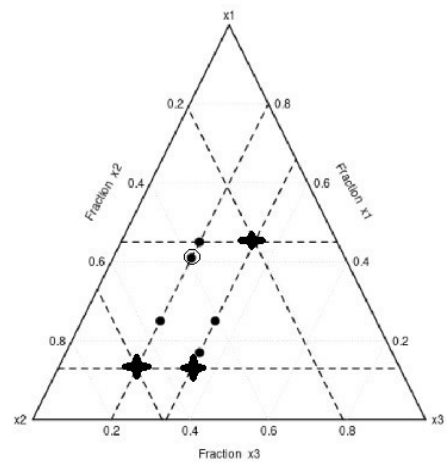
Table 6.30: The MPV design when $\alpha_1 = 0.85$, $\alpha_2 = -0.60$ and β 's=1

Design points	Replications	The pro.var level
$\mathbf{x}_1=(0.45,0.21,0.34)$	7	$z=1$
$\mathbf{x}_2=(0.45,0.21,0.34)$	7	$z=-1$
$\mathbf{x}_3=(0.45,0.35,0.20)$	7	$z=1$
$\mathbf{x}_4=(0.13,0.67,0.20)$	6	$z=-1$
$\mathbf{x}_5=(0.13,0.53,0.34)$	7	$z=1$
$\mathbf{x}_6=(0.45,0.35,0.20)$	7	$z=-1$
$\mathbf{x}_7=(0.13,0.67,0.20)$	3	$z=1$
$\mathbf{x}_8=(0.13,0.53,0.34)$	2	$z=-1$
$\mathbf{x}_9=(0.29,0.51,0.20)$	6	$z=1$
$\mathbf{x}_{10}=(0.29,0.37,0.34)$	5	$z=-1$
$\mathbf{x}_{11}=(0.33,0.33,0.34)$	3	$z=1$

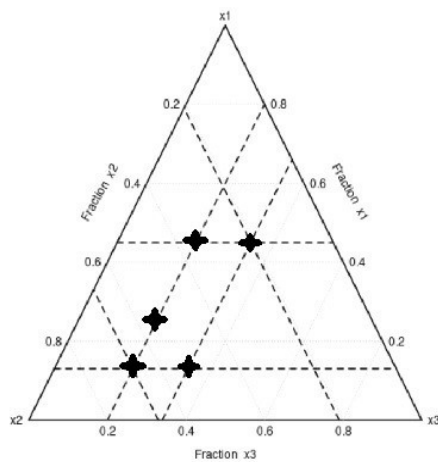
a.



b.



c.



d.

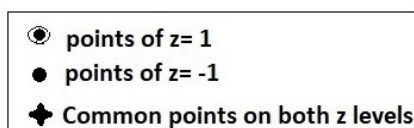
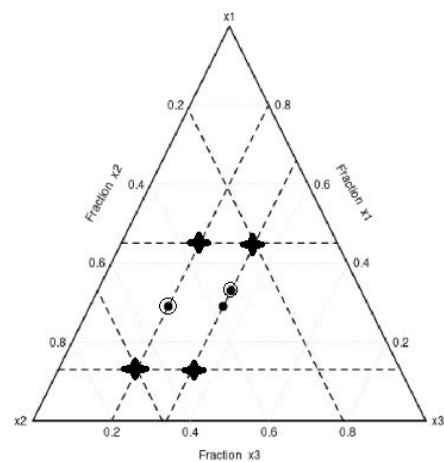


Figure 6.25: MVP designs for CMFP models with two power parameters for the four studied scenarios

The optimized MPV designs have points similar to those generated for the single power parameter case for the four scenarios in general. Three design points, namely $(0.13, 0.67, 0.20)$, $(0.13, 0.53, 0.34)$, and $(0.45, 0.21, 0.34)$, are present at both levels of the process variable and are common to all designs. These three points are, again, vertices of the experimental region, and this set includes the two points that had been seen to feature in all designs for the single power parameter models. The fourth vertex finally features in all designs, but not at every level of z . Again, all design points lie on the boundary of the experimental region. Next, we will find MPV designs for another experimental dataset with a process variable with three levels to make the comparison between two levels and three levels of a process variable evident.

6.4.2 Example 2: MPV Designs for the Opacity of Printable Coating Material Experiment with a 3-level Process Variable

As introduced in Section 4.3, Chau and Kelley (1993) also obtained experimental data on the opacity of the printable coating material when the process variable, coating thickness, was measured at 3 different values, 10, 19, and 28, which correspond to 0, 1, and 2, respectively. Again, the opacity was also affected by the mixture proportions, which were subject to the same limitations as in the first dataset. See Table 8.2 in the appendix for the data. When the power parameters are the same, the first, second, and fourth scenarios resulted in only nine design points, while more design points resulted in the third scenario. When the power parameters are different, the first scenario resulted in twelve design points, the second and fourth scenarios resulted in eleven design points, and the third scenario resulted in only ten design points. All optimized MPV designs in the case of a single power parameter with the levels of the process variable are shown in Table 6.31, Table 6.32, Table 6.33, and Table 6.34 and are visualized in the plots in Figure 6.26.

Table 6.31: The MPV design when all parameter values have the estimated values

Design points	Replications	The pro.var level
$\mathbf{x}_1=(0.45, 0.21, 0.34)$	8	$z=2$
$\mathbf{x}_2=(0.13, 0.53, 0.34)$	7	$z=0$
$\mathbf{x}_3=(0.45, 0.21, 0.34)$	8	$z=0$
$\mathbf{x}_4=(0.13, 0.67, 0.20)$	7	$z=2$
$\mathbf{x}_5=(0.13, 0.67, 0.20)$	6	$z=0$
$\mathbf{x}_6=(0.13, 0.53, 0.34)$	6	$z=2$
$\mathbf{x}_7=(0.37, 0.43, 0.20)$	9	$z=2$
$\mathbf{x}_8=(0.29, 0.51, 0.20)$	4	$z=0$
$\mathbf{x}_9=(0.33, 0.47, 0.20)$	5	$z=0$

Table 6.32: The MPV design when all parameter values have the estimated values but with opposite signs

Design points	Replications	The pro.var level
$\mathbf{x}_1=(0.13,0.67,0.20)$	8	$z=2$
$\mathbf{x}_2=(0.13,0.67,0.20)$	8	$z=0$
$\mathbf{x}_3=(0.45,0.21,0.34)$	7	$z=2$
$\mathbf{x}_4=(0.45,0.21,0.34)$	6	$z=0$
$\mathbf{x}_5=(0.13,0.53,0.34)$	9	$z=2$
$\mathbf{x}_6=(0.45,0.35,0.20)$	6	$z=0$
$\mathbf{x}_7=(0.21,0.45,0.34)$	9	$z=0$
$\mathbf{x}_8=(0.37,0.43,0.20)$	5	$z=2$
$\mathbf{x}_9=(0.45,0.35,0.20)$	2	$z=2$

Table 6.33: The MPV design when $\alpha = 0.88$ and $\beta^s=-1$

Design points	Replications	The pro.var level
$\mathbf{x}_1=(0.13,0.67,0.20)$	8	$z=2$
$\mathbf{x}_2=(0.45,0.21,0.34)$	7	$z=2$
$\mathbf{x}_3=(0.13,0.67,0.20)$	8	$z=0$
$\mathbf{x}_4=(0.45,0.21,0.34)$	7	$z=0$
$\mathbf{x}_5=(0.45,0.35,0.20)$	4	$z=0$
$\mathbf{x}_6=(0.45,0.35,0.20)$	4	$z=2$
$\mathbf{x}_7=(0.21,0.45,0.34)$	3	$z=0$
$\mathbf{x}_8=(0.21,0.45,0.34)$	2	$z=2$
$\mathbf{x}_9=(0.17,0.49,0.34)$	5	$z=0$
$\mathbf{x}_{10}=(0.17,0.49,0.34)$	6	$z=2$
$\mathbf{x}_{11}=(0.33,0.47,0.20)$	3	$z=0$
$\mathbf{x}_{12}=(0.33,0.47,0.20)$	3	$z=2$

Table 6.34: The MPV design when $\alpha = -0.93$ and $\beta^s=1$

Design points	Replications	The pro.var level
$\mathbf{x}_1=(0.45,0.21,0.34)$	9	$z=0$
$\mathbf{x}_2=(0.13,0.53,0.34)$	6	$z=2$
$\mathbf{x}_3=(0.13,0.67,0.20)$	6	$z=0$
$\mathbf{x}_4=(0.13,0.67,0.20)$	6	$z=2$
$\mathbf{x}_5=(0.13,0.53,0.34)$	6	$z=0$
$\mathbf{x}_6=(0.45,0.21,0.34)$	9	$z=2$
$\mathbf{x}_7=(0.25,0.41,0.34)$	4	$z=2$
$\mathbf{x}_8=(0.33,0.47,0.20)$	8	$z=0$
$\mathbf{x}_9=(0.29,0.51,0.20)$	6	$z=2$

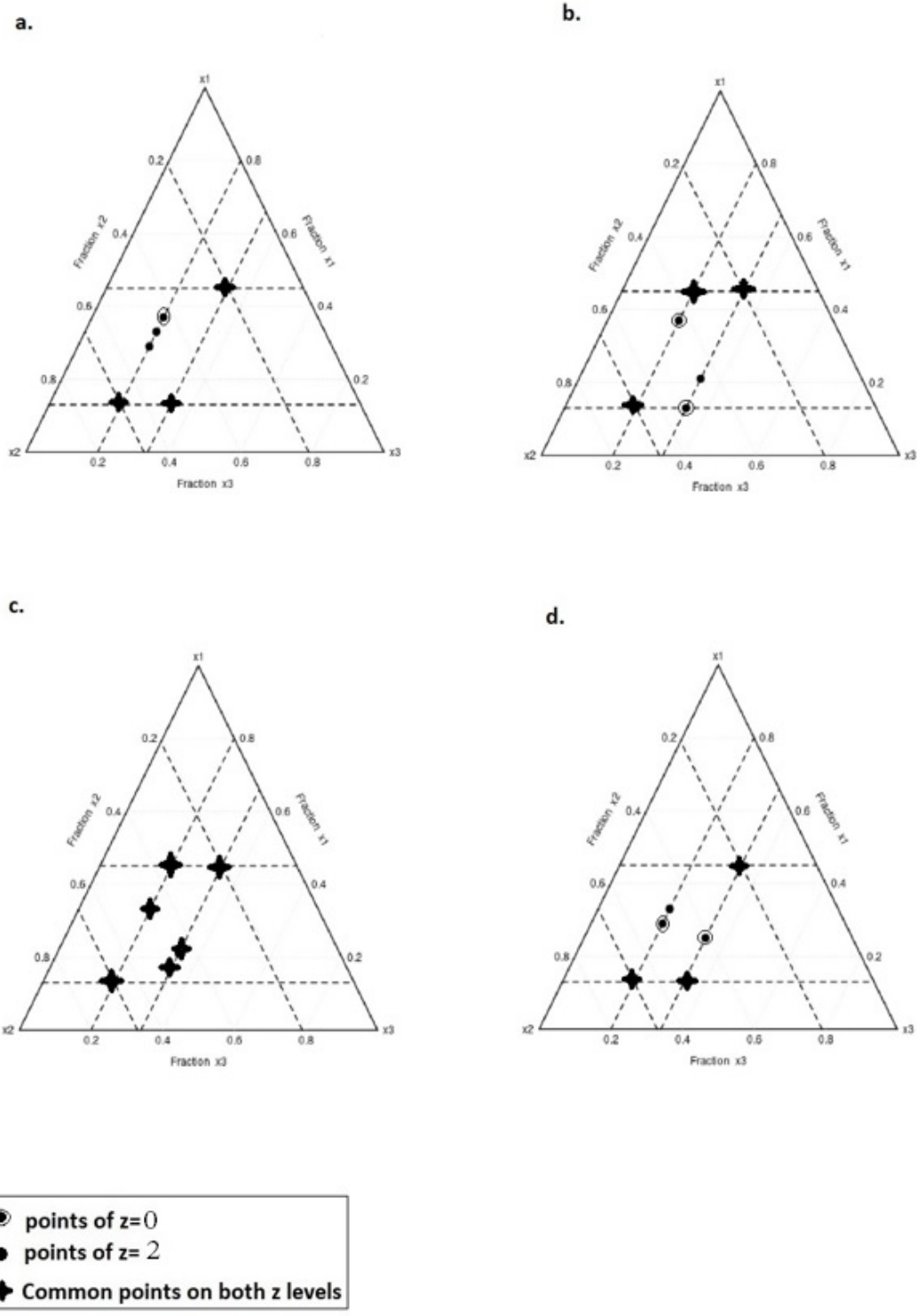


Figure 6.26: MVP designs for CMFP models with a single power parameter for the four studied scenarios

All MVP designs for the four studied scenarios when the dataset has a process variable with three levels are the same as MVP designs for the four studied scenarios when the dataset has a process variable with two levels in the case of one power parameter. Likewise, we need to check the designs in the case of two power parameters when the dataset has a three-level process variable. These MPV designs are evident in Table 6.35, Table 6.36, Table 6.37, and Table 6.38 in addition to the plots in Figure 6.27.

Table 6.35: The MPV design when all parameter values have the estimated values

Design points	Replications	The pro.var level
$\mathbf{x}_1=(0.13,0.67,0.20)$	6	$z=0$
$\mathbf{x}_2=(0.45,0.21,0.34)$	7	$z=0$
$\mathbf{x}_3=(0.45,0.21,0.34)$	7	$z=2$
$\mathbf{x}_4=(0.13,0.53,0.34)$	6	$z=0$
$\mathbf{x}_5=(0.13,0.67,0.20)$	7	$z=2$
$\mathbf{x}_6=(0.13,0.53,0.34)$	7	$z=2$
$\mathbf{x}_7=(0.33,0.47,0.20)$	5	$z=0$
$\mathbf{x}_8=(0.45,0.35,0.20)$	6	$z=2$
$\mathbf{x}_9=(0.29,0.51,0.20)$	4	$z=2$
$\mathbf{x}_{10}=(0.21,0.59,0.20)$	1	$z=0$
$\mathbf{x}_{11}=(0.33,0.33,0.34)$	3	$z=0$
$\mathbf{x}_{12}=(0.29,0.51,0.20)$	1	$z=0$

Table 6.36: The MPV design when all parameter values have the estimated values but with opposite signs

Design points	Replications	The pro.var level
$\mathbf{x}_1=(0.13,0.67,0.20)$	7	$z=0$
$\mathbf{x}_2=(0.13,0.67,0.20)$	8	$z=2$
$\mathbf{x}_3=(0.45,0.21,0.34)$	7	$z=2$
$\mathbf{x}_4=(0.45,0.21,0.34)$	7	$z=0$
$\mathbf{x}_5=(0.45,0.35,0.20)$	6	$z=0$
$\mathbf{x}_6=(0.13,0.53,0.34)$	6	$z=2$
$\mathbf{x}_7=(0.37,0.43,0.20)$	6	$z=2$
$\mathbf{x}_8=(0.13,0.53,0.34)$	4	$z=0$
$\mathbf{x}_9=(0.45,0.35,0.20)$	1	$z=2$
$\mathbf{x}_{10}=(0.29,0.51,0.20)$	3	$z=0$
$\mathbf{x}_{11}=(0.25,0.41,0.34)$	5	$z=0$

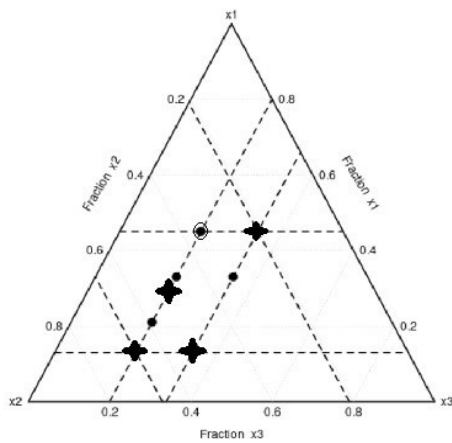
Table 6.37: The MPV design when $\alpha_1 = -0.50$, $\alpha_2 = 0.77$ and β 's=-1

Design points	Replications	The pro.var level
$\mathbf{x}_1=(0.13,0.67,0.20)$	7	$z=2$
$\mathbf{x}_2=(0.13,0.53,0.34)$	7	$z=2$
$\mathbf{x}_3=(0.13,0.53,0.34)$	7	$z=0$
$\mathbf{x}_4=(0.45,0.21,0.34)$	8	$z=2$
$\mathbf{x}_5=(0.13,0.67,0.20)$	7	$z=0$
$\mathbf{x}_6=(0.45,0.35,0.20)$	6	$z=2$
$\mathbf{x}_7=(0.45,0.21,0.34)$	6	$z=0$
$\mathbf{x}_8=(0.25,0.55,0.20)$	4	$z=2$
$\mathbf{x}_9=(0.25,0.55,0.20)$	7	$z=0$
$\mathbf{x}_{10}=(0.45,0.35,0.20)$	1	$z=0$

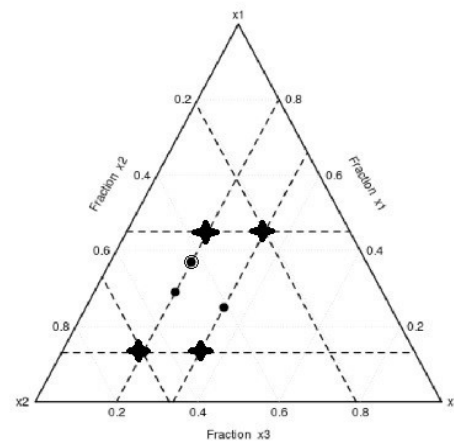
Table 6.38: The MPV design when $\alpha_1 = 0.85$, $\alpha_2 = -0.60$ and β 's=1

Design points	Replications	The pro.var level
$\mathbf{x}_1=(0.45,0.21,0.34)$	7	$z= 2$
$\mathbf{x}_2=(0.45,0.21,0.34)$	7	$z= 0$
$\mathbf{x}_3=(0.13,0.53,0.34)$	7	$z= 2$
$\mathbf{x}_4=(0.45,0.35,0.20)$	7	$z= 2$
$\mathbf{x}_5=(0.45,0.35,0.20)$	7	$z= 0$
$\mathbf{x}_6=(0.13,0.67,0.20)$	6	$z= 0$
$\mathbf{x}_7=(0.13,0.67,0.20)$	3	$z= 2$
$\mathbf{x}_8=(0.13,0.53,0.34)$	2	$z= 0$
$\mathbf{x}_9=(0.29,0.37,0.34)$	5	$z= 0$
$\mathbf{x}_{10}=(0.29,0.51,0.20)$	6	$z= 2$
$\mathbf{x}_{11}=(0.33,0.33,0.34)$	3	$z= 2$

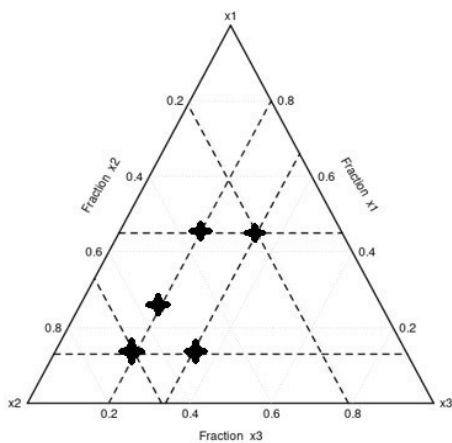
a.



b.



c.



d.

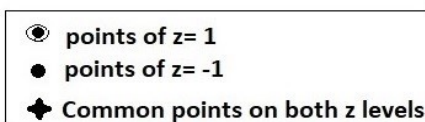
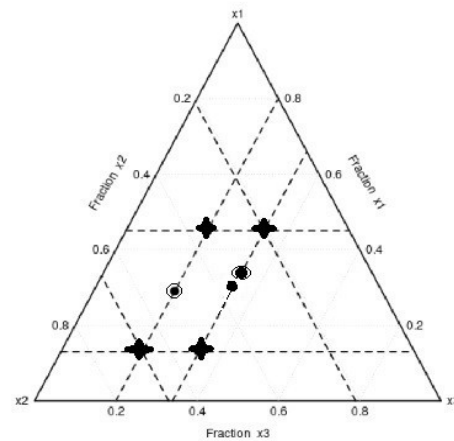


Figure 6.27: MVP designs for CMFP models with two power parameters for the four studied scenarios

In this case, the MPV designs in the four studied scenarios for a 3-level process variable are similar to MPV designs for a 2-level process variable. Yet, there are minor differences between the MPV designs of the first and second datasets in each scenario. For example, in the design of the second dataset, the first scenario resulted in more design points. One more point that became common in both levels is (0.29,0.51,0.20) instead of a point close to it in the first dataset, which exists only at a high level of the process variable, and this point is (0.25,0.55,0.20). In the second scenario, the point (0.45,0.35,0.20) became common in both levels while it only exists at the low level of the design of the first dataset. These differences can be explained by the slightly different values of the estimated model parameters in the two datasets. Again, in all scenarios for this example, the vertices of the experimental region are featured in most designs, and all design points are on the boundary.

After studying two datasets with a process variable, whether it has two or three levels, the optimized MPV designs generated by the exchange algorithm using the CMFP models produced design points at the low and high levels of the process variable only. This is likely to be a consequence of the models only having terms that are linear in the process variable. The similarity of the MPV designs of CMFP models in the cases of one power parameter and two power parameters facilitates the experimenter to generate a good design without overthinking what power parameters case in the CMFP model will be used.

Furthermore, MPV designs for four scenarios of each case of power parameters of CMFP models are generated for the following dataset that contains a three-level process variable.

6.4.3 Example 3: MPV Designs for Oil-Water Separation Experiment with a 3-level Process Variable

The oil-water separation ratio after a week of storage at room temperature was the response of interest in an experiment conducted by Hare (1979). In this experiment, which has been introduced in Section 4.5, three mixture components were used (water x_1 , oil x_2 , and emulsifier x_3) to determine the effectiveness of the unsaturated fatty acid esters of corn oil. The restrictions on the proportions of the mixture components were $0.430 \leq x_1 \leq 0.645$, $0.350 \leq x_2 \leq 0.550$, $0.005 \leq x_3 \leq 0.020$. The response of this experiment is also affected by the agitation time in minutes, which is a three-level process variable ($z = 2, 3$, and 4 , corresponding to $0, 1$, and 2 , respectively). The data are shown in Table 8.4 in the appendix. When the power parameters are the same, the first, second, and fourth scenarios resulted in twelve design points, while more design points resulted in the third scenario. When the power parameters are different, the first and second scenarios resulted in fifteen

design points. The third and fourth scenarios resulted in twelve design points. All optimized MPV designs in the case of a single power parameter are shown in tables 6.39, 6.40, 6.41, and 6.42 and Figure 6.28.

Table 6.39: The MPV design when all parameter values have the estimated values

Design points	Replications	The pro.var level
$\mathbf{x}_1=(0.430,0.550,0.020)$	7	$z= 2$
$\mathbf{x}_2=(0.430,0.550,0.020)$	8	$z= 0$
$\mathbf{x}_3=(0.630,0.350,0.020)$	6	$z= 2$
$\mathbf{x}_4=(0.645,0.350,0.005)$	5	$z= 2$
$\mathbf{x}_5=(0.445,0.550,0.005)$	3	$z= 2$
$\mathbf{x}_6=(0.645,0.350,0.005)$	6	$z= 0$
$\mathbf{x}_7=(0.445,0.550,0.005)$	2	$z= 0$
$\mathbf{x}_8=(0.630,0.350,0.020)$	4	$z= 0$
$\mathbf{x}_9=(0.520,0.475,0.005)$	6	$z= 0$
$\mathbf{x}_{10}=(0.545,0.450,0.005)$	7	$z= 2$
$\mathbf{x}_{11}=(0.530,0.450,0.020)$	3	$z= 0$
$\mathbf{x}_{12}=(0.530,0.450,0.020)$	3	$z= 2$

Table 6.40: The MPV design when all parameter values have the estimated values but with opposite signs

Design points	Replications	The pro.var level
$\mathbf{x}_1=(0.645,0.350,0.005)$	8	$z= 0$
$\mathbf{x}_2=(0.430,0.550,0.020)$	6	$z= 0$
$\mathbf{x}_3=(0.445,0.550,0.005)$	6	$z= 2$
$\mathbf{x}_4=(0.645,0.350,0.005)$	7	$z= 2$
$\mathbf{x}_5=(0.445,0.550,0.005)$	4	$z= 0$
$\mathbf{x}_6=(0.430,0.550,0.020)$	4	$z= 2$
$\mathbf{x}_7=(0.630,0.350,0.020)$	3	$z= 2$
$\mathbf{x}_8=(0.630,0.350,0.020)$	3	$z= 0$
$\mathbf{x}_9=(0.530,0.450,0.020)$	7	$z= 2$
$\mathbf{x}_{10}=(0.555,0.425,0.020)$	6	$z= 0$
$\mathbf{x}_{11}=(0.545,0.450,0.005)$	4	$z= 0$
$\mathbf{x}_{12}=(0.545,0.450,0.005)$	2	$z= 2$

Table 6.41: The MPV design when $\alpha = 0.88$ and $\beta's=-1$

Design points	Replications	The pro.var level
$\mathbf{x}_1=(0.445,0.550,0.005)$	5	$z= 2$
$\mathbf{x}_2=(0.645,0.350,0.005)$	7	$z= 2$
$\mathbf{x}_3=(0.430,0.550,0.020)$	5	$z= 2$
$\mathbf{x}_4=(0.630,0.350,0.020)$	3	$z= 0$
$\mathbf{x}_5=(0.645,0.350,0.005)$	7	$z= 0$
$\mathbf{x}_6=(0.445,0.550,0.005)$	5	$z= 0$
$\mathbf{x}_7=(0.630,0.350,0.020)$	3	$z= 2$
$\mathbf{x}_8=(0.430,0.550,0.020)$	5	$z= 0$
$\mathbf{x}_9=(0.530,0.450,0.020)$	5	$z= 0$
$\mathbf{x}_{10}=(0.555,0.425,0.020)$	3	$z= 2$
$\mathbf{x}_{11}=(0.545,0.450,0.005)$	4	$z= 2$
$\mathbf{x}_{12}=(0.545,0.450,0.005)$	4	$z= 0$
$\mathbf{x}_{13}=(0.530,0.450,0.020)$	3	$z= 2$
$\mathbf{x}_{14}=(0.555,0.425,0.020)$	1	$z= 0$

Table 6.42: The MPV design when $\alpha = -0.93$ and $\beta^i s=1$

Design points	Replications	The pro.var level
$x_1=(0.430,0.55,0.020)$	7	$z=0$
$x_2=(0.430,0.55,0.020)$	7	$z=2$
$x_3=(0.630,0.35,0.020)$	5	$z=0$
$x_4=(0.645,0.35,0.005)$	5	$z=2$
$x_5=(0.645,0.35,0.005)$	5	$z=0$
$x_6=(0.445,0.55,0.005)$	3	$z=0$
$x_7=(0.630,0.35,0.020)$	5	$z=2$
$x_8=(0.445,0.55,0.005)$	3	$z=2$
$x_9=(0.545,0.45,0.005)$	6	$z=2$
$x_{10}=(0.545,0.45,0.005)$	6	$z=0$
$x_{11}=(0.530,0.45,0.020)$	4	$z=0$
$x_{12}=(0.530,0.45,0.020)$	4	$z=2$

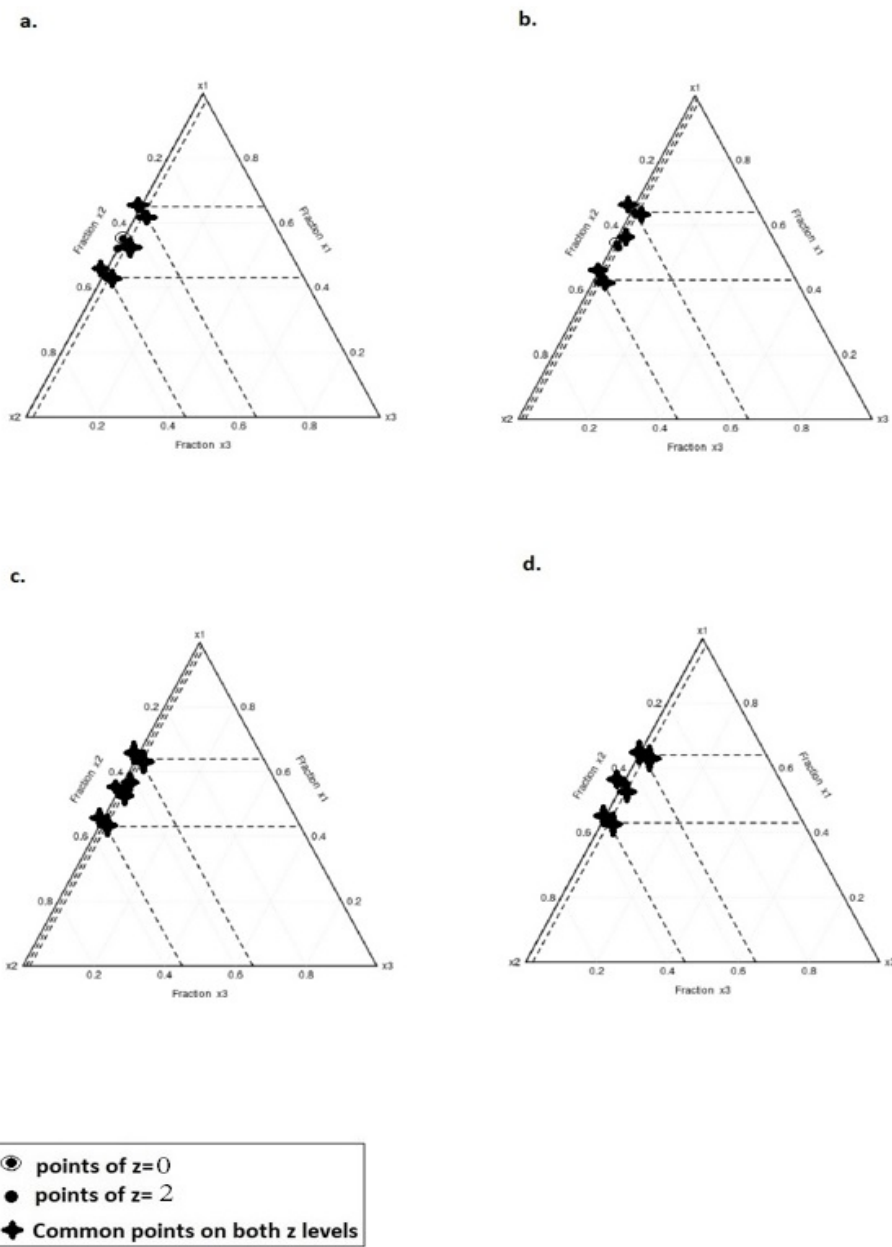


Figure 6.28: MVP designs for CMFP models with one power parameter for the four studied scenarios

Although this experiment was performed on three levels of the process variable, the points of our MPV designs were only generated at low and high levels, as previously when studying the dataset in Section 6.4.2. MPV designs for all four scenarios have at least five points in common at both levels of the process variable, and four of these points are common to all designs. These points are $(0.430, 0.55, 0.020)$, $(0.630, 0.35, 0.020)$, $(0.645, 0.35, 0.005)$, and $(0.445, 0.55, 0.005)$. As shown, all optimized MPV designs are generally similar to each other. Furthermore, four other scenarios were studied to investigate the form of the designs when the model has two power parameters. The designs for this case are shown in tables 6.43, 6.44, 6.45 and 6.46.

Table 6.43: The MPV design when all parameter values have the estimated values

Design points	Replications	The pro.var level
$\mathbf{x}_1 = (0.645, 0.350, 0.005)$	6	$z = 2$
$\mathbf{x}_2 = (0.645, 0.350, 0.005)$	7	$z = 0$
$\mathbf{x}_3 = (0.430, 0.550, 0.020)$	5	$z = 2$
$\mathbf{x}_4 = (0.430, 0.550, 0.020)$	6	$z = 0$
$\mathbf{x}_5 = (0.445, 0.550, 0.005)$	3	$z = 0$
$\mathbf{x}_6 = (0.630, 0.350, 0.020)$	3	$z = 2$
$\mathbf{x}_7 = (0.445, 0.550, 0.005)$	4	$z = 2$
$\mathbf{x}_8 = (0.630, 0.350, 0.020)$	5	$z = 0$
$\mathbf{x}_9 = (0.595, 0.400, 0.005)$	6	$z = 0$
$\mathbf{x}_{10} = (0.495, 0.500, 0.005)$	4	$z = 0$
$\mathbf{x}_{11} = (0.495, 0.500, 0.005)$	2	$z = 2$
$\mathbf{x}_{12} = (0.595, 0.400, 0.005)$	1	$z = 2$
$\mathbf{x}_{13} = (0.561, 0.425, 0.014)$	4	$z = 2$
$\mathbf{x}_{14} = (0.530, 0.450, 0.020)$	2	$z = 2$
$\mathbf{x}_{15} = (0.580, 0.400, 0.020)$	2	$z = 0$

Table 6.44: The MPV design when all parameter values have the estimated values but with opposite signs

Design points	Replications	The pro.var level
$\mathbf{x}_1 = (0.605, 0.375, 0.020)$	1	$z = 0$
$\mathbf{x}_2 = (0.645, 0.350, 0.005)$	6	$z = 0$
$\mathbf{x}_3 = (0.430, 0.550, 0.020)$	5	$z = 2$
$\mathbf{x}_4 = (0.630, 0.350, 0.020)$	5	$z = 2$
$\mathbf{x}_5 = (0.430, 0.550, 0.020)$	4	$z = 0$
$\mathbf{x}_6 = (0.445, 0.550, 0.005)$	4	$z = 2$
$\mathbf{x}_7 = (0.645, 0.350, 0.005)$	5	$z = 2$
$\mathbf{x}_8 = (0.432, 0.550, 0.018)$	2	$z = 0$
$\mathbf{x}_9 = (0.630, 0.350, 0.020)$	5	$z = 0$
$\mathbf{x}_{10} = (0.545, 0.450, 0.005)$	6	$z = 0$
$\mathbf{x}_{11} = (0.445, 0.550, 0.005)$	3	$z = 0$
$\mathbf{x}_{12} = (0.505, 0.475, 0.020)$	1	$z = 0$
$\mathbf{x}_{13} = (0.480, 0.500, 0.020)$	5	$z = 2$
$\mathbf{x}_{14} = (0.480, 0.500, 0.020)$	2	$z = 0$
$\mathbf{x}_{15} = (0.587, 0.400, 0.013)$	6	$z = 2$

Table 6.45: The MPV design when $\alpha_1 = -0.50$, $\alpha_2 = 0.77$ and β 's=1

Design points	Replications	The pro.var level
$\mathbf{x}_1=(0.445,0.550,0.005)$	7	$z= 2$
$\mathbf{x}_2=(0.645,0.350,0.005)$	6	$z= 0$
$\mathbf{x}_3=(0.445,0.550,0.005)$	6	$z= 0$
$\mathbf{x}_4=(0.430,0.550,0.020)$	7	$z= 0$
$\mathbf{x}_5=(0.430,0.550,0.020)$	6	$z= 2$
$\mathbf{x}_6=(0.630,0.350,0.020)$	6	$z= 2$
$\mathbf{x}_7=(0.645,0.350,0.005)$	3	$z= 2$
$\mathbf{x}_8=(0.630,0.350,0.020)$	2	$z= 0$
$\mathbf{x}_9=(0.545,0.450,0.005)$	5	$z= 2$
$\mathbf{x}_{10}=(0.530,0.450,0.020)$	5	$z= 0$
$\mathbf{x}_{11}=(0.505,0.475,0.020)$	4	$z= 2$
$\mathbf{x}_{12}=(0.520,0.475,0.005)$	3	$z= 0$

Table 6.46: The MPV design when $\alpha_1 = 0.85$, $\alpha_2 = -0.60$ and β 's=1

Design points	Replications	The pro.var level
$\mathbf{x}_1=(0.645,0.350,0.005)$	6	$z= 2$
$\mathbf{x}_2=(0.630,0.350,0.020)$	7	$z= 0$
$\mathbf{x}_3=(0.645,0.350,0.005)$	6	$z= 0$
$\mathbf{x}_4=(0.430,0.550,0.020)$	7	$z= 2$
$\mathbf{x}_5=(0.630,0.350,0.020)$	7	$z= 2$
$\mathbf{x}_6=(0.430,0.550,0.020)$	4	$z= 0$
$\mathbf{x}_7=(0.445,0.550,0.005)$	4	$z= 0$
$\mathbf{x}_8=(0.445,0.550,0.005)$	3	$z= 2$
$\mathbf{x}_9=(0.545,0.450,0.005)$	6	$z= 2$
$\mathbf{x}_{10}=(0.570,0.425,0.005)$	4	$z= 0$
$\mathbf{x}_{11}=(0.555,0.425,0.020)$	5	$z= 0$
$\mathbf{x}_{12}=(0.580,0.400,0.020)$	1	$z= 2$

Often, more design points are generated in this case than in the case of a single power parameter. Generally, the designs are similar in both cases. There are slight differences between cases concerning design points. For the first scenario, one more design point appears, which is common on both levels, while the same number of common points appears in the second scenario in both cases. Fewer points that are common at both levels exist in the third and fourth scenarios compared to those in the other case. Thus, more special points are found that appear at only the low level or only the high level in these two scenarios for this case. Again, the vertices of the experimental region feature in most designs, and all design points are on its boundary. Similar to first-order CMFP without process variable, all design points lie on the boundary of the experimental region. Although rare interior design points appear in the designs of first-order CMFP without a process variable, in our examples, none appear in the designs of first-order CMFP with a process variable.

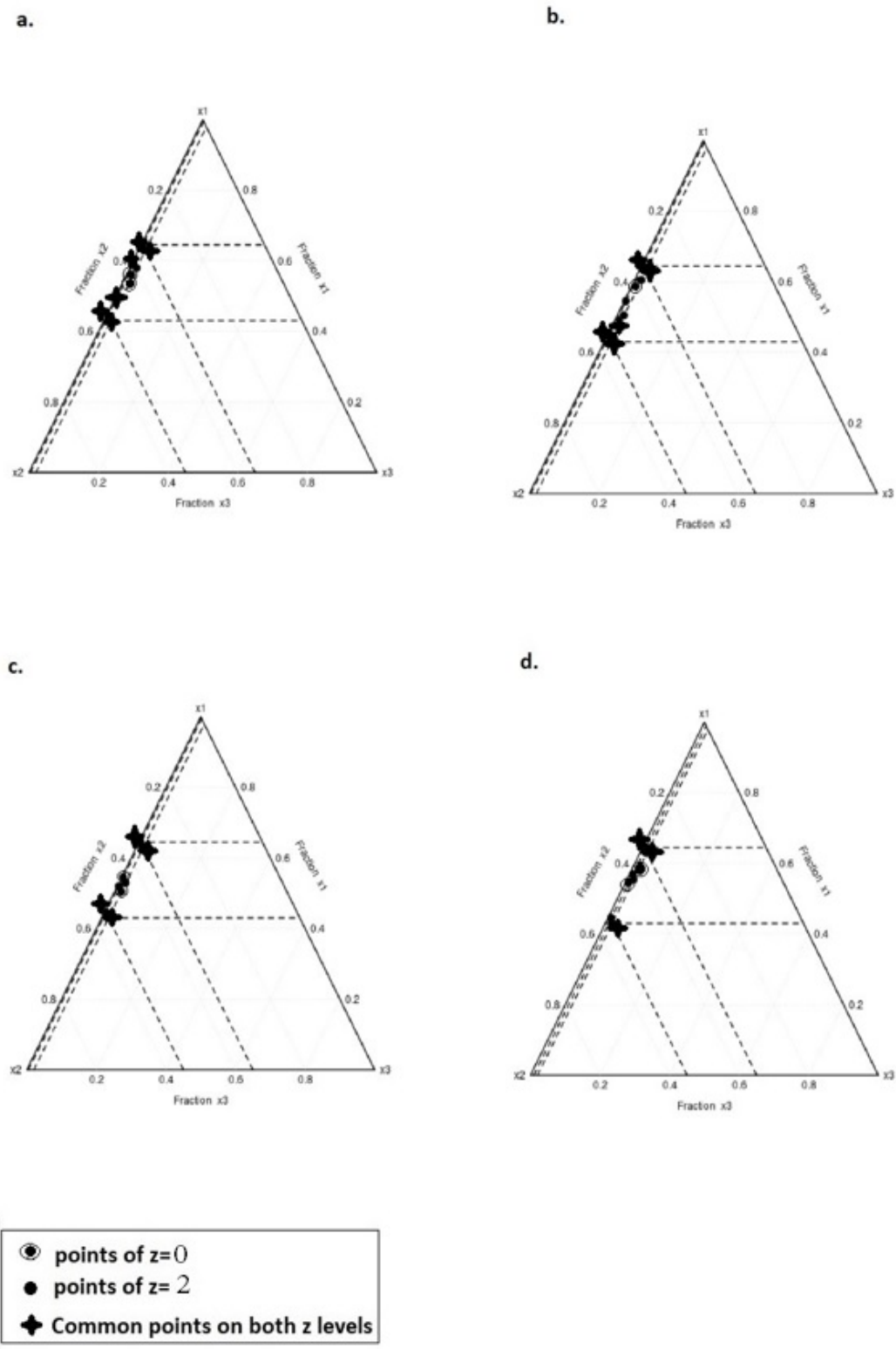


Figure 6.29: MVP designs for CMFP models with two power parameters for the four studied scenarios

Chapter 7

Conclusion and Some Further Recommendations

7.1 Brief Review

Linear models, such as Scheffé's polynomial models, are traditionally used to model data from experiments with mixtures. Recently, nonlinear models, for example, general blending models, have been proposed to be applied to such data. However, existing approaches are either not flexible enough in all situations or are quite complex. Therefore, we seek models that are flexible and parsimonious at the same time. So, we proposed a new class of nonlinear models for fitting the data from mixture and mixture-process variables experiments. These new models propose an additional transformation of the modified fractional polynomial models, which are quite constrained if some proportions may be zero. In addition, we proposed an extended form for the modified fractional polynomial models to fit data from mixture-process variables experiments. Then, these models are compared with several models from the literature. The CMFP models and the MFP models, such as model (3.7), model (3.8), model (3.9), and model (3.10) for mixture experiments, as well as the extended forms of the CMFP and the MFP models such as model (3.15), model (3.16), model (3.17), and model (3.18) for mixture-process variables experiments, were fit to real data and have been found to be good competitor models to the standard and popular models from the literature, and often even outperforming them. The experimental datasets that have been studied in Chapter 4 illustrate that model (3.18) can ideally fit data from three mixture components experiments with a single process variable, whether the number of levels of the process variable is two or three. Model (3.17), on the other hand, best fits experimental datasets that are affected by two process variables. Moreover, model (3.10) demonstrated its ability to find optimal values of the mixture

proportions in the simulation study in Section 5.3 and 5.4, besides its flexible use of either retaining or deleting any term as needed for each different scenario. Additionally, model (3.16) and model (3.18) can find the optimal values of the mixture proportions and the best condition of the process variable for data from mixture experiments that include a process variable as described in Section 5.5. In addition, we note the flexibility of all CMFP models because any of the CMFP models can be simple or more complex as needed (any term can be kept or deleted depending on the dataset under study, or higher order terms could be added).

Constructing a suitable design depends on the chosen model, the region of interest, and the optimality criteria that we consider. In Chapter 6, we find designs for the CMFP models for several scenarios of the model parameter values under the D-optimality criterion. As the component proportions are subject to further constraints in addition to the natural constraints of the mixture in all experimental datasets under study, the experimental regions of all designs are non-simplex-shaped (irregular) regions. We found that the locally optimal designs for each CMFP model under study are similar for all scenarios, with most optimal support points situated on the boundary of the experimental regions. Regarding assessing the robustness of these designs with respect to the model parameters, we calculated the relative D-efficiencies of the D-optimal designs with misspecified parameter values relative to the design with the correctly specified parameter values for all scenarios. The relative D-efficiencies of the designs in Section 6.2 indicate that the optimal designs for first-order CMFP models are more robust to misspecified values of model parameters than the optimal designs for the second-order CMFP models, regardless of the number of power parameters (the same power parameter for all linear terms or different power parameters). In order to study the robustness of the CMFP models with respect to misspecified terms, we assessed the locally optimal designs for models where terms have been misspecified in Section 6.2.5. The D-efficiencies of these designs indicate that the optimal designs for misspecified terms models do not lose too much efficiency if the ranges of the mixture proportions in the misspecified and the correct model are close together. In section 6.3, we investigated strategies to find optimal exact designs. We rounded the continuous optimal design for each scenario and compared it to the exact optimal design for the same scenario. We found that the relative D-efficiency for all scenarios of the CMFP model is almost equal to one. So, there are no significant differences between the exact designs and the rounded continuous designs for all CMFP models, and thus both strategies can be applied to find optimal exact designs.

7.2 Suggested Points for Future Work

In the optimization study that has been done in the present work, we conducted a simulation study in which we evaluated the performance of the CMFP models and compared them with different models from the literature. So, we found the maximum response by determining the corresponding proportions of the mixture components that achieved this. A limitation of a simulation based (rather than a theoretical) approach is that the performance of a model depends on the 'true model' in the simulation, and only a finite number of models can be selected. We tried to mitigate this issue by

- using real datasets from a range of applications to broaden the scope of the study (Chapter 4);
- selecting each type of model in the study to be the true model in turn to incorporate an element of fairness (Chapter 5).

Still, the simulation studies, and indeed our modelling approach, could be extended in various directions. For example, extending our proposed methodology to optimize multiple responses, particularly in mixture-process variables experiments, would be an interesting idea for future research.

Regarding the optimal design research, we found the locally optimal designs for the CMFP models considering the D-optimality criterion that seeks precise model estimation by maximizing the determinant of the information matrix. However, it would be interesting to consider another optimality criterion to build optimal designs, such as the I-optimality criterion, which minimizes the prediction average variance. It seems appropriate for mixture experiments where the aim is to identify the optimal proportion for each mixture component as precise prediction of the response is required in this situation.

When we compared the two different strategies for finding exact optimal designs, we used examples where the mixture has three or four components. In this case, the designs we found had similar performance, with the exact designs found directly by the exchange algorithm always doing slightly better. It would be interesting to see if this advantage persists in higher dimensions and if the candidate set would need to be increased in size to retain this advantage. Further research in this direction would be interesting. To do this, further methods for finding the continuous optimal designs, such as particle swarm optimization (Wong et al., 2015), may need to be explored.

While the optimal designs for first-order CMFP models seem to be reasonably robust with respect to misspecifications of the model parameters or terms, this is not the case for the second-order

models. We only considered locally optimal designs in this thesis, but it would be interesting to investigate robust design approaches, such as sequential design, Bayesian design, or maximin efficient design. In the case of optimizing continuous designs in constrained experimental regions, we have tried various optimization functions in R, such as `constrOptim`, `Solnp`, and `nloptr`. These optimization functions become challenging to run and do not easily give the desired design points and corresponding weights when there are many mixture components. So, more advanced constrained optimization functions are needed in the case of many mixture components, and have to be improved to include process variables. This is an area of research that is important and required, in particular when robust designs are sought.

Chapter 8

Appendix

Table 8.1: Experimental data of the opacity of printable coating material with a 2-level process variable

x_1	x_2	x_3	z	y
0.13	0.53	0.34	-1	0.698
0.13	0.53	0.34	-1	0.711
0.13	0.53	0.34	1	0.912
0.13	0.53	0.34	1	0.930
0.13	0.60	0.27	-1	0.700
0.13	0.67	0.20	-1	0.710
0.13	0.67	0.20	-1	0.680
0.13	0.67	0.20	1	0.908
0.13	0.67	0.20	1	0.901
0.29	0.37	0.34	-1	0.772
0.29	0.51	0.20	-1	0.772
0.45	0.21	0.34	-1	0.823
0.45	0.21	0.34	-1	0.798
0.45	0.21	0.34	1	0.992
0.45	0.28	0.27	-1	0.818
0.45	0.35	0.20	-1	0.802
0.45	0.35	0.20	1	0.976
0.45	0.35	0.20	1	0.940

Table 8.2: Experimental data of the opacity of printable coating material with a 3-level process variable

x_1	x_2	x_3	z	y
0.13	0.67	0.20	0	0.710
0.45	0.35	0.20	0	0.802
0.45	0.21	0.34	0	0.823
0.13	0.53	0.34	0	0.698
0.29	0.51	0.20	0	0.772
0.45	0.28	0.27	0	0.818
0.29	0.37	0.34	0	0.772
0.13	0.60	0.27	0	0.700
0.13	0.67	0.20	1	0.780
0.29	0.44	0.27	1	0.861
0.13	0.53	0.34	1	0.782
0.13	0.67	0.20	2	0.908
0.45	0.35	0.20	2	0.976
0.13	0.53	0.34	2	0.912
0.45	0.21	0.34	2	0.992
0.13	0.67	0.20	0	0.680
0.45	0.35	0.20	0	0.822
0.45	0.21	0.34	0	0.798
0.13	0.53	0.34	0	0.711
0.13	0.67	0.20	1	0.791
0.13	0.67	0.20	2	0.901
0.45	0.35	0.20	2	0.940
0.13	0.53	0.34	2	0.930

Table 8.3: Homemade bubble solution experimental data

x_1	x_2	x_3	$z1$	$z2$	y
0.350	0.600	0.05	-1	-1	23.8
0.350	0.600	0.05	-1	1	14.2
0.350	0.600	0.05	1	-1	4.2
0.350	0.600	0.05	1	1	3.6
0.250	0.600	0.15	-1	-1	12.6
0.250	0.600	0.15	-1	1	13.6
0.250	0.600	0.15	1	-1	2.6
0.250	0.600	0.15	1	1	3.4
0.250	0.650	0.10	-1	-1	12.0
0.250	0.650	0.10	-1	1	12.0
0.250	0.650	0.10	1	-1	5.8
0.250	0.650	0.10	1	1	2.6
0.250	0.750	0.05	-1	-1	12.8
0.250	0.750	0.05	-1	1	15.4
0.250	0.750	0.05	1	-1	4.0
0.250	0.750	0.05	1	1	4.4
0.150	0.700	0.15	-1	-1	10.8
0.150	0.700	0.15	-1	1	9.2
0.150	0.700	0.15	1	-1	3.2
0.150	0.700	0.15	1	1	3.4
0.145	0.775	0.08	-1	-1	8.8
0.145	0.775	0.08	-1	1	11.2
0.145	0.775	0.08	1	-1	4.4
0.145	0.775	0.08	1	1	3.0
0.040	0.810	0.15	-1	-1	2.4
0.040	0.810	0.15	-1	1	4.0
0.040	0.810	0.15	1	-1	3.0
0.040	0.810	0.15	1	1	4.2
0.120	0.850	0.03	-1	-1	12.8
0.120	0.850	0.03	-1	1	8.0
0.120	0.850	0.03	1	-1	1.6
0.040	0.850	0.03	1	1	3.4
0.040	0.880	0.08	-1	-1	2.0
0.040	0.880	0.08	-	1	4.6
0.040	0.880	0.08	1	-1	0.6
0.040	0.880	0.08	1	1	0.6

Table 8.4: Experimental data of oil separation ratio

x_1	x_2	x_3	z	y
0.6375	0.3575	0.0050	0	7
0.6375	0.3575	0.0050	1	7
0.6375	0.3575	0.0050	2	8
0.6338	0.3537	0.0125	0	2
0.6338	0.3537	0.0125	1	3
0.6338	0.3537	0.0125	2	5
0.6300	0.3500	0.0200	0	1
0.6300	0.3500	0.0200	1	1
0.6300	0.3500	0.0200	2	3
0.5412	0.4538	0.0050	0	6
0.5412	0.4538	0.0050	1	10
0.5412	0.4538	0.0050	2	9
0.5375	0.4500	0.0125	0	2
0.5375	0.4500	0.0125	1	6
0.5375	0.4500	0.0125	2	3
0.5338	0.4462	0.0200	0	1
0.5338	0.4462	0.0200	1	2
0.5338	0.4462	0.0200	2	2
0.4450	0.5500	0.0050	0	6
0.4450	0.5500	0.0050	1	6
0.4450	0.5500	0.0050	2	6
0.4412	0.5463	0.0125	0	2
0.4412	0.5463	0.0125	1	4
0.4412	0.5463	0.0125	2	2
0.4375	0.5425	0.0200	0	1
0.4375	0.5425	0.0200	1	3
0.4375	0.5425	0.0200	2	1

Table 8.5: The chick feeding experimental data

x_1	x_2	x_3	y
0.05	0.89	0.06	59.00
0.05	0.73	0.22	60.00
0.05	0.09	0.86	29.00
0.05	0.25	0.70	35.00
0.05	0.57	0.38	53.00
0.05	0.41	0.54	48.00
0.12	0.82	0.06	82.00
0.12	0.66	0.22	90.00
0.12	0.02	0.86	63.00
0.12	0.18	0.70	73.00
0.12	0.50	0.38	100.00
0.12	0.34	0.54	80.00
0.19	0.75	0.06	105.00
0.19	0.59	0.22	105.00
0.19	0.43	0.38	120.00
0.19	0.27	0.54	109.00
0.19	0.11	0.70	110.00
0.26	0.68	0.06	136.00
0.26	0.04	0.70	125.00
0.26	0.20	0.54	133.00
0.26	0.36	0.38	130.00
0.26	0.52	0.22	141.00
0.33	0.61	0.06	141.00
0.33	0.45	0.22	156.00
0.33	0.29	0.38	157.00
0.33	0.13	0.54	153.00
0.40	0.54	0.06	156.00
0.40	0.38	0.22	179.00
0.40	0.22	0.38	163.00
0.40	0.06	0.54	143.00

Table 8.6: The illumination candle experimental data

x_1	x_2	x_3	x_4	y
0.40	0.10	0.47	0.03	75
0.60	0.10	0.27	0.03	195
0.40	0.10	0.42	0.08	180
0.60	0.10	0.22	0.08	300
0.60	0.27	0.10	0.03	220
0.60	0.22	0.10	0.08	350
0.40	0.47	0.10	0.03	145
0.40	0.42	0.10	0.08	230
0.40	0.27	0.27	0.06	190
0.60	0.17	0.17	0.06	310
0.50	0.10	0.35	0.06	220
0.50	0.35	0.10	0.06	260
0.50	0.24	0.24	0.03	260
0.50	0.21	0.21	0.08	410
0.50	0.22	0.22	0.06	425

Table 8.7: The soap processing experimental data

x_1	x_2	x_3	z_1	z_2	y
0.2	0.5	0.3	-1	-1	245.2
0.8	0.15	0.05	-1	-1	381.5
0.8	0.15	0.05	-1	-1	381.0
0.55	0.15	0.3	-1	-1	453.3
0.45	0.5	0.05	-1	-1	172.9
0.2	0.5	0.3	-1	1	285.4
0.8	0.15	0.05	-1	1	409.1
0.8	0.15	0.05	-1	1	411.7
0.55	0.15	0.3	-1	1	450.0
0.45	0.5	0.05	-1	1	245.8
0.2	0.5	0.3	1	-1	213.8
0.8	0.15	0.05	1	-1	378.4
0.8	0.15	0.05	1	-1	377.3
0.55	0.15	0.3	1	-1	408.8
0.45	0.5	0.05	1	-1	180.6
0.2	0.5	0.3	1	1	250.6
0.8	0.15	0.05	1	1	404.2
0.8	0.15	0.05	1	1	406.6
0.55	0.15	0.3	1	1	410.1
0.45	0.5	0.05	1	1	245.44

Bibliography

- Akalin, O., Akay, K. U., Sennaroglu, B., & Tez, M. (2010). Optimization of Chemical Admixture for Concrete on Mortar Performance Tests Using Mixture Experiments. *Chemometrics and Intelligent Laboratory Systems*, *104*(2), 233–242.
- Anderson, M. J., & Whitcomb, P. J. (2016). *RSM Simplified: Optimizing Processes Using Response Surface Methods for Design of Experiments*. Productivity press.
- Anderson-Cook, C. M., Goldfarb, H. B., Borror, C. M., Montgomery, D. C., Canter, K. G., & Twist, J. N. (2004). Mixture and Mixture-Process Variable Experiments for Pharmaceutical Applications. *Pharmaceutical Statistics: The Journal of Applied Statistics in the Pharmaceutical Industry*, *3*(4), 247–260.
- Atchison, J., & Shen, S. M. (1980). Logistic-Normal Distributions: Some Properties and Uses. *Biometrika*, *67*(2), 261–272.
- Atkinson, A. (2014). Optimal Design. *Wiley StatsRef: Statistics Reference Online*, 1–17.
- Atkinson, A., & Donev, A. (1992). *Optimum Experimental Designs* (Vol. 5). Clarendon Press.
- Atkinson, A. (1982). Developments in the Design of Experiments, Correspondent Paper. *International Statistical Review/Revue Internationale de Statistique*, 161–177.
- Atkinson, A., Donev, A., & Tobias, R. (2007). *Optimum Experimental Designs, with SAS* (Vol. 34). OUP Oxford.
- Baty, F., & Delignette-Muller, M. (2004). Estimating the Bacterial Lag Time: Which Model, Which Precision? *International journal of food microbiology*, *91*(3), 261–277.
- Becker, N. (1968). Models for the Response of a Mixture. *Journal of the Royal Statistical Society: Series B (Methodological)*, *30*(2), 349–358.
- Becker, N. (1978). Models and Designs for Experiments with Mixtures. *Australian Journal of Statistics*, *20*(3), 195–208.
- Bello, L. D., & Vieira, A. (2011). Optimization of a Product Performance Using Mixture Experiments Including Process Variables. *Journal of Applied Statistics*, *38*(8), 1701–1715.
- Bhadani, R. (2021). Nonlinear Optimization in R Using nlopt. *arXiv preprint arXiv:2101.02912*.

- Box, G., & Draper, N. (2007). *Response Surfaces, Mixtures, and Ridge Analyses*. John Wiley & Sons.
- Box, G., & Lucas, H. (1959). Design of Experiments in Non-Linear Situations. *Biometrika*, *46*(1/2), 77–90.
- Box, G., & Wilson, K. (1951). On the Experimental Designs for Exploring Response Surfaces. *Ann Math Stat*, *13*, 1–45.
- Brown, L. (2014). *General Blending Models for Mixture Experiments: Design and Analysis*. The University of Manchester (United Kingdom).
- Brown, L., Donev, A. N., & Bissett, A. (2015). General Blending Models for Data From Mixture Experiments. *Technometrics*, *57*(4), 449–456.
- Chau, K., & Kelley, W. (1993). Formulating Printable Coatings via D-optimality. *JCT, Journal of coatings technology*, *65*(821), 71–78.
- Chaudhuri, P., & Mykland, P. A. (1993). Nonlinear Experiments: Optimal Design and Inference Based on Likelihood. *Journal of the American Statistical Association*, *88*(422), 538–546.
- Chen, W., Zhu, W., & Hu, C. (1985). A New Mixture Model with Three or Four Components and Their Quasi D-optimality. *Northern Illinois University, DeKalb, IL*.
- Chernoff, H. (1953). Locally Optimal Designs for Estimating Parameters. *The Annals of Mathematical Statistics*, 586–602.
- Chitra, S., & Ekong, E. (1993). An Alternative Approach to Product Development. *ANNUAL QUALITY CONGRESS TRANSACTIONS-AMERICAN SOCIETY FOR QUALITY CONTROL*, *47*, 837–837.
- Chu, C., & Resurreccion, A. (2004). Optimization of a Chocolate Peanut Spread Using Response Surface Methodology (RSM). *Journal of sensory studies*, *19*(3), 237–260.
- Claringbold, P. (1955). Use of the Simplex Design in the Study of Joint Action of Related Hormones. *Biometrics*, *11*(2), 174–185.
- Cochran, W. G. (1973). Experiments for Nonlinear Functions (ra Fisher Memorial Lecture). *Journal of the American Statistical Association*, *68*(344), 771–781.
- Coetzer, R., & Haines, L. M. (2017). The Construction of D-and I-optimal Designs for Mixture Experiments with Linear Constraints on the Components. *Chemometrics and Intelligent Laboratory Systems*, *171*, 112–124.
- Cook, D., & Fedorov, V. (1995). Invited Discussion Paper Constrained Optimization of Experimental Design. *Statistics*, *26*(2), 129–148.
- Cornell, J. (1973). Experiments with Mixtures: A Review. *Technometrics*, *15*(3), 437–455.
- Cornell, J. (1988). Analyzing Data from Mixture Experiments Containing Process Variables: A Split-plot Approach. *Journal of Quality Technology*, *20*(1), 2–23.

- Cornell, J. (1990). Embedding Mixture Experiments Inside Factorial Experiments. *Journal of quality technology*, 22(4), 265–276.
- Cornell, J. (1995). Fitting Models to Data From Mixture Experiments Containing Other Factors. *Journal of Quality Technology*, 27(1), 13–33.
- Cornell, J. (2000). Developing Mixture Models, Are We Done. *Journal of Statistical Computation and Simulation*, 66(2), 127–144.
- Cornell, J. (2011). *Experiments with Mixtures: Designs, Models, and the Analysis of Mixture Data*. John Wiley & Sons.
- Cox, D. (1971). A Note on Polynomial Response Functions for Mixtures. *Biometrika*, 58(1), 155–159.
- Czitrom, V. (1988). Mixture Experiments with Process Variables: D-optimal Orthogonal Experimental Designs. *Communications in Statistics-Theory and Methods*, 17(1), 105–121.
- Czitrom, V. (1989). Experimental Design for Four Mixture Components with Process Variables. *Communications in Statistics-Theory and Methods*, 18(12), 4561–4581.
- Draper & Pukelsheim, F. (1998). Mixture Models Based on Homogeneous Polynomials. *Journal of statistical planning and inference*, 71(1-2), 303–311.
- Draper & St.John, R. (1977). A Mixtures Model with Inverse Terms. *Technometrics*, 19(1), 37–46.
- Fedorov. (2013). *Theory of Optimal Experiments*. Elsevier.
- Fedorov & Hackl, P. (1997). *Model-Oriented Design of Experiments* (Vol. 125). Springer Science & Business Media.
- Fishman, G. (1996). Monte Carlo Concepts, Algorithms and Applications. Springer-Verlag.
- Focke, W. W., Sandrock, C., & Kok, S. (2007). Weighted-Power-Mean Mixture Model: Application to Multicomponent Liquid Viscosity. *Industrial & engineering chemistry research*, 46(13), 4660–4666.
- Ford, I., Titterton, D., & Kitsos, C. P. (1989). Recent Advances in Nonlinear Experimental Design. *Technometrics*, 31(1), 49–60x.
- Gelfand, A. E., & Ghosh, S. K. (1998). Model Choice: A Minimum Posterior Predictive Loss Approach. *Biometrika*, 85(1), 1–11.
- Gilmour, S. G., & Trinca, L. A. (2005). Fractional Polynomial Response Surface Models. *Journal of agricultural, biological, and environmental statistics*, 10, 50–60.
- Glover, F. (1986). Future Paths for Integer Programming and Links to Artificial Intelligence. *Computers & operations research*, 13(5), 533–549.
- Goldberg, D. E. (1989). Genetic Algorithms in Search. *Optimization, Machine Learning*.
- Goldfarb, H. B., Borrer, C. M., & Montgomery, D. C. (2003). Mixture-Process Variable Experiments with Noise Variables. *Journal of Quality Technology*, 35(4), 393–405.

- Golub, G., & Pereyra, V. (1973). The Differentiation of Pseudo-Inverses and Nonlinear Least Squares Problems Whose Variables Separate. *SIAM Journal on numerical analysis*, *10*(2), 413–432.
- Gorman, J. W., & Cornell, J. A. (1982). A Note on Model Reduction for Experiments with Both Mixture Components and Process Variables. *Technometrics*, *24*(3), 243–247.
- Hackler, W. C., Kriegel, W. W., & Hader, R. J. (1956). Effect of Raw-Material Ratios on Absorption of Whiteware Compositions. *Journal of the American Ceramic Society*, *39*(1), 20–25.
- Hare, L. B. (1979). Designs for Mixture Experiments Involving Process Variables. *Technometrics*, *21*(2), 159–173.
- John, R. S., & Draper, N. R. (1975). D-Optimality for Regression Designs: A Review. *Technometrics*, *17*(1), 15–23.
- Johnson, M. E., Moore, L. M., & Ylvisaker, D. (1990). Minimax and Maximin Distance Designs. *Journal of statistical planning and inference*, *26*(2), 131–148.
- Jones, B. (2011). *Optimal Design of Experiments: A Case Study Approach*. Wiley.
- Kenworthy, O. (1963). Factorial Experiment with Mixtures Using Ratios. *Industrial Quality Control*, *19*(12), 24–26.
- Khashab, R. H. H. (2018). *Optimal Design of Experiments with Mixtures* (Doctoral dissertation). University of Southampton.
- Khudri, M. M., & Sadia, F. (2013). Determination of the Best Fit Probability Distribution for Annual Extreme Precipitation in Bangladesh. *European Journal of Scientific Research*, *103*(3), 391–404.
- Khuri, A. I., & Cornell, J. A. (2018). *Response Surfaces: Designs and Analyses*. Routledge.
- Kiefer, J. (1959). Optimum Experimental Designs. *Journal of the Royal Statistical Society: Series B (Methodological)*, *21*(2), 272–304.
- Kiefer, J. (1961). Optimum Designs in Regression Problems, II. *The Annals of Mathematical Statistics*, *32*(1), 298–325.
- Kirkpatrick, S., Gelatt Jr, C. D., & Vecchi, M. P. (1983). Optimization by Simulated Annealing. *science*, *220*(4598), 671–680.
- Kowalski, S., Cornell, J. A., & Geoffrey Vining, G. (2000). A New Model and Class of Designs for Mixture Experiments with Process Variables. *Communications in Statistics-Theory and Methods*, *29*(9-10), 2255–2280.
- Li, Z., Lu, D., & Gao, X. (2021). Optimization of Mixture Proportions by Statistical Experimental Design Using Response Surface Method-A Review. *Journal of Building Engineering*, *36*, 102101.

- Måge, I., & Næs, T. (2005). Split-Plot Design for Mixture Experiments with Process Variables: A Comparison of Design Strategies. *Chemometrics and intelligent laboratory systems*, 78(1-2), 81–95.
- Meyer, R. K., & Nachtsheim, C. J. (1995). The Coordinate-Exchange Algorithm for Constructing Exact Optimal Experimental Designs. *Technometrics*, 37(1), 60–69.
- Montgomery, D. C. (2017). *Design and Analysis of Experiments*. John Wiley & Sons.
- Næs, T., Færgestad, E. M., & Cornell, J. (1998). A Comparison of Methods for Analyzing Data From a Three Component Mixture Experiment in the Presence of Variation Created by Two Process Variables. *Chemometrics and intelligent laboratory systems*, 41(2), 221–235.
- Nelder, J. A., & Mead, R. (1965). A Simplex Method for Function Minimization. *The computer journal*, 7(4), 308–313.
- Pal, M., & Mandal, N. K. (2006). Optimum Designs for Optimum Mixtures. *Statistics & Probability Letters*, 76(13), 1369–1379.
- Pal, M., & Mandal, N. K. (2008). Minimax Designs for Optimum Mixtures. *Statistics & Probability Letters*, 78(6), 608–615.
- Piepel, G. F., & Cornell, J. A. (1985). Models for Mixture Experiments When the Response Depends on the Total Amount. *Technometrics*, 27(3), 219–227.
- Prescott, P. (2004). Modelling in Mixture Experiments Including Interactions with Process Variables. *Quality Technology & Quantitative Management*, 1(1), 87–103.
- Pukelsheim, F. (1993). *Optimal Design of Experiments*. John Wiley & Sons. Inc., New York, New York.
- Pukelsheim, F., & Rieder, S. (1992). Efficient Rounding of Approximate Designs. *Biometrika*, 79(4), 763–770.
- Quenouille, M. H., et al. (1953). The Design and Analysis of Experiment. *The design and analysis of experiment*.
- Quenouillé, M. (1963). Discussion of “The Simplex-Centroid Design for Experiments with Mixtures” by H. Scheffé. *Journal of the Royal Statistical Society, Series B*, 25, 235–263.
- Royston, P., & Altman, D. G. (1994). Regression Using Fractional Polynomials of Continuous Covariates: Parsimonious Parametric Modelling. *Journal of the Royal Statistical Society Series C: Applied Statistics*, 43(3), 429–453.
- Sahni, N. S., Piepel, G. F., & Næs, T. (2009). Product and Process Improvement Using Mixture-Process Variable Methods and Robust Optimization Techniques. *Journal of Quality Technology*, 41(2), 181–197.
- Scheffé, H. (1958). Experiments with Mixtures. *Journal of the Royal Statistical Society: Series B (Methodological)*, 20(2), 344–360.

- Scheffé, H. (1963). The Simplex-Centroid Design for Experiments with Mixtures. *Journal of the Royal Statistical Society: Series B (Methodological)*, 25(2), 235–251.
- Schwarz, G. (1978). Estimating the Dimension of a Model. *The annals of statistics*, 461–464.
- Sinha, B., Mandal, N., Pal, M., Das, P., Sinha, B., Mandal, N., Pal, M., & Das, P. (2014). Optimal Designs for Estimation of Optimum Mixture in Scheffé's Quadratic Model Under Constrained Factor Space. *Optimal Mixture Experiments*, 123–136.
- Snee, R., & Hoerl, R. (2016). *Strategies for Formulations Development: A Step-by-step Guide Using JMP*. SAS Institute.
- Snee, R., & Marquardt, D. W. (1974). Extreme Vertices Designs for Linear Mixture Models. *Technometrics*, 16(3), 399–408.
- Steiner, S. H., Hamada, M., White, B. J. G., Kutsyy, V., Mosesova, S., & Salloum, G. (2007). A Bubble Mixture Experiment Project for Use in an Advanced Design of Experiments Class. *Journal of Statistics Education*, 15(1).
- Thompson, W. O., & Myers, R. H. (1968). Response Surface Designs for Experiments with Mixtures. *Technometrics*, 10(4), 739–756.
- Tong, H. (2010). Professor Hirotugu Akaike, 1927-2009. *Journal of the Royal Statistical Society. Series A (Statistics in Society)*, 451–454.
- Wald, A. (1943). On the Efficient Design of Statistical Investigations. *The annals of mathematical statistics*, 14(2), 134–140.
- Wong, W. K., Chen, R.-B., Huang, C.-C., & Wang, W. (2015). A Modified Particle Swarm Optimization Technique for Finding Optimal Designs for Mixture Models. *PloS one*, 10(6), e0124720.